A new process for preparing pitches from anthracene oil has been developed. Named the ‘ecopitch process’, it involved four sequential cycles each of which included a thermal oxidative condensation step followed by thermal treatment and distillation. The unreacted anthracene oil obtained in each cycle was used as the feedstock for the next cycle. It was observed that the unreactive anthracene oil required severer operational conditions (i.e. temperature) for being polymerised as the number of processing cycles increased. After four cycles, the polymerisation capability of the anthracene oil was depleted.

Bulk samples and their fractions from all stages of the process were characterised in terms of their molecular mass distribution and structural features. These samples were used to develop and validate methods based on laser desorption mass spectroscopy and nuclear magnetic resonance. The pyrolysis behaviour and the capacity of the anthracene oil derivatives to generate carbon materials were also investigated.

The feasibility of using anthracene oil derivatives as impregnation and binder agents in the production of graphite electrodes was studied. Preliminary results suggest that these pitches are suitable for use as impregnation agents. However, their application as binders requires further study. One of the most important goals attained in this project is the excellent capacity of anthracene oil derivatives to develop mesophase, and, consequently, to produce advanced carbon materials (e.g. carbon fibres, graphitic carbons and activated carbons for application in energy storage).

Modelling of the anthracene oil polymerisation was performed as a base for the scaling-up of the process. Tests in batch mode involved the study of the main parameters that affected the final properties and quality of the pitch obtained from the anthracene oil. A computational model was also developed and tested in order to simulate the experimental conditions inside a pitch production reactor. This model showed that the critical point in the reacting system is the injector which corresponded to the zone of largest energy release.

Price (excluding VAT) in Luxembourg: EUR 7

Publications Office

ISBN 978-92-79-14238-3

9 789279 142383

KI-NA-24193-EN-C

EC

Development of a new generation of coal-derived environmentally- friendly pitches

EUR 24193

EUROPEAN COMMISSION

European Research Area

Development of a new generation of coal-derived environmentally-friendly pitches

Research Fund for Coal & Steel

Interested in European research?

RTD info is our quarterly magazine keeping you in touch with main developments (results, programmes, events, etc.). It is available in English, French and German. A free sample copy or free subscription can be obtained from:

Directorate-General for Research
Information and Communication Unit
European Commission
B-1049 Brussels
Fax (32-2) 29-58220
E-mail: research@ec.europa.eu
Internet: http://ec.europa.eu/research/rtdinfo/index_en.html

How to obtain EU publications

Free publications:

- via EU Bookshop (http://bookshop.europa.eu);
- at the European Commission's representations or delegations. You can obtain their contact details by linking http://ec.europa.eu or by sending a fax to +352 2929-42758.

Publications for sale:

- via EU Bookshop (http://bookshop.europa.eu);
- Priced subscriptions (Official Journal of the EU, Legal cases of the Court of Justice as well as certain periodicals edited by the European Commission) can be ordered from one of our sales agents. You can obtain their contact details by linking http://bookshop.europa.eu, or by sending a fax to +352 2929-42758.

EUROPEAN COMMISSION
Directorate-General for Research
Research Fund for Coal and Steel Unit

Contact: RFCS publications
Address: European Commission, CDMA 0/124, B-1049 Brussels
Fax (32-2) 29-65987; e-mail: rtd-steel@ec.europa.eu

European Commission

Research Fund for Coal and Steel

Development of a new generation of coal-derived environmentally friendly pitches

R. Menéndez, M. Granda ([1]), Rafael Kandiyoti, M. Millán ([2]), I. Gulyurtlu, F. Pinto ([3]), J. J. Fernández ([4]), S. Lacroix, B. Allard ([5]), J. Machnikowski ([6])

([1]) **Consejo Superior de Investigaciones Científicas–Instituto Nacional del Carbón, CSIC —** PO Box 73, 33080 Oviedo, SPAIN
([2]) **Imperial College of Science, Technology and Medicine —** South Kensington Campus, SW7 2AZ London, UNITED KINGDOM
([3]) **Instituto Nacional de Engenharia, Tecnología e Inovação —** Edificio J, Azinhaga dos Lameiros 22, 1649-038, Lisboa, PORTUGAL
([4]) **Industrial Química del Nalón, S.A. (IQNSA) —** Avda. Galicia 31, 33005 Oviedo, SPAIN
([5]) **Carbone Savoie (CS) —** 30 rue Louis Jouvet, BP16, Cedex F-39631, Venissieux, FRANCE
([6]) **Wroclaw University of Technology —** Gdanska 7/9, 50-344 Wroclaw, POLAND

Contract No RFCR-CT-2005-00004
1 July 2005 to 30 June 2008

Final report

Directorate-General for Research

2010 EUR 24193 EN

Europe Direct is a service to help you find answers to your questions about the European Union

Freephone number (*)**:**

00 800 6 7 8 9 10 11

(*) Certain mobile telephone operators do not allow access to 00 800 numbers or these calls may be billed.

A great deal of additional information on the European Union is available on the Internet. It can be accessed through the Europa server (http://europa.eu).

Cataloguing data can be found at the end of this publication.

Luxembourg: Publications Office of the European Union, 2010

ISBN 978-92-79-14238-3

doi 10.2777/82435

ISSN 1018-5593

Printed in Luxembourg

PRINTED ON WHITE CHLORINE-FREE PAPER

CONTENTS

FINAL SUMMARY

Work Package 1. Project coordination

The coordination activities of the project were mainly focused on the distribution of the tasks to be carried out by each partner, the organization of periodical semester meetings, the elaboration of an internal consortium agreement document and the compilation of the information provided by the partners in the semester, mid-term and final reports.

Work Package 2. Processing of anthracene oil at laboratory scale

Task 2.1. Selection and preliminary characterization of the anthracene oil

Standard anthracene oil obtained from coal-tar by industrial fractionated distillation in the temperature range of 280-400 °C was used as feedstock for the preparation of the pitches. The initial characterization of this raw material involved the determination of industrial parameters, such as distillation curves, flash points, etc.

Task 2.2. Oxidative thermal treatment of the anthracene oil under different experimental conditions

According to previous experiences, anthracene oil was polymerized in the presence of air. Pressure was used to avoid the massive release of volatiles and also to improve the yield of the process. Different operational conditions of reaction time, residence time and oxygen/sample ratio were studied in order to obtain a reaction product with different characteristics and a higher degree of polymerization. After thermal treatment (task 2.4) and distillation (task 2.3) pitches with the desired softening point were obtained (~ 90 °C for impregnation pitches and ~ 110 °C for binder pitches). By using this procedure the first cycle of anthracene oil processing was completed, as a result of which a reaction product (RP-1), a pitch (P-1) and unreacted anthracene oil (AO-2) were obtained. In an attempt to upgrade the anthracene oil, the unreacted part was subjected to a second cycle of processing. A second series of products was obtained: RP-2, P-2 and AO-3. A third and a fourth processing cycle completed the transformation of the initial anthracene oil into reaction products (RP-1 to RP-4) and pitches (P-1 to P-4).

Task 2.3. Distillation of oxidized anthracene oil

Distillation was performed in order to adjust the characteristics of the pitches to commercial requirements, especially softening point.

Task 2.4. Thermal treatment of oxidized anthracene oil

The thermal treatment of the reaction products and pitches obtained from anthracene oil processing was performed with a double aim: (i) to refine the commercial parameters of the anthracene oil pitches for use as binder or impregnating agents and (ii) to find the optimum conditions for transforming anthracene oil derivatives into mesophase for the preparation of carbon fibres.

In the first case, softening point and carbon yield were the main parameters to be monitored. In the second case, several reactions (with and without gaseous pressure) were carried out in order to obtain mesophase with adequate viscoelastic properties for further spinning into fibres. An initial thermal treatment under pressure gave rise to a polymerized sample that in a subsequent second thermal treatment was partially transformed into mesophase. Finally, by means of a hot sedimentation step the mesophase was separated from the isotropic part. Despite the promising initial properties exhibited by this mesophase, it was not possible to spin it into fibres. After several approaches, a new strategy consisting in rejecting the mesophase and taking the isotropic part as the feedstock for the preparation of a new mesophase was studied. This fresh mesophase was successfully spun, as will be described in WP-5.

Work Package 3. Characterization and evaluation of the genotoxicity of the anthracene oil-based pitches

Task 3.1. Chemical and rheological characterization

There were two main aims to this part of the work. The first was to perform a detailed characterisation of the pitches produced from the "ecopitch" process in terms of mass distribution and structural features. The second was to validate the analytical procedures used to obtain this information. Overall, the two aims have been successfully achieved.

The results suggest that, in this process, molecules with the largest conjugated aromatic systems are the most reactive species to oxygen and are mostly consumed in the first two cycles. Most of the oxygen is then eliminated during the thermal treatment, which leads to a pitch with a more polymerized structure. The amount of oxygen introduced into the samples increased with the severity of the oxidation conditions. However, during the fourth cycle, the pitch obtained exhibited an unusually high oxygen content compared to the pitches from the earlier cycles, due to its decreased thermal stability compared to the pitches from the earlier stages.

In a more detailed investigation of the anthracene-oils and pitches, significant differences between equivalent samples from successive cycles of the process were observed. The anthracene oils were fractionated into narrow bands of material using planar-chromatography. These fractions were studied as an aid to determining mass distribution (by SEC and LD-MS) and any changes in the relative sizes of aromatic ring systems (by UV-F). Demonstrable evidence of the presence of high mass species (1,000 - 3,000 Da) that were not expected to be in these samples was found. A trend of decreasing average mass was found as the number of cycles increased, which is in keeping with the observations from the study of the bulk samples (by UV-F, SEC, GC-MS and probe-MS).

The pitch samples were also sub-divided into narrow fractions through a two-step process. Solvent separation was used first to produce five solubility-fractions from each pitch. These samples were then further fractionated using planar chromatography. This treatment revealed differences in mass and structure between the pitches that were not apparent from the analysis of the bulk samples. Data from SEC, UV-F, LD-MS, NMR, EA, GC-MS and probe-MS were correlated for characterizing these samples.
Larger molecular sizes and larger polynuclear aromatic ring systems were observed in the pitch samples recovered from the later processing cycles, indicating that samples were getting progressively larger with the increasing severity of the oxidative and thermal treatment steps. The most important differences found during the characterisation were in the amounts of cata-condensed aromatic carbon (Ccata) and aromatic carbon substituted with aromatic groups (Car-AS) detected in samples from different cycles of the process. These changes in structure could be related to the processing conditions and properties of the pitches. From this information it was possible to infer basic reaction mechanisms for the process.

For the pitch produced from the first cycle of the process (P-1), a higher proportion of its carbon is in cata-condensed aromatic environments than the pitch from the fourth cycle. Conversely, the pitch from the fourth cycle has more Car-AS. The data suggest a change from condensation and ring closure reactions for the pitch produced in the first cycle (P-1), leading to increasing sizes of aromatic clusters and to cross linking reactions through biphenyl like aromatic-aromatic single bond formation for P-4. These findings are in keeping with the processing conditions, where P-4 was produced from less reactive species than the P-1 sample, and processed under more severe conditions. The P-1 samples contain molecules that are more planar in geometry and that P-4 is more crossed-linked, with its fused aromatic ring systems possibly held in different planes to one-another. These conclusions on structure also match findings from studies on the pyrolysis behaviour and ability of these pitches to generate mesophase and coke.

In conclusion, the aims of the study are successful achieved. The detailed characterisation of the pitch samples using the ASP method highlighted changes in structure and mass. The basic reaction mechanisms inferred from these studies correlate well with the studies on pyrolysis. In both sets of

studies similar conclusions were reached on the structural make-up of the pitches from different cycles of the process.

Task 3.2. Pyrolysis behaviour
The pyrolysis behaviour of the anthracene oil derivatives corroborated the results previously obtained from the chemical characterization of the samples. The severity of the thermal oxidative condensation determined the pyrolysis behaviour of the samples, especially the capacity of the reaction products and pitches to develop mesophase. In fact, the increase in the severity of the experimental conditions for polymerizing anthracene oil led to samples that required more drastic conditions to generate mesophase (reaction temperature and/or residence time). In the same way, the optical texture of the cokes varied from domains to fine mosaics with the increasing severity of the operational conditions of anthracene oil processing. These results provide a good guidance for further use of the anthracene oil-based pitches. The samples obtained in the first cycle of anthracene oil processing (RP-1 and P-1) seem to be promising candidates for the preparation of carbon fibres.

Task 3.3. Genotoxicity indices
As previously mentioned, the processing of anthracene oil involved the reaction of those components that to a large extent contribute to the genotoxicity of pitches (i.e., benzo[a]pyrene, etc.). With the increase in the number of processing cycles the concentration of these compounds is lower, and consequently, the global genotoxicity of the pitches decreases. This reduction was especially relevant in the pitch obtained in the fourth cycle of anthracene oil processing (BaP-equiv of 3.11 and 0.04 wt.% for P-1 and P-4, respectively).

Work Package 4. Feasibility of trial pitches for graphite electrode, pinstock and cathode preparation

In this study, anthracene oil-based pitches with a softening point of 90 °C (impregnation pitch) and 110 °C (binder pitch) were used and the results were compared with those obtained from standard impregnation and binder coal-tar pitches.

Task 4.0. Preliminary characterization
This task has been spread out over the period under consideration, as it was the first step to be carried out for each round of production for both the 90 °C and 110°C softening point samples.

For each pitch sample, density and carbon yield were measured, as well as their wetting temperature, viscosity curve versus temperature, toluene and anthracene oil insoluble contents. Thermogravimetric analysis was also performed.

Task 4.1. Electrodes testing
The purpose of this task was to evaluate the use of P-1b as an impregnation pitch for electrodes. A large sample of P1-b (4 tons, 90°C SP) has been sent by IQNSA, together with a reference commercial pitch. Despite disappointing results for the filtration rate, 3 pieces of electrode, 150 mm in diameter and 300 mm in length, were impregnated with pitches, baked and then graphitized.

During the impregnation process, the percentage of pitch used was the same than with reference pitch. The final properties of the electrodes were then determined. The density and flexural strength of P-1b were lower than in the case of those with the standard pitch.

These lower properties could be a consequence of a possible problem during industrial pitch production (pitch ageing or pitch contamination). For this reason, these conclusions cannot be taken as definitive.

Finally, this task was completely stopped and the focus was shifted to the cathode blocks only. This was due to the fact that Carbone Savoie no longer belongs to GRAFTECH because it was sold to ALCAN. The large industrial tests initially planned in the GRAFTECH installations could not be performed.

Task 4.2. Simulation of pinstock PI
P-1b was evaluated as an impregnation pitch for pinstocks. This evaluation implied two successive impregnation treatments, each of which followed by a baking treatment. The products were then graphitized. Three pieces of pinstocks (with the same dimensions as the previous electrodes) were impregnated, either with P1-b, or with the reference pitch. The amount of pitch picked up in each case and during the two treatments was similar. However, the final properties of the pinstocks made with P-1b had significantly lower density, Young's modulus and flexural strength. Again, was considered that these poor results could have been due to the problem observed in the 4MT sample. However, as in the case of electrode impregnation, this task has been stopped and GRAFTECH has decided not to pursue it any further.

Task 4.3. Large scale study
This task was not started due to the results with Task 4.1. As this study implies very large amount of product and severe treatment, it has been postponed in order that we first select the appropriate pitch process step. With the focus now directed to cathode block impregnation, Task 4.3 has been cancelled and replaced by task 4.4.

Task 4.4. Evaluation of cathode block pitch impregnation
As GRAFTECH is not interested in pursuing the study on electrode and pinstocks impregnation, CARBONE SAVOIE has decided to focus on cathode blocks only. A subcontract has been signed between GRAFTECH and CARBONE SAVOIE for cathode blocks impregnation in Parma (GRAFTECH's central laboratory). Step 4 (P4-b) has been chosen for the impregnation, as it leads to a significant decrease in the PAH content, especially BaP content. The pitch properties were found appropriate for an impregnation pitch. Therefore 4 MT of P-4b have been sent to Parma. Two graphitized cathode blocks 305 * 305 * 1778 mm have been impregnated in Parma's pilot impregnation facility, one with P4-b pitch and the other with the standard coal tar pitch supplied by IQNSA at the beginning of the project.

The analyses show a large gradient of impregnation along the entire length of the block, independent of the type of pitch, and the final properties are not as high as during an industrial impregnation. However, it cannot be concluded that there is any real difference due to the impregnation pitch. P4-b could therefore be used as an impregnation pitch for cathode blocks. Its use in electrodes and pinstocks impregnation requires further confirmation, as impregnation of cathode blocks is easier than impregnating electrodes or pinstocks.

Parallel studies on the application of Ecopitch as binder pitch have shown that the final properties of carbon cathodes processed with Ecopitch P4-a (step 4, with less BaP content), were lower than those of products processed with standard coal tar pitch, especially the mechanical properties.

According to the above discussed results, the main application at industrial scale of the Ecopitches can be found in the impregnation of cathode blocks. Even if it is a small business, it can be considered of high interest because of the additional value provided by the lower genotoxicity of pitch P-4b, and consequently, its reduced environmental impact. The use of P-4a as a binder pitch requires further studies in order to improve the mechanical properties of the resultant cathode blocks.

Work Package 5. Preparation and testing of advanced carbon materials

Task 5.1. Carbon fibres
The high aromaticity and the total absence of solid particles make anthracene oil-based pitches excellent candidates for carbon fibres. The preparation of fibres from anthracene oil derivatives requires the application of several thermal cycles in order to obtain a precursor that fulfills the requirements of spinnability. Preparation of this precursor was initially limited by the difficulty of producing a homogeneous mesophase with adequate viscoeleastic properties for transformation into fibres. This was because of the different thermal reactivity of the components of the anthracene oil derivatives, which leads to the coexistence of fresh mesophase with mesophase that has already hardened (semicoke). This

problem was successfully overcome by using the isotropic part initially separated from the mesophase by sedimentation. This isotropic part was transformed into mesophase and this mesophase was successfully spun into fibres. Further studies showed that the preparation of anthracene oil derivatives for fibres can be substantially improved by using continuous regime of mesophase production.

Task 5.2. Mesophase-based carbon materials

The processing of anthracene oil at progressively increasing temperatures may be expected to affect the propensity of pitch to develop mesophase and, in consequence, the structural ordering and properties of the resultant carbonaceous materials. The objective of the work performed within this task was to assess and compare carbons produced from P-1, P-2, P-3 and P-4 and select the most appropriate pitches for producing graphitic and activated carbons. The preliminary part of the study was focused on a general characterization of the carbons derived from the pitches in terms of optical texture, graphitizability and reactivity towards alkaline hydroxides. The selected pitches were next used for the synthesis of advanced carbons for application in energy storage: boron doped graphitic carbons, activated carbons of tailored porosity development, nitrogen enriched activated carbons and microporous monolithic adsorbents.

The thermal oxidative condensation of anthracene oil yields a series of practically QI free pitches which can be considered as one family. Despite the similarities between the essential characteristics of the pitches, microscopic and XRD analysis of the resultant cokes revealed a worsening of anisotropic development and graphitizability from P-1 to P-4. P-1 is therefore preferred as a precursor of graphitic carbons of a degree of structural ordering comparable to that of commercial graphites, as evidenced by the values of the structure parameters after heat-treatment at 2900^{o}C: d_{002}=0.3364 nm, L_c=47 nm, L_a=83 nm. In terms of behaviour on activation of the samples with alkaline hydroxide the semi-cokes from all the pitches show similar properties. Activation with KOH yields activated carbons with an extremely developed microporosity at a moderate weight loss. Reaction with NaOH produces carbon with poorly developed porosity. In conclusion, only KOH is a suitable activation agent for pitch derived carbons.

P-1 derived coke and graphitic carbon (HTT 1000^{o}C and 2900^{o}C, respectively) were used for the synthesis of boronated carbons with a good structure for Li-ion cells. The procedure developed involved mixing 2 wt% of both crystalline and amorphous nanopowder of boron, or boron carbide, with the carbon followed by annealing at 2300^{o}C under argon. Boron acts as a graphitization catalyst.

Specific applications of porous carbons require materials with a well defined porous texture and surface properties. We demonstrated that the carbonization degree and KOH/precursor ratio are the most powerful variables for the control of porosity development in the activation of pitch derived materials. Mesophase pitches and semi-cokes rich in hydrogen produced on heat-treatment up to ~550^{o}C show a high and very similar capacity of pore generation on reaction with KOH (S_{BET} 2500-2800 m^2/g, and micropore volume V_{DR} 0.8-0.9 cm^3/g). An additional increase in the pretreatment temperature to 700^{o}C suppresses the generation of porosity (S_{BET} ~1500 m^2/g, V_{DR} ~0.45 cm^3/g), however has a minor effect on pore size distribution. A decreasing KOH/coke ratio from 3:1 to 2:1 results in an activated carbon with a reduced S_{BET} from 2500 to 1940 m^2/g and a reduction in average micropore width L_0 from 1.47 to 1.21 nm. This study demonstrates therefore that activated carbons with tailored porosity development can be successfully produced from anthracene oil derived pitches.

Two routes were tested for the synthesis of nitrogen enriched porous carbons from anthracene oil pitches: co-pyrolysis of the pitches with polyacrylonitrile (PAN) and various forms of melamine (M) followed by activation with steam and CO_2 and the ammonization of pitch-derived KOH activated carbons. The activated carbons derived from pitch/N-polymer blends with a weight ratio of ~50:50 are characterized by moderate porosity development (S_{BET} up to 800 m^2/g) and a nitrogen content of at most 6.2 wt%. The pitch properties have a negligible effect on co-pyrolysis behaviour. A study of the reaction of ammonia with activated carbons of S_{BET} of 2480 and 1560 m^2/g led to a similar total nitrogen content of about 5.5 wt% on treatment at 450 and 700^{o}C. It was found out that under the conditions used nitrogen enrichment occurs preferentially on the outer surface of the particles with little reaction on the pore surface.

To obtain a high volumetric capacity for gas adsorption the system must be made up of tightly packed microporous activated carbon. In the study on monolith formation we used high surface area microporous carbon (S_{BET} = 2550 m^2/g) produced by activating P-4 semi-coke at 750^oC. The powder was compacted into discs of 18 mm diameter and 7-10 mm height baked under nitrogen at 900 °C, using polyfurfuryl alcohol (PFA) and novolac type resin (NOV) as a binder.

Cokes with a well oriented microstructure can be obtained from anthracene oil derivatives by applying thermal cycles that facilitate the formation of oriented domains. The preparation of this type of materials requires, the formation of mesophase, rather than the manipulation of mesophase, as intermediate stage in the preparation of the cokes. The results were obtained when relatively low carbonization temperatures (450 °C) and long residence times (> 10 h) under 1 bar of gaseous pressure were applied.

Task 5.3. Testing of carbon materials

The carbon materials produced from anthracene oil derived pitches in the preceding task were tested for their applicability as anode material in litium-ion batteries, as electrodes in electrochemical capacitors and for methane storage under elevated pressure.

Boronated graphitic carbons from P-1 pitch as anode in Li-ion cell.

The most relevant finding of the study can be summarized as follows. Boron, both nanocrystalline and amorphous, is a very effective catalyst of graphitization when it is heated at 2300^oC. However, voltammetry and galvanostatic experiments show no positive effect of boron on lithium insertion/deinsertion, whichever procedure is used. The most promising electrochemical characteristics – a high reversible capacity X_{rev} =0.83 and a low irreversible capacity X_{irr} = 0.10 are show by pure graphite which is produced by heat-treatment at 2900^oC followed by post-treatment in hydrogen.

Evaluation of electric capacitance properties of anthracene oil derived porous carbons

The materials selected for testing as electrodes in a capacitor system were activated carbons with a tailored porous texture and activated carbons enriched in nitrogen using different procedures. The measurements of the electric charge accumulation were performed with 1 M H_2SO_4 and 6 M KOH as electrolyte using voltammetry, galvanostatic charge/discharge and impedance spectroscopy methods.

Our study demonstrates that anthracene oil derived pitch can be successfully used as a precursor of porous carbons and it is suitable for application as an electric capacitor. High gravimetric capacitance (up to 290 F/g) and a good behaviour under a high current load discriminate KOH activated carbon with a BET surface area in the range of 1500-2000 m^2/g which is produced from pitch coke pre-treated about 650^oC in terms of performance as electrode material. Ammonization has a harmful effect on electrochemical performance, probably due to the reduction in pseudocapacitance, resulting from the removal of oxygen groups. The effect is in a part only compensated by nitrogen generated pseudocapacitance. Amongst the routes tested for producing nitrogen enriched activated carbons the most promising seems to be the co-pyrolysis of pitch with preoxidized melamine due to its high potential for nitrogen enrichment. The drawback of using steam and CO_2 activated carbons from pitch/N-polymer blends is the rather moderate development of porosity (S_{BET} ~800 m^2/g).

Performance of monolithic methane adsorbents from pitch derived activated carbons

Monoliths made of activated carbon powder from P-4 semi-coke using polymeric binder, PFA and NOV, were assessed in terms of porous texture by applying N_2 adsorption at 77K (micro- and mesopores), mercury porosimetry (meso- and macropores) and capacity of methane adsorption under elevated pressure. Compared to the activated carbon powder the surface area and micropore volume of the monoliths were reduced by about 40% due to the presence of binder coke and micropore blockage. The characteristics of methane uptake at elevated pressure demonstrate that the best monolith performance is achieved using PFA binder and post-treatment under hydrogen to reduce surface polarity. Gravimetric adsorption expressed as mmol/g and volumetric storage capacity as V/V at 3.5 MPa amount to 10.2 mmol/g and 131 V/V, respectively. The results of the project reveal the feasibility of using KOH activated carbon produced from anthracene oil derived pitch for moulding monolithic gas adsorbents. It seems that optimization of the porosity of the powder material and the formation of

monolith to reduce microporosity blockage can result in an additional improvement of volumetric storage capacity.

Work Package 6. Modeling the process and scaling up the production of anthracene oil based pitches

As an essential step in scaling up the process for producing anthracene oil based pitches, INETI contributed to the know-how with experimental tests performed in batch mode. These experimental tests started with literature surveys to find out the best analytical methods for the characterization of anthracene oil, anthracene oil derived products and anthracene oil pitch. Additional information was collected to evaluate the best experimental conditions for converting anthracene oil into pitch. This survey gave rise to a set of experimental parameters that could be adjusted to optimize the quality of the obtained pitches. The experimental runs were made at atmospheric pressure in batch mode, with a lab-scale reactor, where possible, to adjust the initial amount of fuel, the reaction temperature, the reaction time and the flow rates of nitrogen and air used in the heating and reacting phases.

The quality of the products was evaluated according to the degree of similarity between the characteristics of each pitch and a sample of industrially produced pitch. The best adjustment corresponded to a pitch obtained at a reaction temperature of 275ºC, a run time of between 11 and 12 hours and an air flow rate of 0.30 g/min. The results also confirmed that small variations in the reaction parameters may affect pitch quality. The pitch softening point may also be altered making it unsuitable for the intended applications.

In the context of WP 6.1 INETI also carried out some modelling work using “FLUENT” computing package. This model included an accurate representation of both the physical process and the chemical reactions inside the reactor. It was possible to conclude from the model developed that the reaction occurs in a very short time and that due to the exothermal nature of the process it would be difficult to adjust the operating reactor conditions. The high velocity of the conversion reaction was found to be related to the higher temperatures found, by the model, in the injector area. There is a zone of high turbulence, with a noticeable release of energy, which, due to the high flow velocities involved in the process, allow the chemical species to be quickly mixed. It was possible to conclude from the model that this zone near the injector can be considered as a critical point in the whole reactor. Any changes due to the accumulation of residues on the injector or near the reactor walls could have a noticeable effect on the high turbulence zone, and therefore, a very negative impact on the whole process, with significant changes to the pressure and temperature profiles and a disruption of the flows of chemical species.

The model simulation included all the available data. However, a better validation could be achieved if internal values from a real system were included. The installation did not offer the possibility of acquiring data so as to obtain access to internal properties inside the reactor, especially near the injector area, e.g., temperature, pressure or gas composition. The best way to change the reaction of pitch production would be to change the air/anthracene oil ratio.

The industrial installation showed some problems after long operation times, which may be associated with the slow accumulation of solid pitches inside the reactor. It would be advisable to take periodic samples at different distances from the injector to evaluate the evolution of the reactor is performance over a period of time. The data thus gathered could be used to predict possible problems arising in process, allowing preventive measures to be taken regarding the temperature profile or air flow rates that would prevent a total shut-down of the pitch production process.

Scientific and technical description of the results

Objectives of the project

The overall objective of this project is the development of the technology and the establishment of optimal operating conditions for the efficient transformation of anthracene oil into pitch-like materials with appropriate properties for use as impregnant in the steel-making industry.

More specifically the following aspects are addressed:

- Acquisition of fundamental data on the air-blowing conditions of anthracene oil (temperature, residence time, air flow rate) for producing pitch-like materials with different compositions and different properties at laboratory scale.
- Modelling of the air-blowing with a view to obtain designing parameters for scaling up the process: mass balance, heat-flow changes, air-oil contact times, air-bubble size, sparger design. The model will be validated with results from the results.
- Assessment of benefits of anthracene oil based pitches in terms of environmental impact reduction.
- Examining the impregnating capability of the anthracene oil based pitches as a function of reaction conditions in order to design products with enhanced properties.
- Exploring the technical feasibility of using anthracene oil based pitches in specialty fields, such as high-modulus carbon fibres, and mesophase-based carbon materials for new generation lithium-ion batteries and supercapacitors.

Comparison of initially planned activities and work accomplished

In general terms, it can be said that the initially posed objectives have been reached. A set of pitches with different properties was obtained from anthracene oil by oxidative thermal condensation and subsequent thermal treatment. Preliminary analyses have shown that pitches, with reduced genotoxicity, can be applied as impregnation agents for graphite cathode blocks and also for the preparation of advanced carbon materials (e.g., carbon fibres and mesophase-based materials).

Modifications in the initially planned activities were due to the changes in the internal organization of Carbone Savoie (this enterprise was transferred from the Graftech group to the Alcan group). As a result of this, some of the activities programmed to be carried out in the Graftech headquarters had to be readapted. Anthracene oil pitches could not be tested for the industrial production of electrodes or the simulation of pinstocks. In compensation, Carbone Savoie tested anthracene oil pitches as possible binders for graphite electrodes, while IQNSA studied the possibility of introducing these pitches into the market.

The other activities planned at the initial stage have been successfully accomplished.

Description of activities and discussion

WORK PACKAGE 1. Project coordination

The coordination activities were focussed on the following points:

1. Organization of periodical meetings. The 'Kick-off' meeting was held at INCAR-CSIC (Oviedo-Spain, September 16th 2005). After this initial meeting, five semester meetings were held in the different places where the partners are located: Carbone Savoie (Lyon-France, March 2nd 2006), Wroclaw University of Technology (Wroclaw-Poland, September 28th 2006), Imperial College (London-UK, March 28th 2007), INETI (Lisbon-Portugal, October 4th 2007) and Industrial Química del Nalón, S.A. (Oviedo-Spain, June 5th 2008).

2. Selection and delivery of samples to each partner according to the sequence of steps shown in Table 1.1 and Figure 1.1.

3. Approval of an internal consortium agreement (a copy of it has been sent to the Commission).

4. Presentation of the state of progress of the project within the Spring-Meeting of the TG2 Commission Committee (Coal Preparation, Conversion and Upgrading). This meeting was held in Oviedo (Spain) on March 31st 2007.

5. In the last year of the project execution, Carbone Savoie (enterprise originally involved in the project on behalf Graftch) ceased to belong to the Graftech Group. This motivated some changes in the activities programmed to be carried out by CS, because some of them were to be done at the headquarters of Graftech in Parma (USA). Due to this, CS incurred a substantial reduction in the initially proposed budget. Nevertheless, anthracene oil-based pitches were tested by CS in order to prepare graphite electrodes.

6. Compilation of the information provided by partners for the elaboration of this final report.

Table 1.1. Identification of the samples prepared by IQNSA and distributed among the other partners.

Sample	Identification	Addressee
Parent Anthracene Oil	AO-1	CSIC/ICSTM/INETI
1st Cycle Reaction Product	RP-1	CSIC/ICSTM/INETI
1st Cycle Pitch	P-1a P-1b	CSIC/ICSTM/WUT/INETI CSIC/ICSTM/WUT/CS
1st Cycle Unreacted Fraction = 2nd Cycle Feedstock	AO-2	CSIC/ICSTM
2nd Cycle Reaction Product	RP-2	CSIC/ICSTM
2nd Cycle Pitch	P-2	CSIC/ICSTM/WUT/CS
2nd Cycle Unreacted Fraction = 3rd Cycle Feedstock	AO-3	CSIC/ICSTM
3rd Cycle Reaction Product	RP-3	CSIC/ICSTM
3rd Cycle Pitch	P-3, P-3a P-3b	CSIC/ICSTM/WUT/CS CSIC/ICSTM/WUT/CS
3rd Cycle Unreacted Fraction	AO-4	CSIC/ICSTM
4th Cycle Reaction Product	RP-4	CSIC/ICSTM
4th Cycle Pitch	P-4, P-4a P-4b	CSIC/ICSTM/WUT/CS CSIC/CS
4th Cycle Unreacted Fraction	AO-5	CSIC

P-X and P-Xa are the same pitch but produced in different batches.

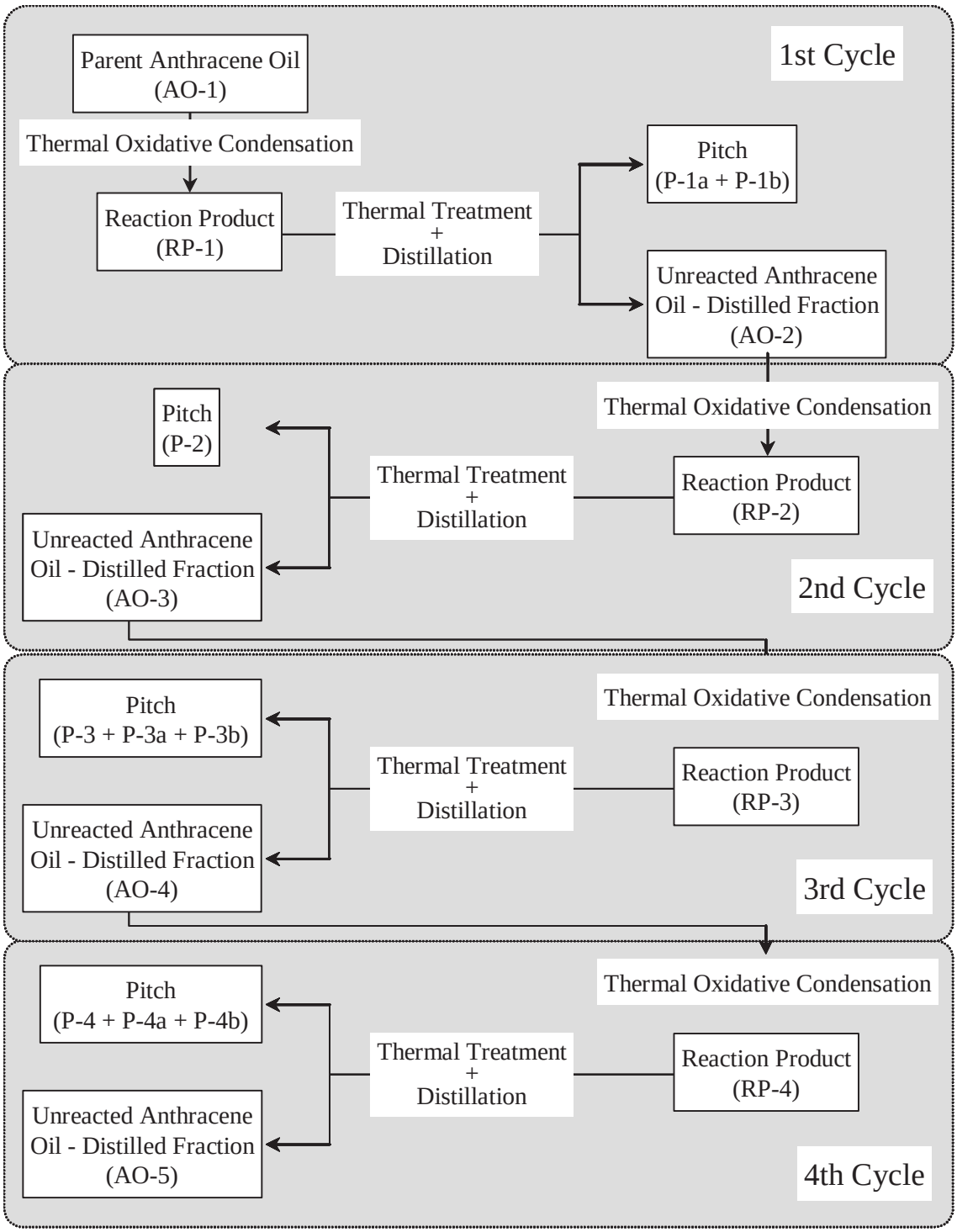

Figure 1.1. Sequence of steps followed for the preparation of pitches from anthracene oil by thermal oxidative condensation.

WORK PACKAGE 2. Processing of anthracene oil at laboratory scale

This work package involved the selection, characterization and processing of anthracene oil in order to prepare the pitches. The processing included oxidative thermal treatment to promote the polymerization/condensation of the anthracene oil components. The resultant reaction product was then thermally treated in order to remove any oxygen and redirect the polymerization towards the formation of condensed structures. This was followed by a distillation step in order to adjust the softening point of the pitch. The partners involved in this work package were INCAR-CSIC (CO-1), ICSTM (CR-2), IQNSA (CR-4) and Carbone Savoie (CR-5). The ICSTM contribution to this Work Package was related to the characterization of the feedstocks by means of different advanced analytical techniques. These techniques included size exclusion chromatography (SEC), UV-Fluorescence spectroscopy (UV-F), laser desorption-mass spectroscopy (LD-MS), Nuclear Magnetic Resonance (NMR) and Fourier transform Infra-red spectroscopy (FT-IR). The results from these analyses are shown in the description of WP3 in order to facilitate comparison between the various reaction products obtained from the process, including the pitches. Likewise, the contribution of Carbone Savoie (CR-5) to this work package was specifically made in WP 4.

Task 2.1. Selection and preliminary characterization of the anthracene oil (IQNSA)

Molecular weight distribution analysis and distillation profile have been used to characterize anthracene oil and the results are summarized in Table 2.1. Some elemental analysis and crystal point values are also reported. These are the critical parameters to control the reaction.

After producing the pitch by thermal treatment and distillation, the un-reacted anthracene oil is very similar in chemical nature to the parent one but slightly different in terms of its distillation profile and molecular weight distribution. This anthracene oil was suspected to be also a good raw material to improve the global yield of the reaction.

According to these results IQNSA developed some additional trials, feeding the reactor with the un-reacted anthracene oil in several stages.

Even thought the un-reacted product has similar physical and chemical characteristics regarding to distillation profile and molecular weight distribution, its behaviour during reaction is clearly different. The un-reacted anthracene oil differs in its reactivity because the reactive components are progressively exhausted, as it is shown by the increase of the crystal point. This means that concentration in anthracene and phenanthrene (less reactive components) is progressively increasing. Because of that it was needed a higher reaction temperature in order to get the same yield (about 20-25 ºC per cycle) but with the same air ratio.

The different anthracene oils mainly differ in their distillation profiles. However, minor influence in the pitch yield was observed but never pitch quality was affected. The analyses shown in Table 2.1 correspond to the average values.

The residual anthracene oil properties (AO5) indicates that it is still suitable for further reaction, but IQNSA considered not to proceed with the fifth cycle because of the following arguments,

- The crystallizing point of the anthracene oil obtained in each cycle is progressively increased, being AO5 the limit to meet the specification for carbon black feedstock purposes. Higher crystallizing point would not allow the product to be commercialised and would generate a residue which imbalance the economy of the process.
- The remaining anthracene oil represents only 40% of the initial one. The recovery of the additional 20% (8%) has no economical sense in terms of the supplementary investment needed in the industrial plant.

- The higher reaction temperatures the process needs to generate the small extra pitch increases the plant maintenance cost, it is not possible to work in large campaigns because of pipes blocking due to soot generation.

Table 2.1. Analytical comparison of different cycle raw materials.

Anthracene Oil (original; #1)
Project reference: AO-1
Mol. Weight: 235 uma
Crystal Point: 53 ºC
C/O: 99,62

Distillation profile (TGA)

T ºC	%
100	99,75
125	99,25
150	98,12
175	95,98
200	91,69
225	83,88
250	71,74
275	56,37
300	38,62
325	22,25
350	8,41
375	3,12

Un-reacted Anthracene Oil #2
Project reference: AO-2
Mol. Weight: 229 uma
Crystal Point: 74 ºC
C/O: 87,39

Distillation profile (TGA)

T ºC	%
100	99,83
125	99,36
150	98,07
175	95,24
200	90,15
225	81,88
250	69,29
275	51,79
300	32,18
325	12,27
350	2,91
375	2,08

Un-reacted Anthracene Oil #3
Project reference: AO-3
Mol. Weight: 220 uma
Crystal Point: 82 ºC
C/O: 81,95

Distillation profile (TGA)

T ºC	%
100	99,76
125	99,12
150	97,49
175	94,36
200	89,18
225	80,66
250	67,52
275	49,07
300	26,79
325	5,47
350	1,42
375	1,30

Un-reacted Anthracene Oil #4
Project reference: AO-4
Mol. Weight: 211 uma
Crystal Point: 86 ºC
C/O: 69,61

Distillation profile (TGA)

T ºC	%
100	99,64
125	98,59
150	95,77
175	90,35
200	82,61
225	72,50
250	59,97
275	44,62
300	21,76
325	4,06
350	1,06
375	0,88

Un-reacted Anthracene Oil #5
Project reference: AO-5
Mol. Weight: 211 uma

Distillation profile (TGA)

T ºC	%
100	99,75
125	99,03
150	97,02
175	92,94
200	86,77
225	77,51
250	63,83
275	44,71
300	21,05
325	1,85
350	0,76
375	0,69

Task 2.2. Air-blowing of anthracene oil under different experimental conditions (IQNSA)

The global process for the transformation of anthracene oil into pitch involved two consecutive steps: (i) oxidative treatment of the anthracene oil with air at moderate temperatures (250-310 °C) and (ii) thermal treatment of the resultant reaction product in an inert atmosphere (375-400 ºC) and subsequent distillation (preferable under vacuum) to obtain a pitch with the desired softening point (90 and

110 °C). Although these two steps are crucial in the transformation of the anthracene oil, the first one seems to be the most relevant. For this reason, the operational parameters for an appropriate polymerization of the anthracene oil with air were widely studied. Special emphasis was put on final temperature, air pressure and sample/air ratio.

The reactions have been carried out under different process conditions trying to establish the best parameters in terms of yield, pitch quality and plant productivity. Different batches of produced anthracene oil were also studied to see the influence of the starting raw material. Table 2.2 summarizes the optimised process conditions for the four cycles that makes the pilot plant work in large campaigns (above 45 days) with an acceptable pitch yield (above 20%) and with the best pitch quality.

Table 2.2. Optimised process conditions.

Anthracene Oil flow rate:		800-1000	kg/hour
Air ratio:		0,15-0,18	kg/kg Anthracene Oil
Inlet pressure:		10-11	bar g
Outlet pressure:		> 2,5	bar g
Inlet temperature:	Cycle 1	250-255	ºC
	Cycle 2	270-275	ºC
	Cycle 3	290-295	ºC
	Cycle 4	305-310	ºC

Task 2.3. Distillation of air-blown anthracene oil (IQNSA)

After the oxidative treatment, the resultant reaction product was thermally treated (see task 2.4) and then distilled to obtain pitches with a softening point of 90 and 110 °C, which were characterized according with the standards for impregnating and binder coal-tar pitches. Table 2.3 and Table 2.4 summarize the main characteristics of these pitches in comparison with standard binder and impregnating carbochemistry pitches. Also, information about parents RP production conditions, pitch distillation conditions and yields is included.

Table 2.3. Binder anthracene oil pitch quality.

		Std	**AO (P-1a)**	**AO (P-2a)**	**AO (P-3)**	**AO (P-3a)**	**AO (P-4)**	**AO (P-4a)**	**AO (P-4a) #2**
S.P	ºC, Mettler	110	110	112	112	113,4	112	114,5	108
TI	%	30	23-25	26,2	30,1	28,7	24	25,8	27,5
QI	%	9,5	0,3	0,6	0,7	1,0	0,4	0,4	0,6
Carbon Value	%Sers	53,8	45-46	48,1	47,2	47,1	46,3	46,3	44,5
Wetting	ºC	135	135-137	145	141 (50%)	155	145 (30%)	145 (30%)	
S	%	0,5	0,5	0,5	0,5	0,5	0,5	0,5	
Mol. Weight	uma	850	1100-1300	1285	1533	1500	1757	1750	
B[a]P equiv	***mg/g***	***28,2***	***30-32***	***17,9***	***13,3***	***9,0***	***10,3***	***9,9***	
B[a]P	***mg/g***	***10,8***	***13-14***	***6,2***	***3,8***	***1,7***	***2,7***	***2,2***	
Flash Point	ºC								
Filtration Rate	g								
Temperature	ºC		250	270	290	290	305	305	305
Air Ratio	kg/kg AO		0,18	0,18	0,18	0,16	0,18	0,15	0,15
Distillation conditions		Std	Std	Std	Std	TT +1h +5ºC	Std	Lab from P4-b	Lab from P4-b
Yield	%		23,6	21,3	16,2	19,2	19	17	17
Total Yield	%		23,6	39,9	49,6	51,4	59,2	59,7	59,7

AO: Anthracene Oil Pitch (in brackets the reference for the project)

Std: Standard Carbochemical Pitch

Table 2.4. Impregnation anthracene oil pitch quality.

		Std	AO (P-1b)	AO (P-3b)	AO (P-4b)
S.P	ºC, Mettler	90	90	90,3	88,6
TI	%	17,4	20-22	23,1	20,8
QI	%	1,3	0,3	0,5	0,4
Carbon Value	%Sers	40,6	39-40	41,4	38,7
Wetting	ºC				
S	%	0,5	0,5	0,5	0,5
Mol. Weight	uma	710	1000-1100	1350	1700
B[a]P equiv	***mg/g***	***25,5***	***30,4***	***13,5***	***10,7***
B[a]P	***mg/g***	***12,8***	***13-14***	***3,4***	***2,3***
Flash Point	ºC	270	240-250	240-250	240-250
Filtration Rate	g	17,8 (80 min)	60 (48-50 min)	22,5 (80 min)	25,7 (80 min)
Temperature	ºC		250	295	305
Air Ratio	kg/kg AO		0,18	0,15	0,15
Distillation conditions		Std	TT +1h +5ºC	TT +1h +5ºC	TT +1h +5ºC
Yield	%		23,1	21	17
Total Yield	%		23,1	52,2	60,3

AO: Anthracene Oil Pitch (in brackets the reference for the project)

Std: Standard Carbochemical Pitch

The B[a]P content diminishes markedly after each cycle, showing an almost linear trend with respect pitch yield. Besides these pitches keep the good properties for binding and impregnating purposes but lose wettability/filtering capacity after consecutive cycles. Nevertheless pitches still maintain enough rheological capacity to be considered as an appropriate carbon precursor. Such rheological behaviour suggested the necessity to study different carbon materials applications (not only carbon fibres), where global mechanical properties are more interesting than local ones.

Task 2.4. Thermal treatment of oxidized anthracene oil (IQNSA, INCAR-CSIC)

Thermal treatment was a critical stage in the production of anthracene oil based pitches as the presence of cross-linked structures needed to be reduced.

This thermal treatment was carried out at a higher temperature in order to favour condensation reactions and the cleavage of side-chains and naphthenic bridges. In addition, temperatures above 350 ºC (free radical minimum formation temperature) promoted the formation of planar molecules and the release of oxygen from the pitch structures.

This intermediate inert atmosphere thermal treatment needed also to be enhanced cycle-by-cycle, because the cross-linked structures generated are more stable (they were also created at higher temperatures). Increasing cycle number generates un-reacted anthracene oil with higher oxygen concentration (Table 2.1). These oxygen compounds promotes the generation of cross-linked structures during the reaction stage.

Moreover, high temperatures for the inert thermal treatment caused the molecular weight distribution to narrow at the same conversion ratio, which favoured the future commercial quality of the pitch and enhanced the chemical characteristics of the un-reacted anthracene oil.

On the basis of the results obtained from the characterization and pyrolysis behaviour of the anthracene oil derived samples (Task 3.1 and Task 3.2), the reaction product obtained in the first cycle of anthracene oil processing (RP-1) was thermally treated in order to produce mesophase suitable for the preparation of advanced carbon materials. This task was carried out by INCAR-CSIC. Initially, an exhaustive study of the operational parameters for the conversion of RP-1 into mesophase was carried out. To this end, several treatments under different experimental conditions were performed in order to assess the effect of temperature, soaking time and pressure on the quality and quantity of the resultant mesophase (Table 2.5). The original procedure involved three steps: (i) thermal treatment to favour polymerization and to assist in the establishment of a pre-graphitic-order necessary for the formation of mesophase. This treatment was performed in an inert atmosphere (nitrogen) under a pressure of 10 bar;

Table 2.5. Summary of experimental conditions tested for the preparation of mesophase from RP-1.

Test	Treatment-1	Treatment-2	Sedimentation	PY	SP	Meso
1	450°C, 3h, 5bar	450°C, 3.50h	420°C, 1h	10.0	237	3.0
2		450°C, 4h		26.0	268	8.0
3		450°C, 4.25h		19.0	331	9.0
4		450°C, 4.50h		12.8	>350	12.8
5	450°C, 3.25h, 5bar	450°C, 4h		12.0	348	11.5
6	450°C, 3.50h, 5bar	450°C, 4h		12.5	>350	12.0
7	450°C, 3.50h, 5bar	450°C, 4.50h		15.6	> 350	15.6

PY, global process yield (wt.%)
SP, Mettler softening point (°C)
Meso, mesophase yield (wt.%)

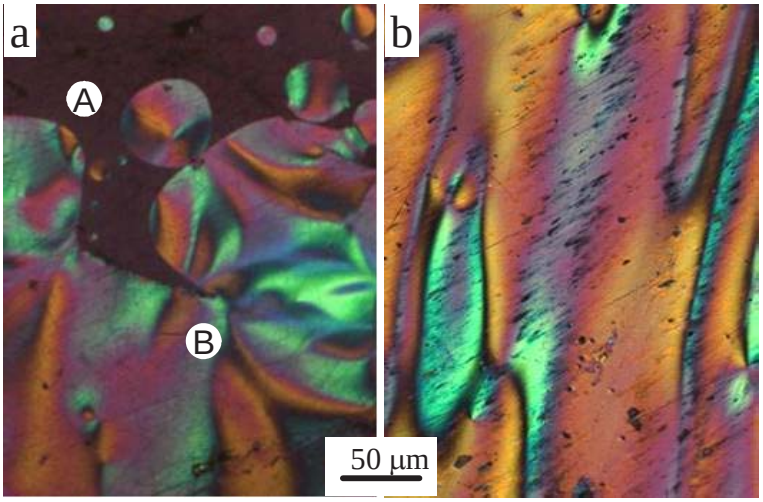

Figure 2.1. Optical microscopy of reaction product RP-1 after (a) thermal treatment and (b) sedimentation.

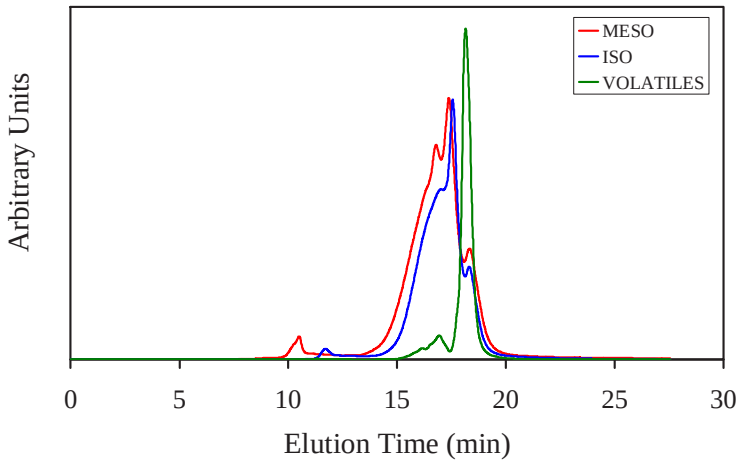

Figure 2.2. SEC profiles of the mesophase, isotropic phase and volatiles.

(ii) a second thermal treatment, in the absence of pressure, which was aimed at a higher formation of mesophase (Figure 2.1) and the removal of unreactive volatiles; and (iii) hot sedimentation to separate the polymerized product (isotropic phase at the top of the reactor, Figure 2.1a, position A) from the mesophase (anisotropic phase at the bottom of the reactor, Figure 2.1a, position B). This separation step results in a material, which consists of ~ 95-100 vol.% of mesophase (Figure 2.1b).

Table 2.6. Main characteristics of the mesophases and intermediate products obtained during the preparation of the carbon fibre precursors from RP-1.

Sample	Elemental analysis (wt.%)					NMPI	SP
	C	H	N	S	O		
Meso-1	94.3	3.7	1.0	0.3	0.7	28	235
Iso-1	93.8	3.7	1.0	0.4	1.1	12	135
Meso-2	94.1	4.2	0.8	0.3	0.6	25	227

NMPI, N-methyl-2-pyrrolidinone insoluble content (wt.%)
SP, Mettler softening point (°C)

An important feature of this study was the release of pressure after the first step because this affected the amount of volatiles in the reaction media, and consequently, the fluidity and softening point of the mesophase. These were crucial parameters that determined the future applications of the mesophase.

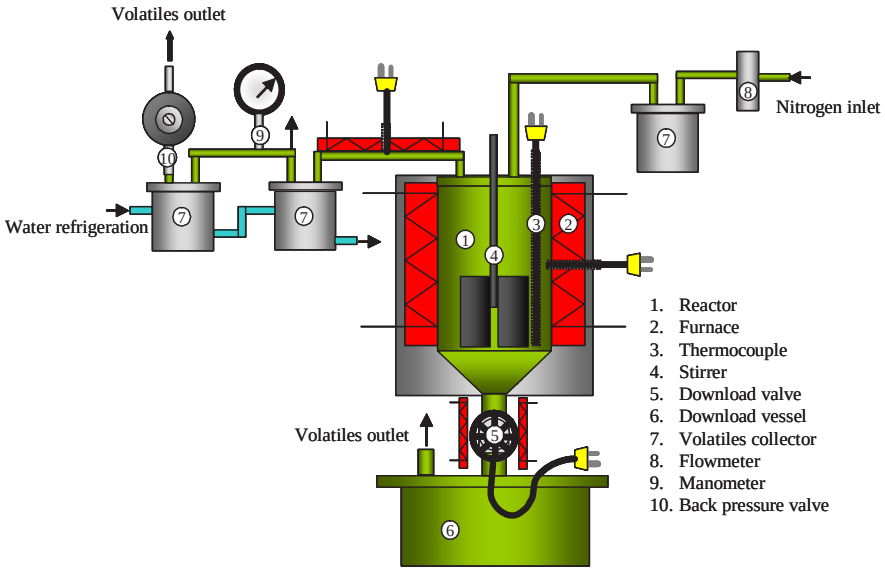

Figure 2.3. Schematic illustration of the equipment used for the processing of the anthracene oil-based samples.

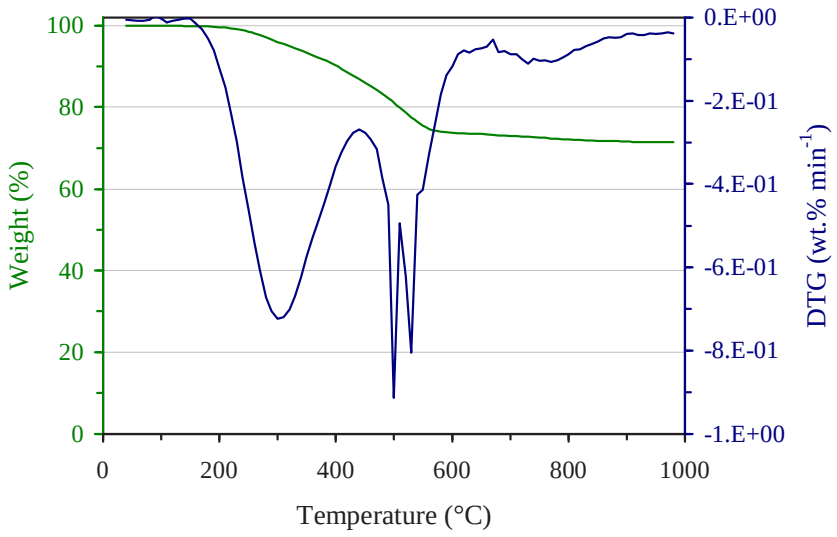

Figure 2.4. TG and DTG curves of the mesophase from RP-1.

The presence of these volatiles was a key factor in the development of mesophase because they not only contributed to form a more fluid system but they were also a source of hydrogen which facilitated polymerization reactions. Some of the parameters used to monitor the presence of volatiles in the mesophase and to determine the optimal operational conditions for the production of suitable mesophase from RP-1 at laboratory scale were the reaction yield, the mesophase yield and the softening point. Additionally, the SEC profiles of the volatiles, isotropic phase and mesophase (Figure 2.2) provided valuable information for establishing the most appropriate conditions for mesophase preparation. After several studies the optimum operational conditions for the production of mesophase from RP-1 at laboratory scale were established: (i) thermal treatment at 450 °C for 3 h under a dynamic pressure of 5bar, (ii) a second treatment in which the pressure was reduced to atmospheric pressure and the reaction product from the first treatment was thermally treated at 450 °C for 3.5 h, (iii) and finally,

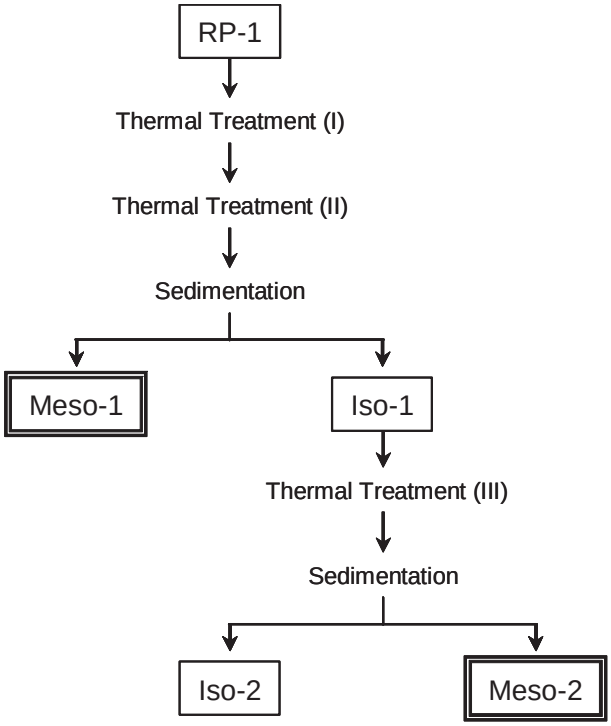

Figure 2.5. Sequence of steps followed for the preparation of Meso-2.

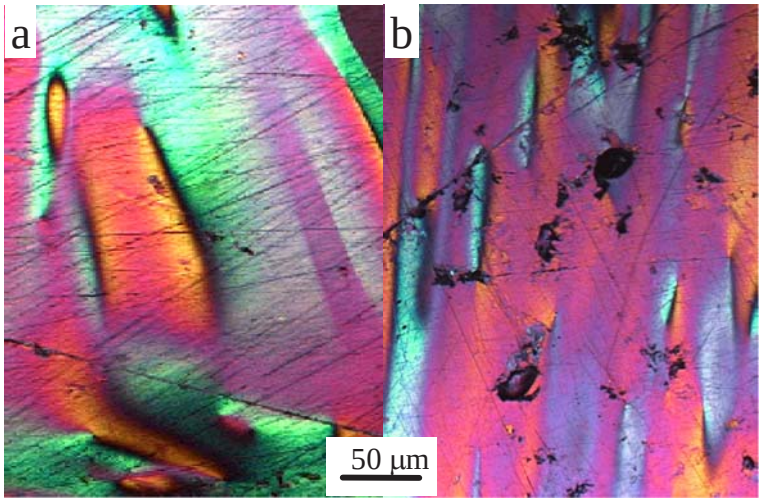

Figure 2.6. Optical microscopy of (a) Meso-1 and (b) Meso-2.

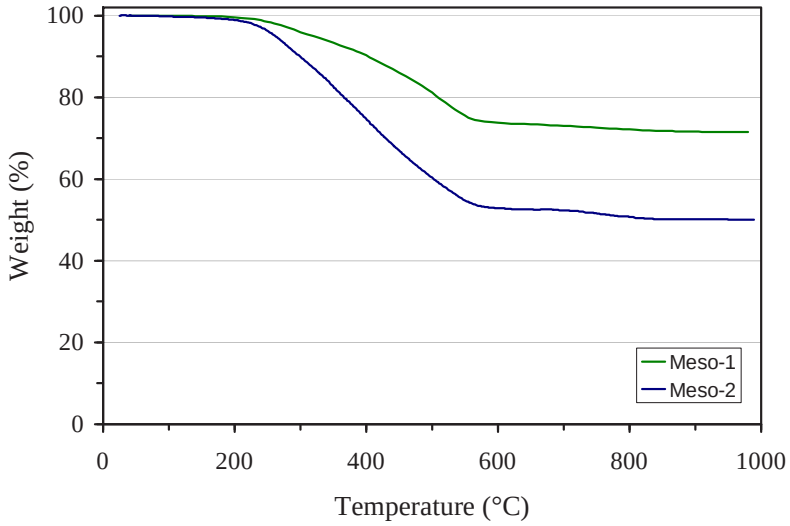

Figure 2.7. TG curves of Meso-1 and Meso-2.

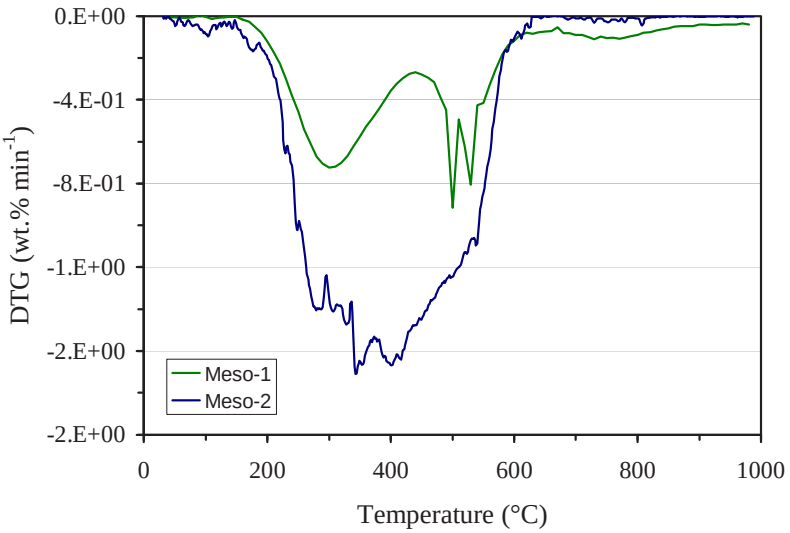

Figure 2.8. DTG curves of Meso-1 and Meso-2.

sedimentation at 420 °C for 1 h. Once these conditions were defined, the autoclave was modified and adjusted to allow the three steps to be performed consecutively in one single batch (Figure 2.3), thus enabling to produce enough mesophase enough to prepare carbon fibres. Following this procedure a material consisting of 99-100 vol.% of mesophase was obtained (Meso-1). Table 2.6 summarizes the main characteristics of this mesophase. The process yield (RP-1 to mesophase) was ~20 wt.%, consisting mainly of carbon (94.3 wt.%) and, to a lesser extent hydrogen (3.7 wt.%). The pyrolysis behaviour of the different samples generated during the transformation of RP-1 into mesophase shows that polymerization occurs in all the steps. As a result not only was there a decrease in weight loss but also a modification of the way in which the samples lost weight (Figure 2.4).

Despite having such promising properties, using this mesophase to prepare carbon fibres afforded poor results. The spinning of the mesophase into fibres encountered the problem that the viscoelastic behaviour of the mesophase at spinning temperature was not suitable for this purpose. Although the mesophase was successfully spun into fibres, these were not uniform in diameter. Moreover, the spinning temperature had to be constantly increased so that extrusion could be maintained. As a

consequence of this, spinning was found to be unfeasible in this case. Further studies carried out with this mesophase showed the inconsistency of the sample. In fact, the different reactivities of the anthracene oil components led to the rapid polymerization of the most reactive compounds, while the less reactive underwent polymerization to a lesser extent. The result was a sample in which fresh mesophase coexisted with hardened mesophase (even semi-coke).

Based on this hypothesis, some modifications in the procedure of mesophase preparation were introduced (Figure 2.5). These modifications were aimed at eliminating the most reactive compounds that seemed to be responsible for the formation of heterogeneous mesophase. For this reason, the isotropic phase (Iso-1) obtained during the formation of Meso-1 was thermally treated at 450 °C for 2 h and subsequent sedimentation at 420 °C for 1 h to produce a new mesophase (Meso-2), with a process yield of ~ 18 wt.%. The main characteristics of this mesophase are highlighted in Table 2.6. The elemental composition, NMP solubility and softening point are similar to those of Meso-1. Similarly, the microstructure of Meso-2, observed under the optical microscope, is almost identical to that of Meso-1 (Figure 2.6. However, the pyrolysis behaviour, studied by thermogravimetric analysis, as revealed that the degree of polymerization reached by Meso-2 is lower than in Meso-1 (Figures 2.7 and 2.8). In fact, the thermogravimetric curve of the new mesophase is below of that of Meso-1 throughout the entire temperature range of weight loss.

Work Package Conclusions

An optimum process for the transformation of anthracene oil into pitch by means of oxidative treatment, thermal treatment and distillation was developed.

According to the characterization performed, the unreacted anthracene oil obtained from the production of the pitch is of good enough quality to be used as raw material for further reaction. In addition four cycles can be performed with good results by increasing the reaction temperature to 25 ºC per cycle in order to obtain same yield with the same air ratio.

The pitches obtained promise good results for many reasons. Their impregnating capacities are greater than those of standard coal-tar pitches and their carcinogenic potential has been reduced drastically with the successive cycles of production.

For binder purposes the key factor is the primary QI, so blends with standard coal tar pitches are necessary in order to achieve optimum primary QI levels. According to the genotoxicity index, these blends can be expected to reduce their carcinogenic potential significantly.

After several consecutive cycles the pitches retain good properties for binding and impregnating purposes but they lose wettability/filtering capacity. Moreover their B[a]P content diminishes markedly.

Mesophase and cokes with different optical textures can be obtained by thermal treatment. Thermal treatment led to partially anisotropic pitches in which mesophase could be selectively separated by hot sedimentation. In this regard, the reaction product from the first cycle of anthracene oil processing (RP-1) proved to be the most adequate for this purpose. Although carbon fibres could be obtained from the anthracene oil derivatives, multiple and complex steps were necessary to prepare a spinnable mesophase.

WORK PACKAGE 3. Characterization and evaluation of the genotoxicity of anthracene oil based pitches

This work package included a detailed structural characterization of the samples obtained during the anthracene oil processing. Special attention was paid to the study of the genotoxicity of the pitches with a view to using them as impregnating agents in the preparation of graphite electrodes. The partners involved in this work package were INCAR-CSIC (CO-1), ICSTM (CR-2) and IQNSA (CR-4).

Task 3.1. Chemical characterization (INCAR-CSIC, ICSTM, IQNSA)

INCAR-CSIC carried out and exhaustive study of the elemental composition and main characteristics of the samples supplied by IQNSA. The main characteristics of these samples are summarized in Table 3.1. The parent anthracene oil (AO-1) is mainly composed of C and H and to a lesser extent of N, S and O. In general terms, it can be said that thermal oxidative condensation leads to the formation of reaction products (RP-1, RP-2, RP-3 and RP-4), whose main characteristic is the uptake of a certain amount of oxygen and the formation of moieties which are soluble in toluene and NMP, but which at the same time, may remain in the resulting coke (carbon yield between 6-8 wt.%). Most of the oxygen is subsequently lost in the transformation of the reaction product into pitch (P-1a, P-2, P-3a and P-4a). Moreover, this transformation involves the removal of unreactive anthracene oil (distilled fraction, AO-2, AO-3, AO-4 and AO-5) and a more acute polymerization of the components. In fact, the solubility parameters and carbon yield of the anthracene oil-based pitches are much higher than in the corresponding reaction products (Table 3.1). An important point to bear in mind is that the unreactive anthracene oil (distilled fractions) has an elemental composition similar to that of the parent anthracene oil. Nevertheless, gas chromatography studies revealed that components containing aliphatic hydrogen are preferentially consumed during the process. This means that the thermal reactivity of the feedstocks used in the subsequent cycles of anthracene oil processing decreased, making it necessary to use severer conditions in each consecutive processing cycle. The effect of this severity is patent in the characteristics of the pitches. As an example, the toluene-insoluble content follows the trend P-1 < P-2 < P-3, indicating that the severer reaction conditions lead to more condensed or cross-linked products. An exception is P-4 whose parameters do not follow the previous trend (Table 3.1), displaying values between P-1 and P-2. A possible explanation for this could be that the severity of the reaction led to

Table 3.1. Elemental composition and main characteristics of the samples.

Sample	Elemental Analisis (wt.%)					SP	TI	NMPI	CY
	C	H	N	S	O				
AO-1	92.0	5.6	0.9	0.5	1.0	-	0	0	0.0
RP-1	91.6	5.4	1.0	0.5	1.5	-	1	0	8.2
P-1a	93.3	4.5	1.1	0.5	0.6	112	23	3	59.9
AO-2	91.4	6.0	0.9	0.6	1.1	-	0	0	0.0
RP-2	91.6	5.6	0.9	0.5	1.4	-	0	0	7.7
P-2	93.3	4.3	1.1	0.5	0.8	127	31	10	55.0
AO-3	91.4	6.1	0.9	0.5	1.1	-	0	0	0.0
RP-3	91.5	5.5	0.8	0.5	1.7	-	1	0	6.1
P-3a	93.2	4.2	1.0	0.5	1.1	118	33	12	52.3
AO-4	91.7	5.7	0.6	0.6	1.4	-	0	0	0.0
RP-4	91.6	5.4	0.7	0.6	1.7	-	0	0	-
P-4a	92.4	4.5	0.8	0.5	1.8	116	29	10	51.0
P-4b	92.8	4.6	0.7	0.5	1.4	93	21	7	-
AO-5	91.4	5.6	0.7	0.6	1.7	-	0	0	0.0

SP, Mettler softening point (°C)
TI, toluene-insoluble content (wt.%)
NMPI, 2-methyl-N-pyrrolidinone-insoluble content (wt.%)
CY, Alcan carbon yield (wt.%)

moieties in which the oxygen content was too high to be subsequently lost, giving rise to large condensed structures. It might be inferred, therefore, that the fourth cycle of anthracene oil processing seems to be unnecessary. Additionally, the decrease in the carbon yield from P-1 to P-4 also points to the presence of a higher contribution of the cross-linking structures in P-4.

IQNSA was also involved in the development of simple and rapid techniques for the characterization of the anthracene oil based pitches. In this regard, IQNSA has proved that the thermogravimetric analysis is a powerful tool for establishing the capacity of the anthracene oil to generate pitch, just by its thermal behaviour. The tool includes database and software development. By a very quick thermo-gravimetric analysis it is possible to confirm the pitch yield at a certain softening point.

IQNSA also was involved in optimising the experimental conditions to provide and guarantee analyses of the toxicity of the pitches. In this sense IQNSA have been searching other possibilities than the present standards. It results in the development of a new method by high-performance liquid chromatography. It has been performed an inter-laboratory round robin to check IQNSA results. The conclusions indicate that IQNSA analyses are one of the most reliable in terms of repeatability and reproducibility. This technique try to diminish the effect of the high temperatures needed in the injector area working with a standard GC-MS; this technology is common used by outsourcing laboratories.

As indicated before (task 2.3), the results show that the different pitches produced are promising for many purposes. First cycle has an excellent impregnating behaviour that could results in a better impregnation performance or in improved impregnation productivity by diminishing time or impregnating temperature (this pitch has not any toxicity benefit).

Third cycle pitch has not the same rheological and impregnating capacities but still presents better properties than standard coal tar derived pitch. This pitch major advance is the great reduction in carcinogenic potentiality.

For binding applications within aluminium industry the use of anthracene oil pitches depends on the minimum primary QI they are able to work with. Blends with standard coal tar pitches can be performed for meeting the minimum QI that the process requires.

Although anthracene oil binder pitches present low carbon values, it is necessary to take into account their very low QI contents. Normalizing carbon value for the same QI content (QI is almost a net carbon) results in similar figures.

Completely different is the situation for the impregnating pitch. In this case pitch quality is improved by several times in terms of impregnating capacity (filtration rate), promoting higher productivity for customers and also improving their electrode quality.

To complement this characterization, ICSTM carried out a detailed study of the samples by different analytical advanced techniques. Initially, the samples were studied as bulk samples. However, in order to study in a greater depth the chemical composition of the samples and establish a more direct connection between the anthracene oil processing and sample characteristics, the samples were fractionated. The fractions were then characterized in a similar way to the bulk samples.

3.1.1. Analysis of the bulk samples

Size Exclusion Chromatography (SEC) Analysis

The SEC chromatograms of all samples from the first cycle, AO-1, RP-1, and P-1 are shown in Figure 3.1. The SEC chromatogram of AO-2 was found to be similar to that observed for AO-1. Analogous results showing similar trends for subsequent cycles have been obtained but are not shown. Some of these data has already been published[2].

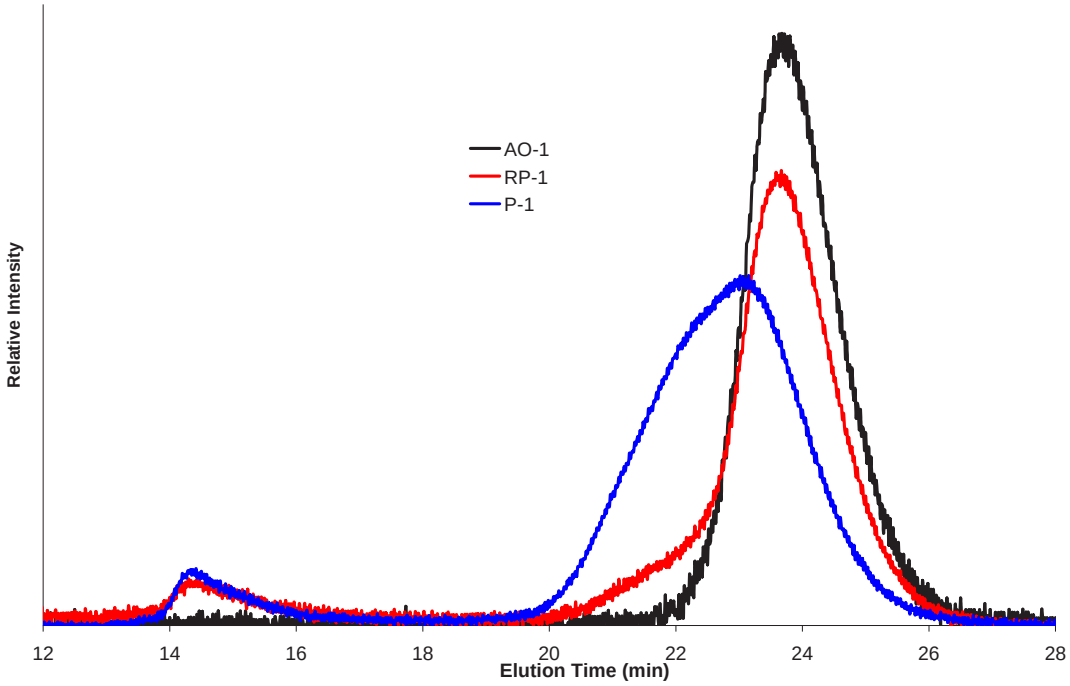

Figure 3.1. SEC chromatograms at 350nm, area normalised, of the samples from the first processing cycle: parent anthracene oil (AO-1), reaction product (RP-1) and pitch (P-1).

The SEC chromatograms of reaction products and pitches (Figures 3.3-3.4) all showed two significant differences in comparison with those of the parent anthracene oils (Figure 3.2). First, they showed bimodal size distributions. The peak at longer retention times consists of material resolved by the column ("retained peak"; 18-25 min), while the early-eluting peak ("excluded peak"; 10-18 min) represents material excluded from column porosity. A valley of nearly zero intensity separates the two peaks. This bimodal distribution is consistently observed in coal-derived samples[6,7]. Second, the resolved (later eluting) peak was observed to progressively shift towards shorter retention times (larger molecules) in the series anthracene oil, reaction products, pitches for each stage. According to a polystyrene (PS) calibration of the SEC column[6], the upper mass limits (early rising edge) of the retained peak in the pitch samples increases from about 4,000 to 7,000 u, from P-1 to P-4 (Figure 3.4). This general shift of the SEC chromatograms towards shorter elution times is consistent with the expected increase in the molecular sizes of the reaction products leading to pitch formation.

The relative intensities of the excluded peaks in the chromatograms were also observed to increase after each stage of the process. In Figures 3.1-3.4, the anthracene oils (AO-x) showed weak/low intensity excluded peaks, whilst the 'whole' reaction products (RP-x) and the corresponding pitches (P-x) showed a pronounced signal in the excluded region (14-16 min). The molecular mass range of the excluded region is thought not to be well represented by the polystyrene calibration[6]. According to this calibration, masses from 70,000 to several million units are predicted. It has been suggested, however, that the excluded material might instead correspond to material with spherical-like or globular conformations that would produce larger solution volumes than would be warranted by their molecular masses[6].

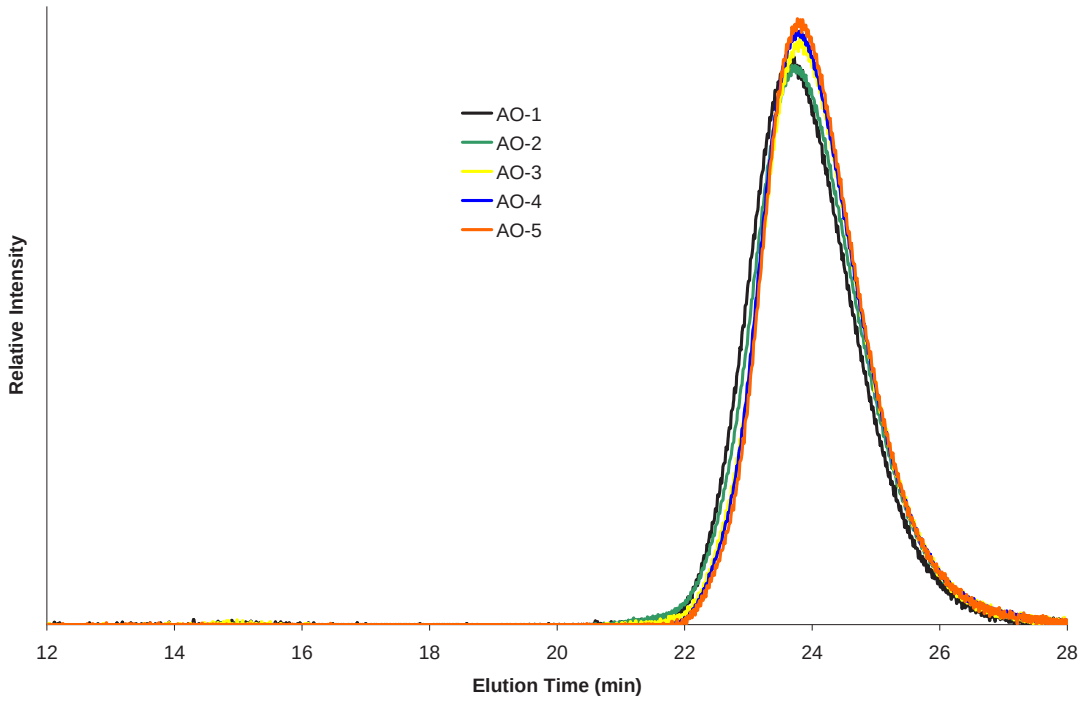

Figure 3.2. SEC curves at 300 nm, area normalised, of the anthracene oils AO-x obtained in the 1st (x=1), 2nd (x=2) , 3rd (x=3) and 4th (x=4) processing cycle of the anthracene oil.

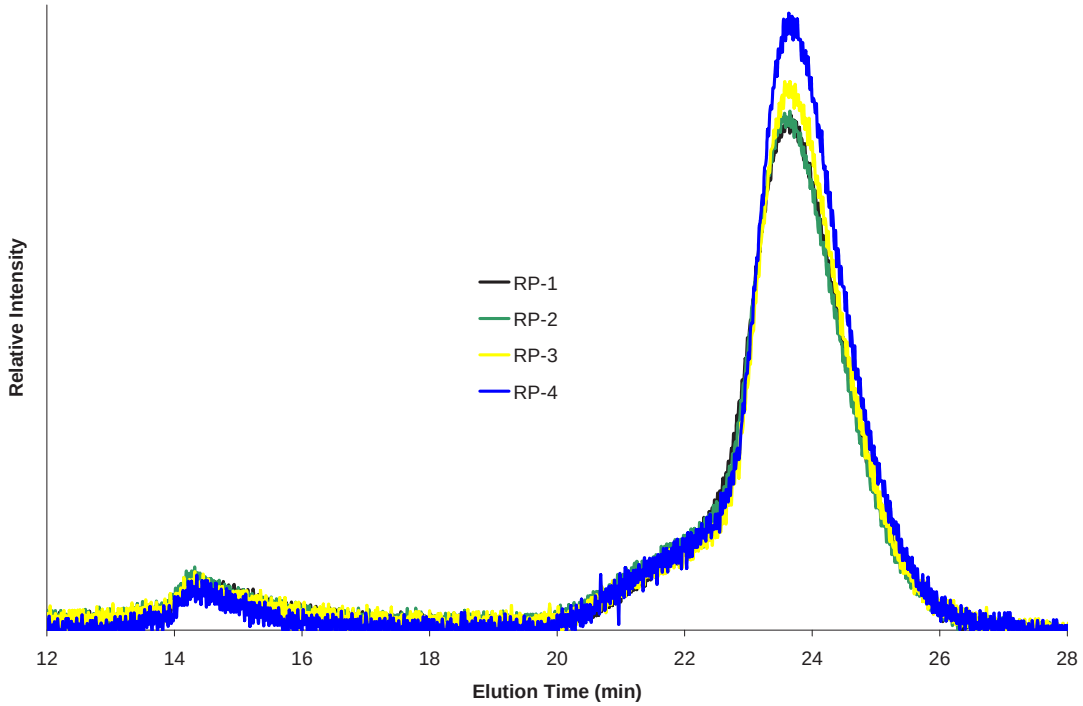

Figure 3.3. SEC curves at 350 nm, area normalised, of the reaction products, RP-x obtained in the 1st (x=1), 2nd (x=2) , 3rd (x=3) and 4th (x=4) processing cycle of the anthracene oil.

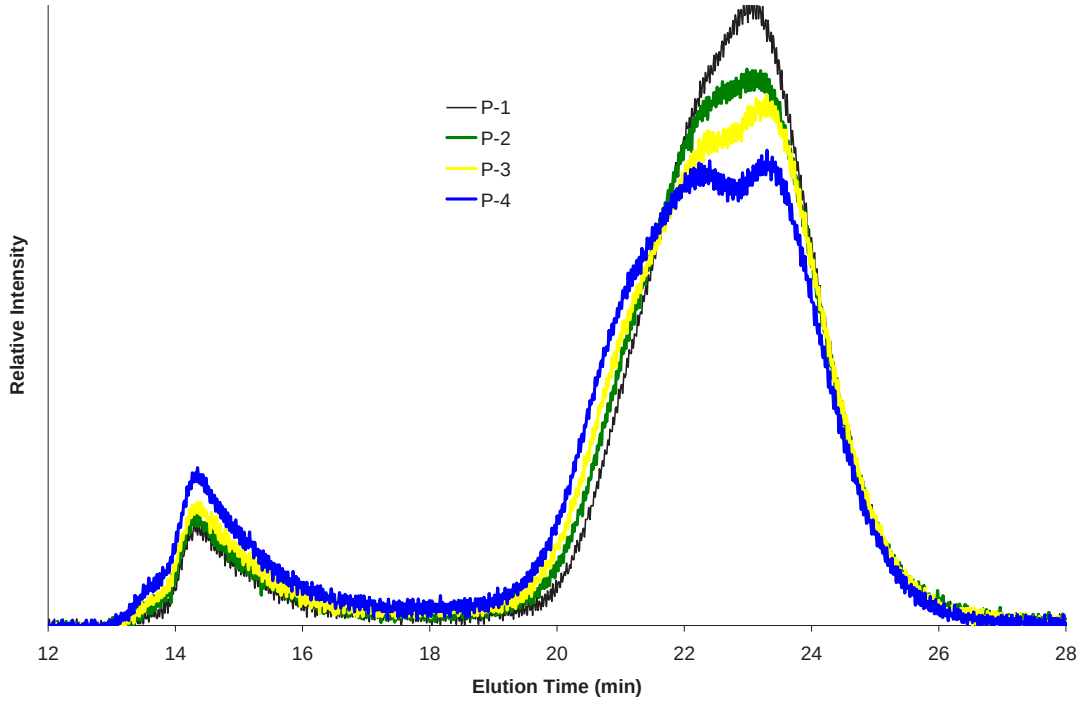

Figure 3.4. SEC curves at 350 nm, area normalised, of the pitches P-x (c) obtained in the 1st (x=1), 2nd (x=2) , 3rd (x=3) and 4th (x=4) processing cycle of the anthracene oil.

Further insight into the reaction process can be gained by comparing the SEC chromatograms of samples from equivalent stages of successive cycles. The anthracene oils (AO-x) are shown in Figure 3.2, the whole reaction products (RP-x) and the resulting pitches, (P-x), are shown in Figures 3.3-3.4 respectively. For the anthracene oils, a small shift to longer elution times (smaller molecules) was observed as the number of processing cycles increased. The anthracene oils showed only faint traces of signal in the excluded region.

The SEC chromatograms of the pitches (Figure 3.4) also exhibit differences. A shift towards shorter elution times (larger molecules) is observed in the retained region as the sample is taken through successive cycles of processing. Signal intensity in the excluded region also showed a clear trend in the order: P-4 > P-3 > P-2 > P-1. The chromatograms of the set of reaction products covered almost identical ranges in both the retained and excluded regions. The only difference between the RP-x samples was an increase in intensity of the lowest mass region of the retained peak as the number of cycles increases (Figure 3.3). This suggests that reactions with the oxygen also involved some cracking reactions, this later being more likely to occur under the more sever reaction conditions.

In summary, the SEC chromatograms showed the expected increases in the molecular size from the anthracene oils to their corresponding pitches. A clear trend of increasing molecular size was observed for the pitches produced from the later stages This indicates that samples were getting progressively heavier with the increasing severity of partial-oxidation and heat-treatment stages.

Ultraviolet Fluorescence (UV-F) Spectroscopy Analysis

Large shifts towards longer wavelengths have been observed in the UV-F spectra of pitches in comparison with those from the corresponding anthracene oils and reaction products. Figure 3.5 shows the UV-F spectra of the samples from the first cycle, AO-1, RP-1, P-1 and AO-2. Figures 3.6-3.8 present the results for samples from equivalent stages of different cycles, AO, RP and Pitches respectively. The UV-F spectra have been peak normalised.

The spectra point at the presence of larger aromatic groups in the pitches compared to the anthracene oils. This interpretation is reinforced by the lower fluorescence intensities exhibited by the pitch

samples. It is likely that similar large fused aromatic compounds are also present in the reaction products, but their presence would be masked by the presence in larger amounts of lighter material. Smaller molecules (carrying smaller polynuclear aromatic groups) are expected to fluoresce more intensely than the larger molecules and effectively mask signal from the larger molecules[7].

Comparison between the UV-F spectra of the AO-x samples, Figure 3.6, shows that all the anthracene oils exhibit fluorescence in the same regions of the spectrum. Differences in relative intensity are observed as the number of processing cycles increases, shifting towards shorter wavelengths (smaller polynuclear aromatic groups).

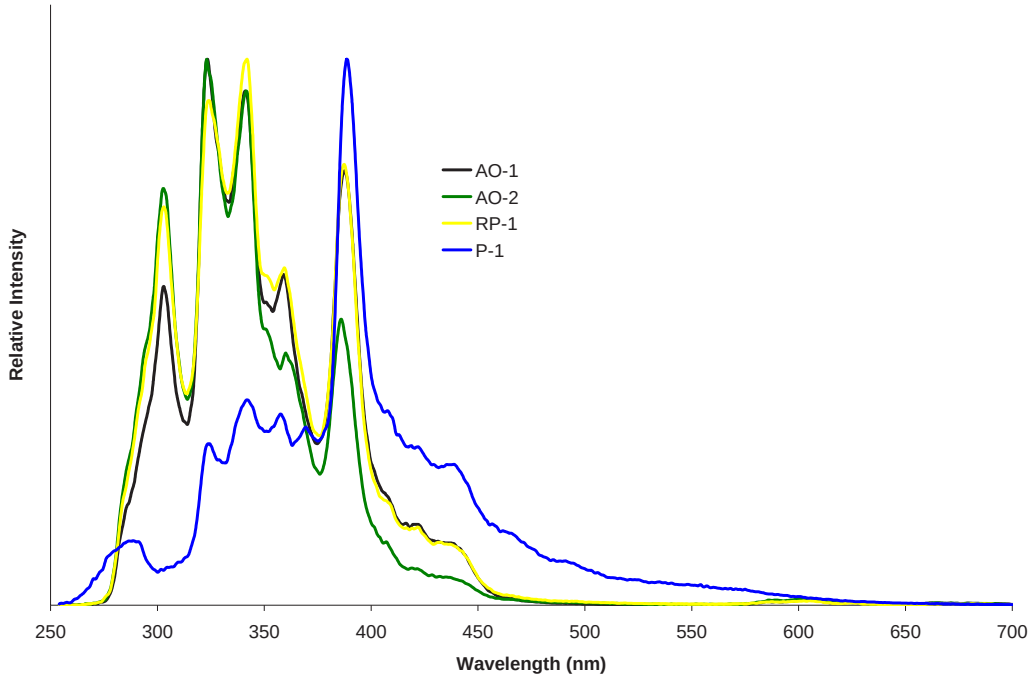

Figure 3.5. Peak normalised UV-F spectra of the samples from the first cycle: anthracene oil (AO-1), reaction product (RP-1), pitch (P-1) and the unreactive anthracene oil (AO-2).

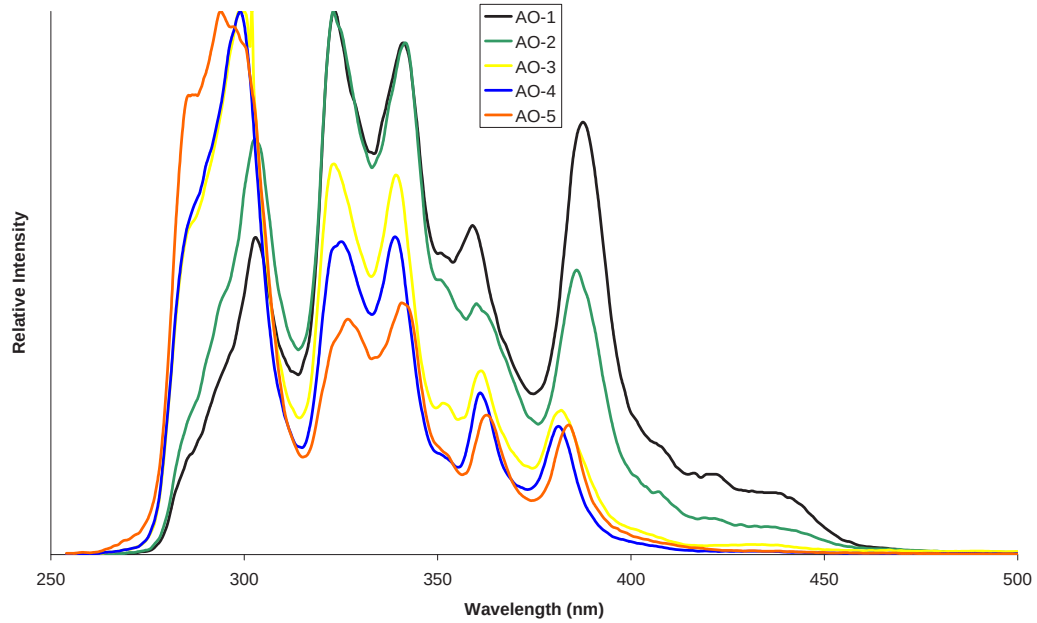

Figure 3.6. Peak normalised UV-F spectra of the anthracene oils AO-x obtained in the 1st (x=1), 2nd (x=2), 3rd (x=3) and 4th (x=4) processing cycle of the anthracene oil.

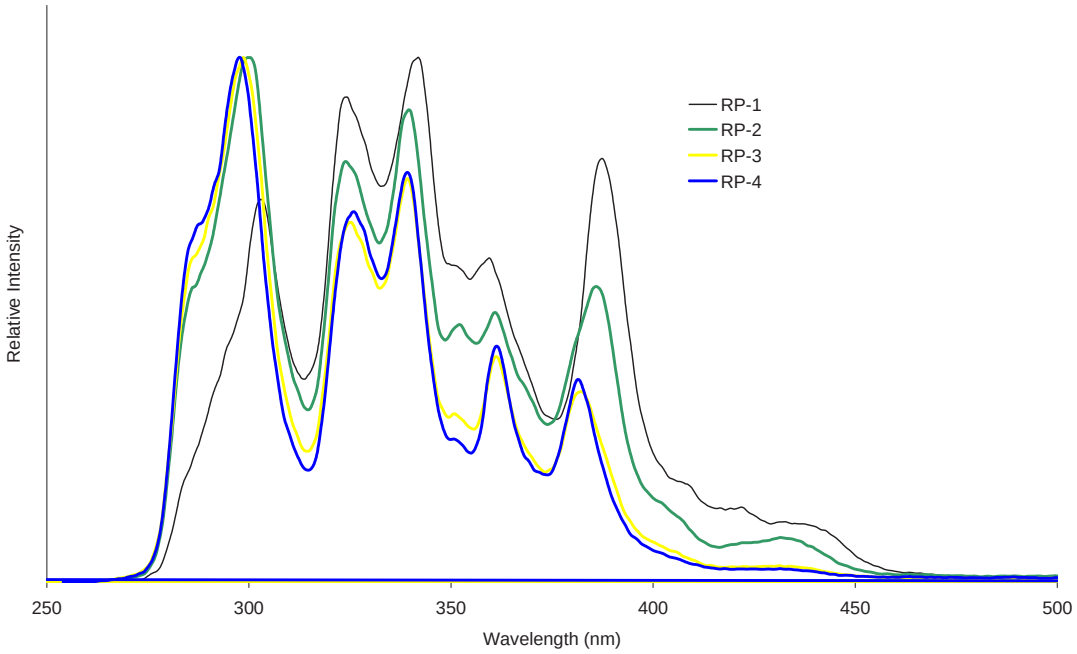

Figure 3.7. Peak normalised UV-F spectra of the reaction products RP-x obtained in the 1st (x=1), 2nd (x=2), 3rd (x=3) and 4th (x=4) processing cycle of the anthracene oil.

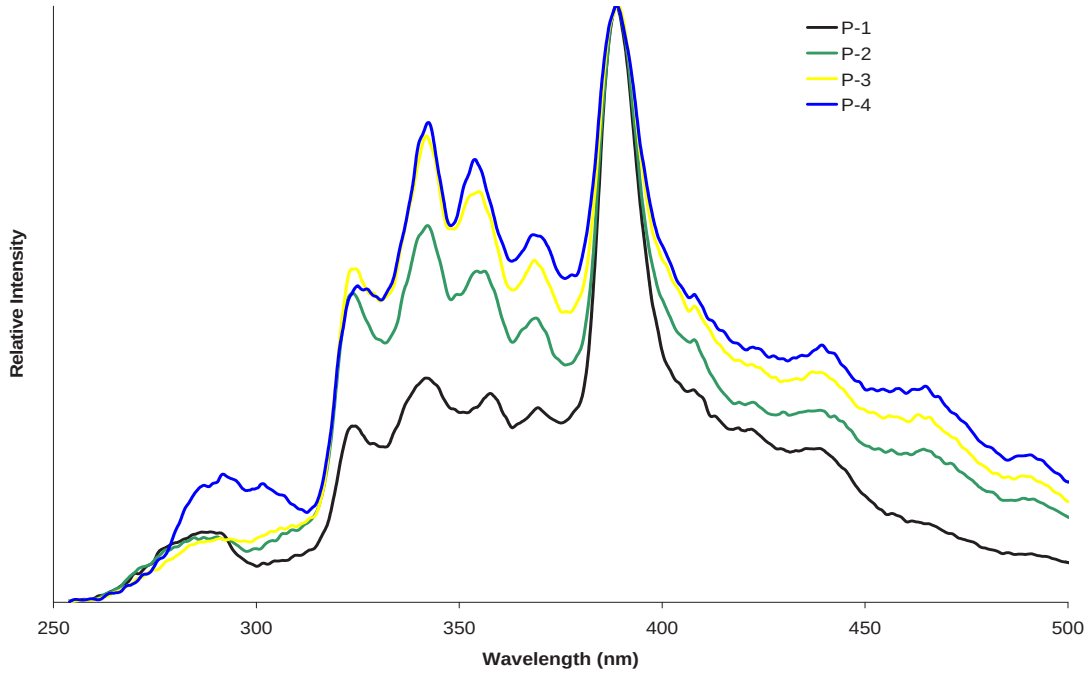

Figure 3.8. Peak normalised UV-F spectra of the pitches P-x obtained in the 1st (x=1), 2nd (x=2), 3rd (x=3) and 4th (x=4) processing cycle of the anthracene oil.

These data suggest that molecules with the largest conjugated aromatic systems are the more reactive species and are consumed in the first two stages of the process. This leaves molecules with smaller aromatic ring systems in the anthracene oils of the later cycles, which apparently are more stable compounds. AO-3 and AO-4 also show a small amount of signal in 600-700 nm region which is not observed in the other oils. Similar signal between 600-700 nm is observed for RP-2, 3 and 4 (Figure 3.7). This signal is reproducible and suggests the presence of larger molecular mass materials produced during the process. The UV-F spectra for the reaction products closely resembled those for the anthracene oils. Almost identical trends were observed, with shifts in maximum intensity from longer to

shorter wavelengths as the number of cycles increased. The similarity of the corresponding AO-x and RP-x samples highlights the influence the smallest molecules over the observed UV-F spectra.

UV-fluorescence spectra of P-1, P-2, P-3 and P-4 are presented in Figure 3.8. The main feature was a large peak at 390 nm, which decreased in relative intensity compared to the rest of the spectrum - with successive stages of processing. Signal at both higher wavelengths (~460 and ~490 nm) and lower wavelengths (between 310-370 nm) increased in relative intensity. Taking into account the SEC results showing larger molecules in the pitches obtained from successive cycles, these data suggest that these pitches contain broader spreads of molecular sizes as well as broader distribution of polycyclic aromatic units. To confirm these findings a more detailed NMR based study has been undertaken on the solubility fractions of these pitches.

The findings from UV-F are consistent with earlier findings suggesting that higher concentrations of larger polynuclear aromatic groups are produced in the pitches obtained from successive cycles, alongside the incremental increase in oxygen functionalities.

3.1.2. Analysis of Sub-Fractions of the Eco-Pitch Samples

3.1.2a. Planar Chromatography Fractions

A more thorough characterisation of the eco-pitch samples was achieved through the analysis of their sub-fractions. This was performed to determine the mass ranges of the anthracene-oils (and pitches) more completely. The anthracene oils were fractionated using planar chromatography (PC) according to the procedure outlined elsewhere[3]; the findings of that study are also reported in Section 8.2.1 of Ref 1 and briefly below.

Images of the developed PC plates containing the AO-1 sample are shown in Figure 3.9. A similar procedure has been applied to the anthracene oils from the other stages (PC plates not shown). Differences are observed from the PC runs of AO samples from different cycles of the process. The clearest of these is the amount of material that remains at the origin of the plate (PC fraction 1). This immobile material is of relatively high mass (>500 Da). The quantity of this material decreases as the number of cycles progresses; for AO-3 to AO-5 very little material is observed at the origin. These findings match those observed from the SEC and UV-F analysis of the bulk samples as discussed earlier, where the AO-1 sample was found to contain molecules of higher average mass with larger PNA ring systems than the other oils.

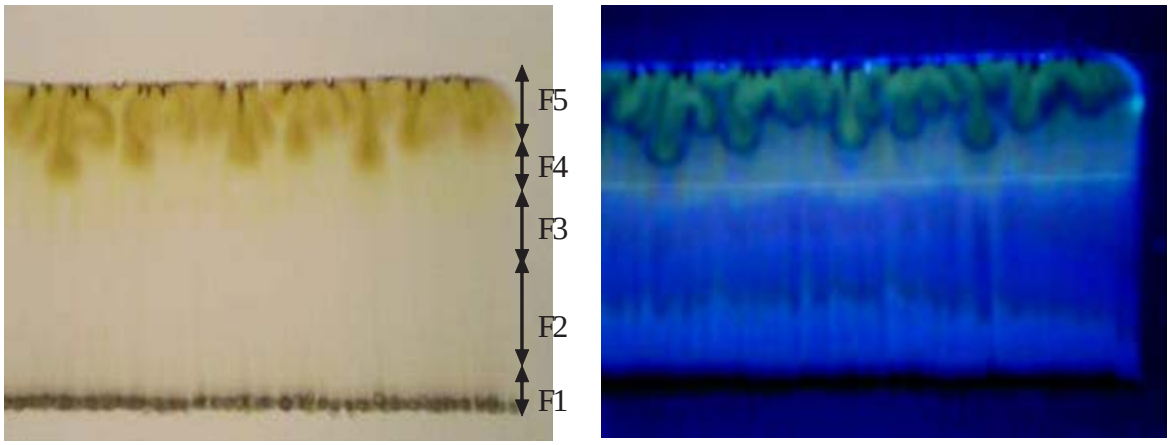

Figure 3.9. PC plate of Anthracene –oil AO-1 eluted with acetone and then $CHCl_3$, the image on the left hand side was taken under visible light; that on the right under UV light (260nm).

The different bands of material isolated by the PC-fractionation of the AO-x samples were examined using SEC, UV-F and LD-MS. The results of these analyses are briefly discussed in the following sections and elsewhere (Ref 1, Chapters 6 & 8). Only the results from the analysis of the AO-5 sample will be presented here with the findings from the other samples summarised, but not shown.

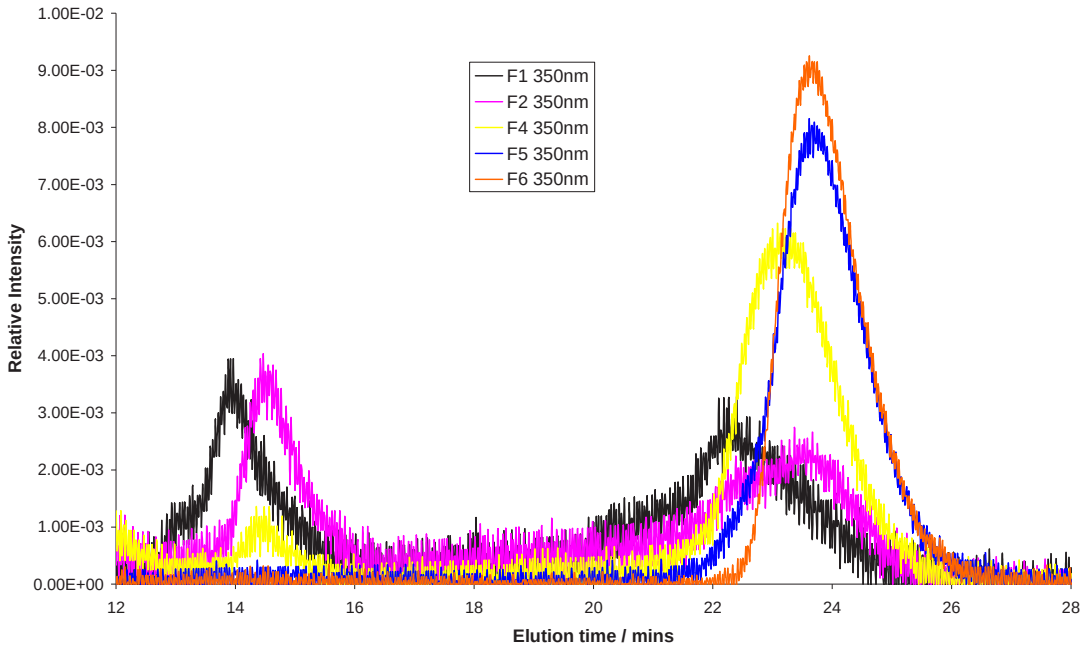

Figure 3.10. SEC curves at 350 nm, area normalised, of the AO-5 PC-fractions F1, F2, F4, F5 and F6, obtained from a Mixed-A column operating with NMP as eluent.

Analysis of the AO-x PC Fractions by SEC

Figure 3.10 shows the SEC chromatograms of the planar chromatography fractions of the AO-5 sample. In all cases (AO-1 to AO-5), there is a shift to shorter elution times (corresponding to higher masses) for the less mobile PC fractions. From the comparison of equivalent PC fractions from the AO-1 and AO-5 samples, the most mobile fractions (F5 and F6) elute about 30 seconds later for AO-5 relative to AO-1. PC fractions F1 to F4 from AO-1 show a similar elution range and profile as those from AO-5. In general, the PC fractions from AO-1 showed more pronounced excluded peaks than AO-5. However, AO-5 PC fraction F1 showed the earliest eluting excluded peak of all the AO fractions.

The SEC chromatograms of the bulk AO samples (cf. Figure 3.2) were found to be identical to those of their most mobile PC fractions (F5 - F6). This highlights the masking effect smaller molecules have on the SEC chromatogram of the bulk sample, even for these relatively narrow samples (narrow in contrast to pitch and asphaltene samples).

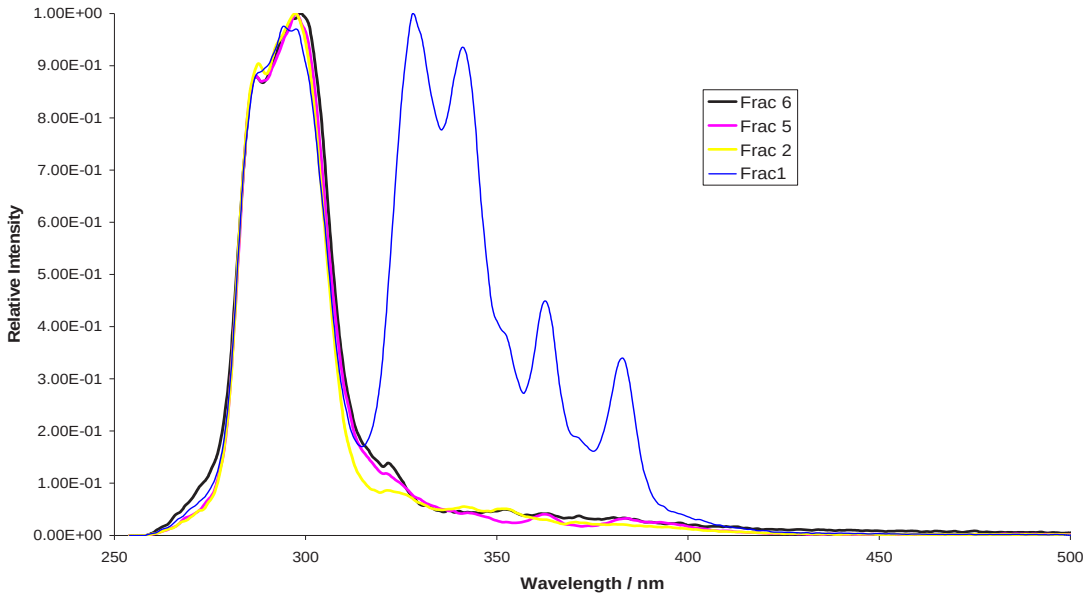

Figure 3.11. Peak normalised UV-F spectra of the AO-5 planar-chromatography fractions F1, F2, F5 and F6.

Analysis of the AO-x PC-Fractions by UV-F Spectroscopy

An example of the UV-F results obtained from the examination of the AO-5 PC fractions is shown in Figure 3.11 for fractions F1, F2, F5 and F6 (the F3 fraction is not shown due to its low response). Overall, the same trend is observed for all the AO samples, where the PC fraction 1 shows fluorescence at the longest wavelengths of all the PC-fractions. For AO-1, a large peak is observed at 450nm which tails off towards ~500nm, whereas for AO-5 the signal decays back to base-line at ~400nm. The other samples fall in-between these results showing progressively less signal at longer wavelengths as the number of cycles increases.

The UV-F results for AO-1 PC fractions showed the greatest diversity of all the AO samples. A trend of decreasing complexity of UV-F spectra was observed as the number of cycles increased. AO-5 PC fractions F2 - F6 all look very similar. In all cases, the PC fractionation uncovered fluorescence at longer wavelengths than was apparent from the examination of the bulk AO samples.

Analysis of the AO-x PC-Fractions by LD-MS

A summary of the findings from the LD-MS analysis of the AO-5 PC-fractions is outlined below. Similar results were obtained for the other AO-x samples (not shown). A full account of the LD-MS analysis of the AO-1 PC fractions has been presented elsewhere[1,3]. Figure 3.12 shows the LD-mass spectra obtained from the AO-5 PC-fractions.

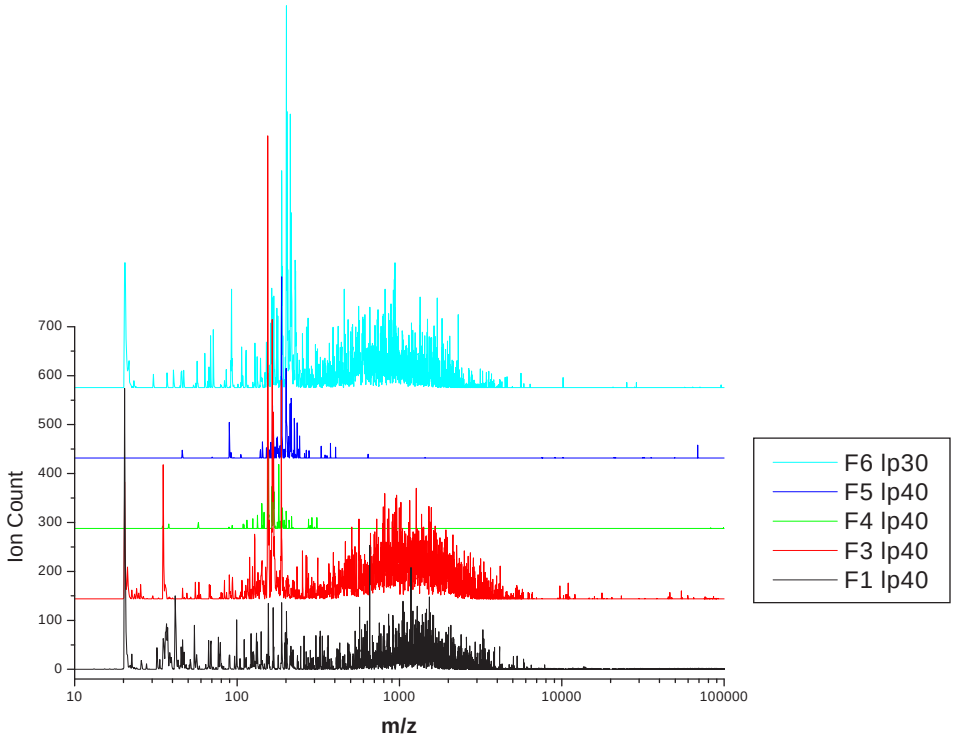

Figure 3.12. LD-mass spectra from the AO-5 PC-fractions, linear mode operation with no Delay Ionisation Extraction (DIE) time and maximum High Mass Acceleration (HMA) voltage (10 kV).

PC fraction F1 of the AO-5 sample showed a main band of ions centred around m/z 1,500, with very little ion intensity at values below m/z 500. This implies that the ions centred ~ m/z 1,500 in PC fraction F1 are from molecular ions. This interpretation is reinforced by the low abundance of low mass ions, which reduces the likelihood of multimer ions being formed. PC fraction F3 has a similar distribution to fraction F1, although for fraction F3 the most intense ions are between m/z 150 – 200. PC fraction 4 showed the lowest masses of all the fractions with a narrow distribution ranging from m/z 100 - 200. PC fraction F5 has a similar narrow distribution but at slightly higher m/z values (150 - 250). PC Fraction F6 has a wider distribution, most similar to fraction F3, with the most intense ions between m/z 150 - 300 and a second band of less intense ions between m/z 400 - 2,500.

These results confirm the presence of high mass species (m/z >500) in these samples. Analogous results were obtained for all five anthracene-oil samples. The results from this study of the AO-x PC mobility fractions were used to aid the interpretation of the LD-MS data obtained from the analysis of the bulk AO-x samples. These data are used to estimate number average molecular weight, Mn, for each sample. These results are discussed next.

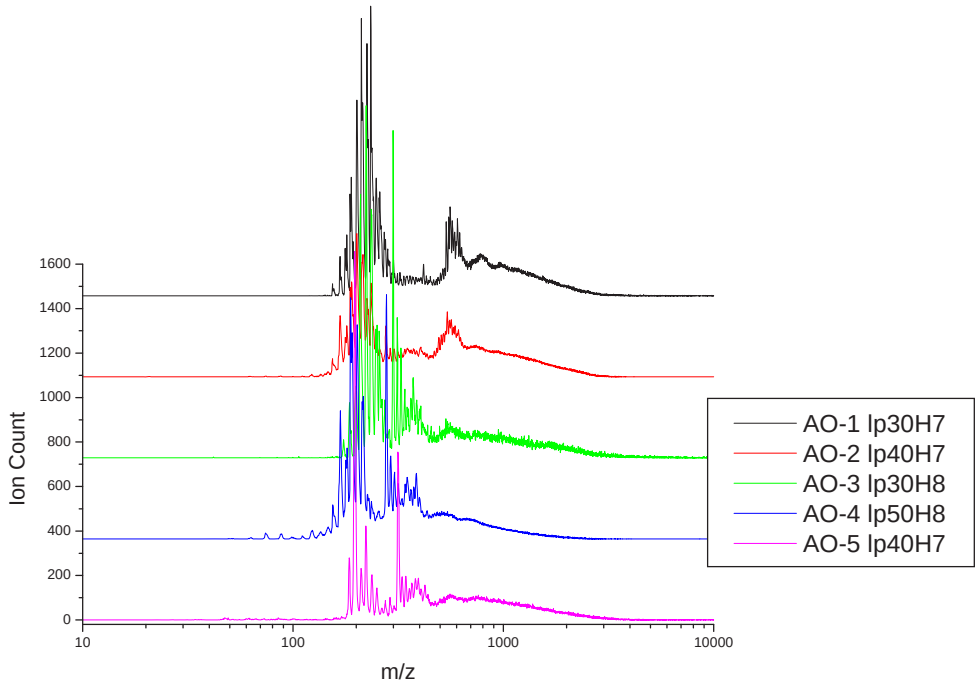

Figure 3.13. LD-MS spectra of the bulk (neat) anthracene-oils, linear mode operation with no DIE time, where the HMA voltage was reduced to keep the ion count below 100 units per shot. Each mass spectrum shown has been summed from 10 scans.

Analysis of the Bulk AO Samples by LD-MS

The mass spectra acquired from the analysis of bulk neat AO samples (neat refers to placing the sample on the LD-MS target without the aid of solvent, cf. Ref 2) by LD-MS showed a large amount of variation depending on the conditions used. For an example of the range of distributions observed for the AO-1 sample refer to Ref 1. The data acquired from the analysis of the PC-fractions of the AO-x samples were used to aid in deciding which of the spectra obtained from the neat sample best represents the actual molecular mass distribution of the bulk sample. The LD-mass spectra presented in Figure 3.13 were selected as 'best representations' of the bulk AO-x samples among the sets of spectra acquired for each neat sample at different laser powers.

The band of high mass ions centred around m/z 800, which is seen in the LD-mass spectra of all the AO samples (Figure 3.13), was initially thought to be from multimer ions. However, the results from the analysis of the PC fractions (Figure 3.12) provide strong evidence for these being molecular ions from the samples. This was inferred from PC fraction F1 that showed no low mass ions with only one band of ions between m/z 1,000 - 3,000 (Figure 3.12). A more comprehensive account of the interpretation of these results is given elsewhere[1,3]. Once the origin of the higher m/z ions was established, it was possible to make a more detailed analysis of the results. Caution is still needed, however, as the relative proportions of high mass and low mass species can not be accurately determined. Nevertheless, by using similar conditions to acquire the data, relative comparisons can be made between samples.

Figure 3.13 shows that all the AO samples have broadly similar distributions, with AO-1 having the highest proportion of high mass ions. There is an observable decrease in the count of ions centred in the vicinity of m/z 600, as the number of cycles increases. The less intense bands of ions centred ~ m/z 800 and 1,000 also decrease after the first cycle. From the 3rd cycle onwards, a new band of low mass ions appears around m/z 350. Also, as the number of cycles increases, the main band of ions (m/z 150 - 300) progressively shifts towards smaller values. These findings are consistent with those from SEC, UV-F and FT-IR studies of the bulk AO-x samples[1,2].

3.1.2b. Solvent Solubility Fractions

The fractionation of the sample by planar-chromatography has increased the certainty to which the LD-MS data can be interpreted. This has made a more detailed characterisation possible. A similar approach was used to characterise the pitch samples. The pitches were first fractionated by solubility (sequentially using heptane, acetone, toluene and finally pyridine), which produced five solubility-fractions from each of the four pitches[1] (Table 3.2). The solubility-fractions from the pitches were then further sub-divided using planar-chromatography. A thorough examination was made of the solubility-fractions using Elemental Analysis (Table 3.3), SEC, UV-F, NMR, and LD-MS; the PC-fractions were studied by SEC, UV-F and LD-MS (this work is being prepared for publication).

The results from SEC, UV-F and LD-MS are presented below, followed by a summary of the Mn estimations for the samples. The mass estimates were based on the analysis of PC-fractions of the solubility-fractions. In turn, the Mn estimates and EA results were then combined in Average Structural Parameter (ASP) calculations to characterise the pitches in terms of mass and structure (cf. Ref 1). A summary of this work is given below.

Table 3.2. Mass Balance for the pitch solubility fractionation, in weight percent

Solvent	P-1 (%)	P-2 (%)	P-3 (%)	P-4 (%)
1-Heptane soluble	16.5	18.3	20.5	21.5
2-Acetonitrile soluble	37.0	33.0	33.1	24.5
3-Toluene soluble	20.0	12.5	14.0	18.5
4-Pyridine soluble	13.5	13.5	12.4	16.0
5-Pyridine Insoluble	13.0	22.7	20.0	19.5

Table 3.3. Elemental analysis result for the pitch solubility-fractions

Sample	C / %	H / %	N / %	S / %	O / %
1P01	92.0	5.1	0.9	0.8	1.2
2P01	91.4	5.0	1.3	0.7	1.6
3P01	92.3	4.3	1.2	0.6	1.6
4P01	90.8	3.9	2.0	0.5	2.8
5P01	91.1	3.5	1.9	0.6	2.9
1P02	92.0	4.9	0.8	0.9	1.4
2P02	91.0	5.0	1.2	0.7	2.1
3P02	91.3	4.5	0.9	0.6	2.7
4P02	90.8	3.9	2.0	0.5	2.8
5P02	91.2	3.5	2.1	0.5	2.7
1P03	92.0	5.2	0.6	0.8	1.4
2P03	91.1	4.9	1.1	0.7	2.2
3P03	91.5	4.3	1.1	0.6	2.5
4P03	89.4	4.2	2.3	0.5	3.7
5P03	90.8	3.5	1.6	0.5	3.6
1P04	91.7	5.2	0.8	0.8	1.5
2P04	91.2	4.8	1.0	0.7	2.3
3P04	91.8	4.4	0.9	0.6	2.3
4P04	90.3	3.9	2.0	0.5	3.3
5P04	90.9	3.6	1.9	0.6	3.0

Summary of the SEC and UV-F Results for the Pitch Samples

The results from the SEC and UV-F analysis of the pitch solubility-fractions are presented in Figures 3.14 and 3.15 respectively. Only results for pitch P-1 will be shown here. The area normalised SEC chromatograms of the solubility-fractions of P-1 acquired using a Mixed-D column operating with NMP as eluent, with detection at 300nm UV-A are presented in Figure 3.14. Analogous results for the solubility fractions of P-2, P3 and P4 are presented elsewhere[1]. UV-F spectra for the P-01 solubility-fractions are shown in Figure 3.15.

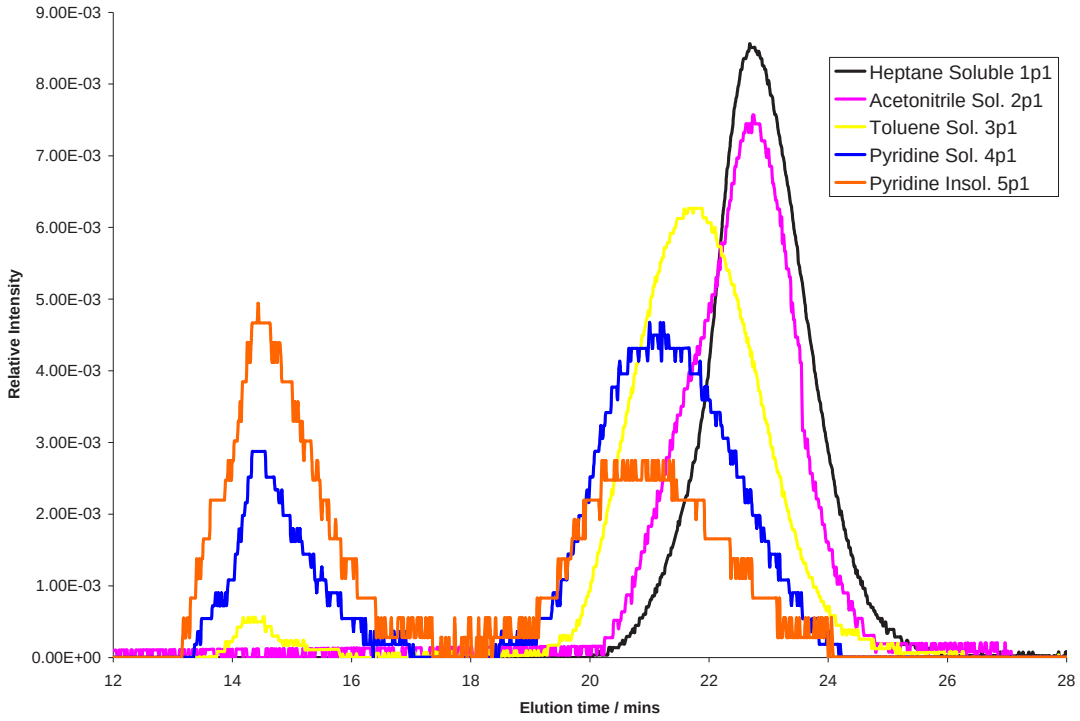

Figure 3.14. Area normalised SEC chromatograms of the solubility fraction of P-1, Mixed-A column operating with NMP as eluent, detection at 300nm UV-absorbance.

The SEC results show a trend towards shorter elution times from the 1P-x fractions to the 5P-x fractions. Similar results are seen for the four pitches, where the 1P-x fractions elute at the longest times with the narrowest distribution and barely any signal in the excluded region of the chromatogram. The 2P-x fractions also show signal solely in the retained region, but shifted to shorter elution times and with a broader distribution than the 1P-x fractions. The 3P-x fractions are the first to show a peak in the excluded region, with their retained peaks eluting at earlier times than the 2P-x fractions. The 4P-x fractions have more pronounced excluded peaks and their retained peaks shift to shorter times. For the 5P-x fractions, the majority of the signal was recorded in the excluded region. The retained peak is in a similar position to that of the 4P-x fractions but slightly shifted to shorter times.

Summarising the SEC examination, it is interesting to note that equivalent solubility-fractions from different pitches show signal in the same areas of the chromatogram; the only difference was the ratio of materials eluting in the retained and excluded regions. In this case, the equivalent solubility-fractions of the pitches from the later cycles generally showed more signal in the excluded region.

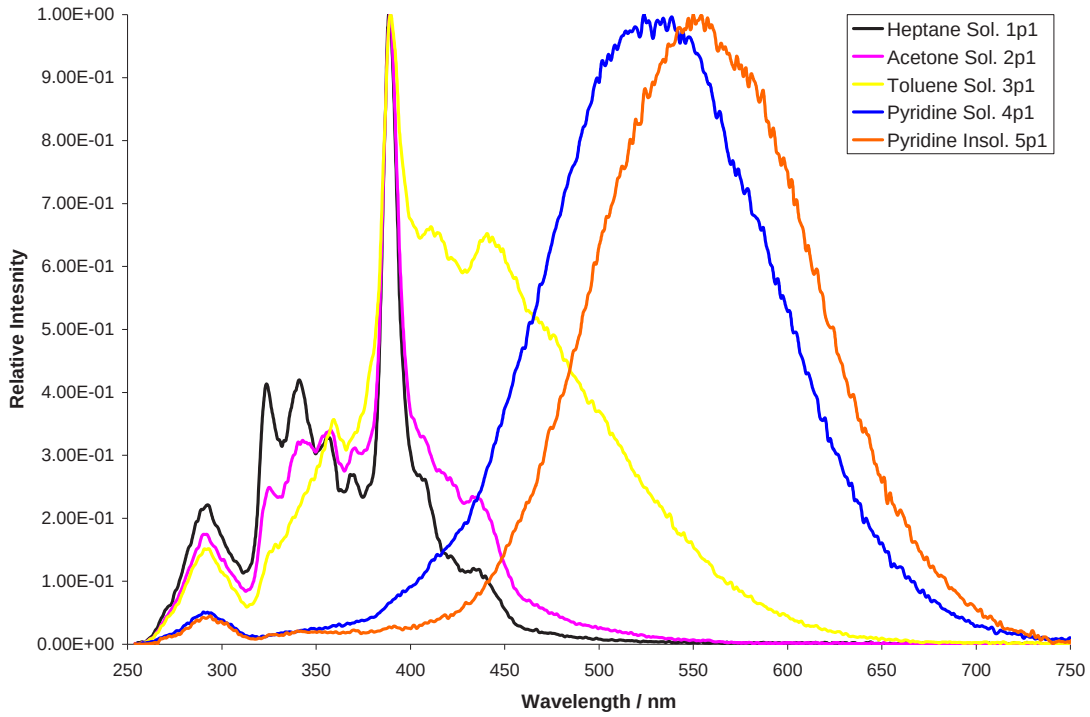

Figure 3.15. Peak normalised UV-F spectra of the solubility-fractions of P-1.

The UV-F spectra of the solubility-fractions from the four pitches all show the same trend, where the signal red-shifts from the 1P-x fractions to the 5P-x ones. This is generally interpreted as an increase in the sizes of conjugated systems and PNA groups. By comparing equivalent solubility-fractions from the different pitches another trend is observed. For the first three solubility-fractions of P-1 (1P-1, 2P-1 and 3P-1) the peak maximum is at 390nm and as the number of cycles increases, the intensity of this peak progressively decreases for those fractions. For the 1P-2 and 2P-2 fractions, the fluorescence shifted towards shorter wavelengths, whereas the fluorescence of 3P-2 fractions shifts to longer wavelengths as the number of cycles increases. The trend becomes more pronounced for the corresponding P-3 and P-4 solubility-fractions.

This implies that samples from equivalent solubility-fractions of pitches from different cycles of the process show peaks in the same regions as one another, although the proportions of signal relating to larger and smaller PNA groups changes. The amount of smaller PNA groups increases as the number of cycles increase, for the 1P-x and 2P-x samples. For the 3P-x samples there is a shift to larger PNA groups as the number of cycles increased.

All the 4P-x samples showed fluorescence at similar wavelengths independent of which pitch they were produced from, as did the 5P-x samples. This suggests all these samples contain large PNA groups that are of similar size. To obtain more detailed information about the structures present in these samples, they were examined using NMR spectroscopy. The findings of that study are summarised next.

Summary of Mass Estimates for the Pitches

A detailed examination of the mass distributions of the pitch solubility-fractions was made according to the procedure outlined in Section 6.3 of Ref 1. The samples were fractionated by planar chromatography and analysed by SEC, UV-F and LD-MS. The Mn estimates obtained from that study are summarised in Table 3.4. Overall, there is a steady increase of average mass from the 1P-x fractions to the 5P-x samples.

Table 3.4. Mn and Mw estimates from the LD-MS analysis of the P-1 and P-4 solubility-fractions

Sample	LD-MS Conditions		Mn / Da	Mw / Da
	Laser power / %	HMA / kV		
1P-01	10	8.0	320	350
2P-01	20	8.0	420	520
3P-01	20	8.0	1,100	1,300
	40	7.0	1,100	1,400
4P-01	30	7.5	1,600	2,300
	60	6.5	2,000	6,000
5P-01	40	6.7	2,100	5,300
	50	6.5	2,600	9,900
1P-04	10	10.0	400	610
2P-04	20	8.0	500	570
	50	6.0	660	900
3P-04	30	8.0	1,500	2,100
4P-04	40	7.0	1,800	2,500
5P-04	30	7.5	1,900	2,800
	50	6.7	2,900	10,700

Nuclear Magnetic Resonance (NMR) Spectroscopy Analysis

The solubility-fractions of the pitches were examined by liquid-state NMR under the conditions and method reported elsewhere[1,8]. Due to the large number of samples (5 fractions from each of the four pitches) only the pitches from the first and last cycles have been examined (P-1 and P-4). In addition, as the errors in this type of NMR analysis are relatively significant (~ ±2-5%), the difference between the samples needs to be relatively large to be measured. Therefore, using the P-1 and P-4 samples should allow any changes between these two samples to be detected.

The proton NMR results are presented in Table 3.5, and the 13C (Inverse Gated - IG) results in Table 3.6. The standard deviations for these values are presented elsewhere[1], as are the chemical shift classifications[1,8].

Table 3.5. Proton NMR-Results (values given as fractions), based on the chemical shift classifications defined in Ref. 1

Label	1p-1	1p-4	2p-1	2p-4	3p-1	3p-4	4p-1	4p-4	5p-1	5p-4
Hγ	0.001	0.009	0.002	0.002	0.006	0.016	0.029	0.009	0.000	0.000
Hβ1	0.005	0.020	0.008	0.007	0.017	0.034	0.070	0.007	0.042	0.000
Hβ2	0.001	0.001	0.013	0.001	0.009	0.007	0.019	0.016	0.031	0.051
Hα1	0.065	0.052	0.081	0.065	0.083	0.070	0.066	0.048	0.010	0.001
HA	0.011	0.004	0.016	0.008	0.020	0.011	0.001	0.000	0.000	0.034
Hα2	0.018	0.012	0.020	0.020	0.022	0.020	0.006	0.000	0.014	0.000
Har1	0.790	0.831	0.769	0.817	0.758	0.759	0.690	0.771	0.605	0.614
Har2	0.110	0.071	0.091	0.081	0.085	0.083	0.120	0.149	0.299	0.299
Tot HAli	0.100	0.097	0.140	0.102	0.157	0.158	0.190	0.080	0.097	0.087
Tot HAr	0.900	0.903	0.860	0.898	0.843	0.842	0.810	0.920	0.903	0.913

Table 3.6. ^{13}Carbon Inverse Gated NMR-Results, (values given as fractions), based on the chemical shift classifications defined in Ref. 1

Label	1p-1	1p-4	2p-1	2p-4	3p-1	3p-4	4p-1	4p-4	5p-1	5p-4
CH3	0.012	0.013	0.014	0.011	0.008	0.014	0.010	0.003	0.031	0.010
CH2	0.017	0.017	0.017	0.016	0.017	0.022	0.010	0.005	0.005	0.017
CA	0.009	0.009	0.012	0.009	0.007	0.009	0.008	0.003	0.021	0.014
CF	0.011	0.010	0.010	0.010	0.010	0.011	0.005	0.003	0.000	0.001
Cα2	0.011	0.010	0.007	0.014	0.010	0.008	0.005	0.007	0.000	0.000
Car1	0.514	0.574	0.562	0.524	0.538	0.556	0.559	0.580	0.427	0.521
Car2	0.426	0.367	0.379	0.415	0.410	0.380	0.404	0.398	0.516	0.437
Tot CAli	0.060	0.059	0.060	0.061	0.052	0.064	0.038	0.022	0.057	0.042
Tot Car	0.940	0.941	0.940	0.939	0.948	0.936	0.963	0.978	0.943	0.958

The main differences observed from the proton NMR results are as follows: the 4P-1, 5P-1 and 5P-4 fractions are the only samples to have more than 5% of their hydrogen atoms in an aliphatic environment, which are beta or further from an aromatic ring (Hβ + Hγ), Table 3.5. These were also the only samples where (Hβ + Hγ) >> Hα, and hence have values of n (length of aliphatic-side-chain) larger than 2.0. However, in the cases of the 5P-1 and 5P-4 fractions, the data suffers because of low solubility. Consequently the signal-to-noise ratio (s/n) was low.

In all cases, the following observations were made from the ^{13}C NMR results: the majority of the aliphatic carbons are alpha to an aromatic ring. The aliphatic carbon is mainly in the form of CH_2

groups. All the samples are primarily aromatic (>93% for carbon, and >80% proton – excluding the 5P-x samples). Aromaticity changed for the different fractions in the following order: 1P-x ≥ 2P-x ≤ 3P-x, < 4P-x. The results for 5P-x are less clear due to the low solubility of this sample leading to poor s/n in its NMR spectra.

Further insight can be gained by comparing the same solubility-fractions from the first and fourth cycles. The results of the1P-x fractions are almost identical to one another, as are the results for the 2P-x, and the 3P-x fractions. For the 4P-x samples, proton aromaticities (Har) differ by more than 10%, whilst their Car values are almost the same. A similar result is seen for the 5P-x samples, along with a large decrease in their Har values compared to the other fractions. It is unclear if these results can be relied upon for the 5P-x samples, due to the poor s/n of these spectra.

To obtain a more detailed characterisation of these samples in terms of their mass and structure, these NMR data have been combined with Mn estimates and EA results in ASP calculations, there results are presented next.

Average Structural Parameters (ASP) Calculations for the Pitches

In this section, the results from the application of average structural parameter calculations to the solubility-fractions of the pitches are presented. Data from EA, NMR and Mn were used in these calculations; the method is based on work by Dickinson[9] and Rongbao[10]. Values from Table 3.4 were used in the ASP calculations. Due to uncertainty in some of the Mn results, ranges of Mn were used in the ASP calculations rather than discrete values.

The calculations used in this work have been defined elsewhere[1,8]. The main types of carbon studied are aromatic carbons substituted with aromatic groups (Car-AS) pericondesed aromatic carbon (Car-P) and cata-condensed aromatic carbon (Ccata). A summary of the experimental values used in the ASP calculations is given in Table 3.7. Heteroatoms are not accounted for in the ASP calculations for the reasons outlined elsewhere[1]. The results of the ASP calculations that are independent of Mn are presented in Table 3.8 and those dependent on Mn in Table 3.9 (duplicated values are for repeat calculations using a different Mn).

Table 3.7. Experimental values used in the ASP calculations

Sample	HAr	Hα	Hβ + Hγ	HAl	CAr	CAl	Mn / Da	%C	%H
1p-01	0.900	0.093	0.007	0.100	0.940	0.060	320	92	5.1
1p-04	0.903	0.067	0.030	0.097	0.941	0.059	400	91.7	5.2
2p-01	0.860	0.117	0.023	0.140	0.940	0.060	420	91.4	5
2p-04	0.898	0.093	0.009	0.102	0.939	0.061	600	91.2	4.8
3p-01	0.843	0.126	0.031	0.157	0.948	0.052	1100	92.3	4.3
3p-04	0.842	0.101	0.057	0.158	0.936	0.064	1500	91.8	4.4
4p-01	0.810	0.072	0.118	0.190	0.963	0.038	1600-2000	90.8	3.9
4p-04	0.920	0.048	0.031	0.080	0.978	0.022	1800	90.3	3.9
5p-01	0.625	0.024	0.073	0.097	0.943	0.057	2100-3600	91.1	3.5
5p-04	0.728	0.036	0.051	0.087	0.958	0.042	1900-2900	90.9	3.6

Table 3.8. ASP Results Independent of Mn (based on definitions given elsewhere[1,8]). Values are given as fractions, except 'n' which is the average number of carbon atoms

Sample	n	Cs	Cn	Cal	Car-US	Car-PC	Car-s	Car-P	Φ
1p-01	1.08	0.06	0.05	0.01	0.59	0.00	0.06	0.65	0.31
1p-04	1.45	0.06	0.05	0.01	0.61	0.00	0.04	0.65	0.31
2p-01	1.19	0.06	0.05	0.01	0.56	0.00	0.05	0.61	0.35
2p-04	1.10	0.06	0.05	0.01	0.56	0.00	0.06	0.62	0.34
3p-01	1.25	0.05	0.04	0.01	0.47	0.07	0.04	0.51	0.46
3p-04	1.57	0.06	0.05	0.01	0.48	0.08	0.04	0.52	0.44
4p-01	2.64	0.04	0.03	0.01	0.41	0.14	0.01	0.43	0.55
4p-04	1.65	0.02	0.02	0.00	0.47	0.11	0.01	0.49	0.50
5p-01	4.04	0.06	0.03	0.03	0.29	0.14	0.01	0.30	0.68
5p-04	2.44	0.04	0.03	0.01	0.34	0.18	0.02	0.36	0.62

Negative values were rounded up to zero

Table 3.9. ASP Results Dependent on Mn, based on Ref 10. Values are given as average 'numbers' of rings or atoms, except 'N', Car-AS and Ccata which are fractions

Sample	Mn	m	H	C	N	Car-AS	Ccata	RA	RN
1p-01	320	1	16	25	0.04	0.03	0.34	2.4	1.3
1p-01	280	1	14	21	0.06	0.00	0.37	1.9	1.1
1p-04	400	1	21	31	0.05	0.13	0.20	3.0	1.4
1p-04	280	1	13	19	0.08	0.01	0.32	1.9	0.9
2p-01	420	1	21	32	0.04	0.09	0.24	3.5	1.2
2p-04	600	1	29	46	0.02	0.13	0.23	4.9	2.6
3p-01	1100	1	47	85	0.01	0.07	0.30	12.4	2.4
3p-04	1500	1	65	115	0.01	0.13	0.21	15.9	4.5
4p-01	1600	1	62	121	0.02	0.00	0.39	21.5	-0.4
4p-01	2000	1	77	151	0.02	0.00	0.39	26.9	-0.5
4p-04	1800	1	70	135	0.01	0.06	0.33	22.1	1.2
5p-01	2100	1	73	159	0.03	0.00	0.50	34.1	-3.5
5p-01	3600	1	125	273	0.01	0.00	0.50	58.5	-6.0
5p-04	1900	1	68	144	0.02	0.00	0.42	28.7	-2.0
5p-04	2900	1	104	219	0.01	0.00	0.42	43.7	-3.1

Summary of ASP Results for the Pitch Samples

Samples 1P-x: Values of 90% Har and 94% Car were found for the two samples, 1P-1 and 1P-4, respectively. They mainly contain compounds with isolated single aromatic-cores with no peri-condensed carbon. Aliphatic-bridges account for ~1-2% of the total carbon and hydrogen detected. It is likely that that some di- and higher- aromatics are present, bound by biphenyl-like aromatic-aromatic bonds, (Car-AS ~ 0-3% for 1P-1, and 0-13% for 1P-4). The Mn value of 1P-1 appears to be at least 280 u; otherwise a negative value is obtained for Car-AS. 1P-4 has a value of at least 250 Da. However, all the mass estimations suggest that 1P-4 is the heavier of the two samples.

The average number of aromatic rings for 1P-1 is 2.0-2.5, and 2.0-3.0 for 1P-4 depending on the Mn used (cf. Table 8.9). 1P-1 seems to contain significantly more cata-condensed carbon than the 1P-4 sample; 34-37% for 1P-1, compared to 20-32% for 1P-4, depending on Mn. Roughly equal amounts of methyl and ethyl groups were detected (Cal ~1% in total). The majority of aliphatic species are in naphthenic-like environments (Cn ~5%) for both fractions.

These results suggest a change in structure from 1P-1 to 1P-4, with 1P-1 having more cata-condensed carbon and fewer Car-AS than the 1P-4 sample.

Samples 2P-x: 2P-1 and 2P-4 have Har values of 86 and 90% respectively, and Car values of 94%. These samples also contain no peri-condensed carbon and are mainly composed of compounds containing isolated single aromatic-cores as only 1-2% of the total carbon could be in aliphatic-bridge like environments. It is possible that some di- and higher- aromatics are also present, linked through biphenyl-like aromatic–aromatic bonds (Car-AS ~ 9-13% for 2P-1 and 2P-4 respectively). The Mn estimates (Table 3.9) used in the ASP calculations seem plausible. The average number of aromatic rings for 2P-1 is 3.5, and 5.0 for 2P-4. Both samples contain roughly the same quantity of Ccata (23-24%). Approximately equal amounts of methyl and ethyl groups were detected (Cal ~1% in total); however, the majority of aliphatic species are in naphthenic-like environments (Cn ~5%) for both fractions.

Overall the results for the 2P-x samples are more similar to 1P-4 than 1P-1.

Samples 3P-x: 3P-1 and 3P-4 both have Har values of 84% and Car values of 94-95% respectively. The 3P-x fractions are the first to show evidence of peri-condensed carbon environments (7-8%), and 3P-4 could have an average of 2 aromatic-cores per molecule, although, the low abundance of bridging aliphatic species (<2% for both fractions) makes this unlikely. Larger amounts of biphenyl-like aromatic-aromatic bonds were calculated (Car-AS 7-13% for 3P-1 and 3P-4 respectively). The difference in Car-AS values for the 3P-x samples are similar to those seen for the 2P-x fractions but more pronounced. The Mn estimates used in the ASP calculations seem plausible.

The average number of aromatic rings for 3P-1 is 12, and 16 for 3P-4. The 3P-1 sample contains ~30% cata-condensed (Ccata) whilst the 3P-4 fraction contains ~21%. Approximately equal amounts of methyl and ethyl groups were detected (Cal ~1% in total). However, the majority of aliphatic species are in naphthenic like environments (Cn 4-5%), for both samples. 3P-4 has the highest number of naphthenic rings per average molecule (RN = 4.5) of all the fractions.

Overall, the results suggest a change in structure from 3P-1 to 3P-4, with 3P-1 having more cata-condensed carbon and fewer aromatic-aromatic-single-bonds than the 3P-4 sample. Meanwhile, both samples maintain similar condensation indices (0.44 – 0.46). The results indicate an increase in the size of molecules and the sizes of aromatic clusters in these fractions compared to the 2P-x results.

Samples 4P-x: 4P-1 and 4P-4 have Har values of 81 and 92%, and Car values of 96-98% respectively. For 4P-1 it is not possible for both the Har and Car values to be correct. It is likely that the Har value is lower than its real value due to the effect of molecular size on relaxation times, which causes a broadening of the peaks and a loss of intensity. The 4P-x samples show an increase in Car-PC compared to the corresponding 3P-x fractions. 4P-1 had a higher Car-PC value than the 4P-4 fraction, 14% compared to 11%. The only parameter to be influenced by the uncertainty in Mn, was RA (average-number-of-aromatic-rings) for the 4P-1 fraction, where a value of 22 – 27 was found. The 4P-4 fraction has an average of 22 rings.

4P-1 and 4P-4 seem to contain mainly molecules with one aromatic core as there is little evidence of bridging-aliphatic species (<1% for both fractions). There is also no evidence of biphenyl like aromatic-

aromatic bonds in the 4P-1 fraction (Car-AS = 0%). 4P-4 could contain di- or higher-aromatic compounds due to its larger Car-AS value (~6%). 4P-1 has a higher percentage of Ccata than the 4P-4 sample (39% compared to 33%). 4P-1 appeared to contain the largest amount of propyl groups. However, the total amount of aliphatic moieties in side-chains is <1% of the total carbon. 4P-4 was found to have no aliphatic groups in side-chains, with all the aliphatic signal in naphthenic like environments (Cn 2-3%). 4P-1 has no naphthenic rings per average molecule (RN), while 4P-4 has ~1.0.

Overall, the results suggest a change in structure from 4P-1 to 4P-4, with 4P-1 having more cata-condensed carbon and fewer Car-AS than the 4P-4 sample. 4P-1 has a higher condensation index than the 4P-4 fraction (0.55 compared to 0.50) and more peri-condensed carbon (14 and 11% respectively). The results indicate an increase in the size of aromatic clusters in these fractions compared to the 3P-x samples; they also contain less aromatic-aromatic substitution (Car-AS).

Samples 5P-x: The poor signal-to-noise ratio of the NMR data for these samples made their analysis less exact. 5P-1 and 5P-4 have Har values of 90-91%, and Car values of 94-96% respectively. The 5P-x samples have the highest proportion of Car-PC of all the fractions with values of 14% for 5P-1 and 18% for 5P-4. It is likely that most of the molecules contain only one aromatic core, as there is little evidence of bridging-aliphatic species in these samples (0-1%). In addition, there is no evidence of any biphenyl-like bonding in either fraction (Car-AS = 0%). Ccata was found to equal 50% for the 5P-1 fraction and 42% for 5P-4.

The only parameter affected by the different Mn values used in the calculations, for the 5P-x fractions, is RA. For 5P-1 the average-number-of-aromatic-rings is between 34 and 59. For 5P-4 RA equals 29 – 44 rings. The majority of aliphatic species are in naphthenic like environments (Cn ~3%). 5P-1 has the highest condensation index of all the samples with a value of 0.68; 5P-4 has a value of 0.62.

Overall, the 5P-x results show the same change in structure as seen for 3P-x and 4P-x, i.e. the xP-1 fractions have more cata-condensed carbon and less aromatic-aromatic single bonds (Car-AS) than the corresponding xP-4 samples. The results show that the 5P-x fractions are the most condensed and contain the largest sizes of fused aromatic-cores.

In summary of the ASP study, the data suggests changes due to condensation and ring closure reactions, which lead to increasing sizes of aromatic clusters for the pitch produced in the first cycle (P-1). Cross linking reactions through biphenyl-like aromatic-aromatic single bond formation appear to increase on going from P1 to P-4. These conclusions can be related to the fact that the P-4 was produced from less reactive species than P-1 and was processed at a higher temperature.

3.1.3. References

1. T.J. Morgan. PhD Thesis, 2008 “Molecular Mass and Structural Characterization of Heavy Hydrocarbon Materials.” Department of Chemical Engineering, Imperial College London.
2. Álvarez, P.; Granda, M.; Sutil, J.; Menendez, R.; Morgan, T. J.; Millan, M.; Herod, A.A.; Kandiyoti, R. Submitted to *Energy & Fuels.* 2008. “Characterisation and pyrolysis behaviour of novel anthracene oil derivates.”
3. Morgan, T.J.; George, A.; Alvarez, P.; Millan, M.; Herod, A.A.; Kandiyoti, R. Submitted to *Energy & Fuels*, 2008. “Characterization of molecular mass ranges of two coal tar distillate fractions (creosote and anthracene oils) and aromatic standards by LD-MS, GC-MS, probe-MS & SEC.”
4. Fernandez A.L., Granda M., Bermejo J., Menendez R. *Carbon.* 2000, 38, (9), 1315. “Air-blowing of anthracene oil for carbon precursors.”
5. Metzinger, T.; Huttinger, K. Carbon. 1997, 35, 885. “Investigations on the cross-linking of binder pitch matrix of carbon bodies with molecular oxygen - Part 1 Chemistry of reactions between pitch and oxygen.”
6. Karaca, F.; Islas, C.A.; Millan, M; Behrouzi, M.; Morgan, T.J.; Herod, A.A.; Kandiyoti, R. *Energy & Fuels*. 2004, 18, 3, 778. “The calibration of size exclusion chromatography columns: molecular mass distributions of heavy hydrocarbon liquids”

7. Morgan, T. J.; Millan, M.; Behrouzi, M.; Herod, A A.; Kandiyoti, R. *Energy & Fuels*. 2005, 19, 164. “On the limitations of UV-Fluorescence spectroscopy in the detection of high-mass hydrocarbon molecules.”
8. Morgan, T. J., George, A., Davis, D.B., Herod, A A. and Kandiyoti, R. *Energy & Fuels*. 2008, 22, (3), 1824. “Optimization of ^{1}H & ^{13}C-NMR methods for structural characterization of acetone & pyridine soluble / insoluble fractions of a coal tar pitch.”
9. Dickinson, E. M. *Fuel*. 1980, 59, 290. “Structural comparison of petroleum fractions using proton and ^{13}C n.m.r spectroscopy.”
10. Rongbao, L.; Zengmin, S.; Bailing, L. *Fuel*. 1988, 67, 565. “Structural analysis of polycyclic aromatic hydrocarbons from petroleum and coal by ^{13}C and ^{1}H-n.m.r spectroscopy.”

Task 3.2. Pyrolysis behaviour (INCAR-CSIC)

The study of the pyrolysis behaviour of the different samples corroborates the results obtained by ICSTM and INCAR-CSIC (Task 3.1). The thermogravimetric curves show that for samples from the same sequence of processing (i.e., feedstock~distilled fraction, reaction product and pitch), thermal stability follows the trend of pitch > reaction product > feedstock~distilled fraction (Figure 3.16). However, the reaction products and pitches exhibit different thermogravimetric behaviours. The thermal stability of the reaction products follows the trend RP-1 > RP-2 > RP-3 > RP-4. On the other hand, the TG profiles of the pitches evidenced that below 375 °C weight loss follows the trend P-4a ~ P-3a > P-2 > P-1a. However, at about this temperature the tendency changed and even P-2, P-3 and P-4 yield a similar carbonaceous residue at 1000 °C (Figure 3.16). This could be related to the loss of selectivity during the thermal oxidative condensation processing of the different feedstocks, as a consequence of the lower thermal reactivity of the components (i.e., the polymerization capacity of the remaining anthracene oil is exhausted). It is interesting to note that both reaction products and pitches are totally isotropic, independently of the operational conditions used for their preparation. However, the reaction products and pitches have a chemical composition that makes them attractive precursors for the preparation of mesophase. In this regard, pitches form mesophase under more moderate conditions than their reaction products (Table 3.10). This is merely a consequence of the higher degree of polymerization attained by the pitches during their preparation with respect to the reaction products (additional thermal treatment and distillation steps). Moreover, the reaction products need to be subjected to pressure in order to avoid the massive production of volatiles. The ability of the reaction products to generate mesophase decreases from RP-1 to RP-4 (Table 3.10 and Figure 3.17), which corroborates the loss of selectivity and the higher contribution of the cross-linked structures as the preparation of these samples becomes severer. These effects are more pronounced in the case of the cokes (Figure 3.18). The cokes from RP-1 and P-1a show a predominantly optical texture of flow domains (Figure 3.18a and 3.18e), while the cokes from RP-4 and P-4 mainly consist of mosaics (Figures 3.18d and 3.18h). RP-2 and P-2 generated cokes with an optical texture intermediate to RP-1/P-1a and RP-3/P-3 (Figure 3.18b and 3.18f). The higher contribution of cross-linked structures in the samples as the preparation process becomes severer seems to be the factor mainly responsible for this.

Table 3.10. Capacity of mesophase formation under different experimental conditions.

Sample	Treatment	PY	Meso	Sample	Treatment	PY	Meso
RP-1	440°C, 3h, 5bar	57	-	P-1a	440°C, 1h	84	15
	460°C, 3h, 5bar	11	**63**		440°C, 3h	81	**70**
					450°C, 2h	53	57
RP-2	440°C, 3h, 5bar	54	-	P-2	440°C, 1h	80	15
	460°C, 3h, 5bar	11	**62**		440°C, 3h	66	**50**
					450°C, 2h	45	36
RP-3	440°C, 3h, 5bar	48	-	P-3	440°C, 1h	74	11
	460°C, 3h, 5bar	9	**60**		440°C, 3h	59	**40**
					450°C, 2h	39	35
RP-4	440°C, 3h, 5bar	20	-	P-4	440°C, 1h	61	10
	460°C, 3h, 5bar	5	**58**		440°C, 3h	57	**37**
					450°C, 2h	26	32

PY, global process yield (wt.%)
Meso, mesophase content, determined by optical microscopy (vol.%)

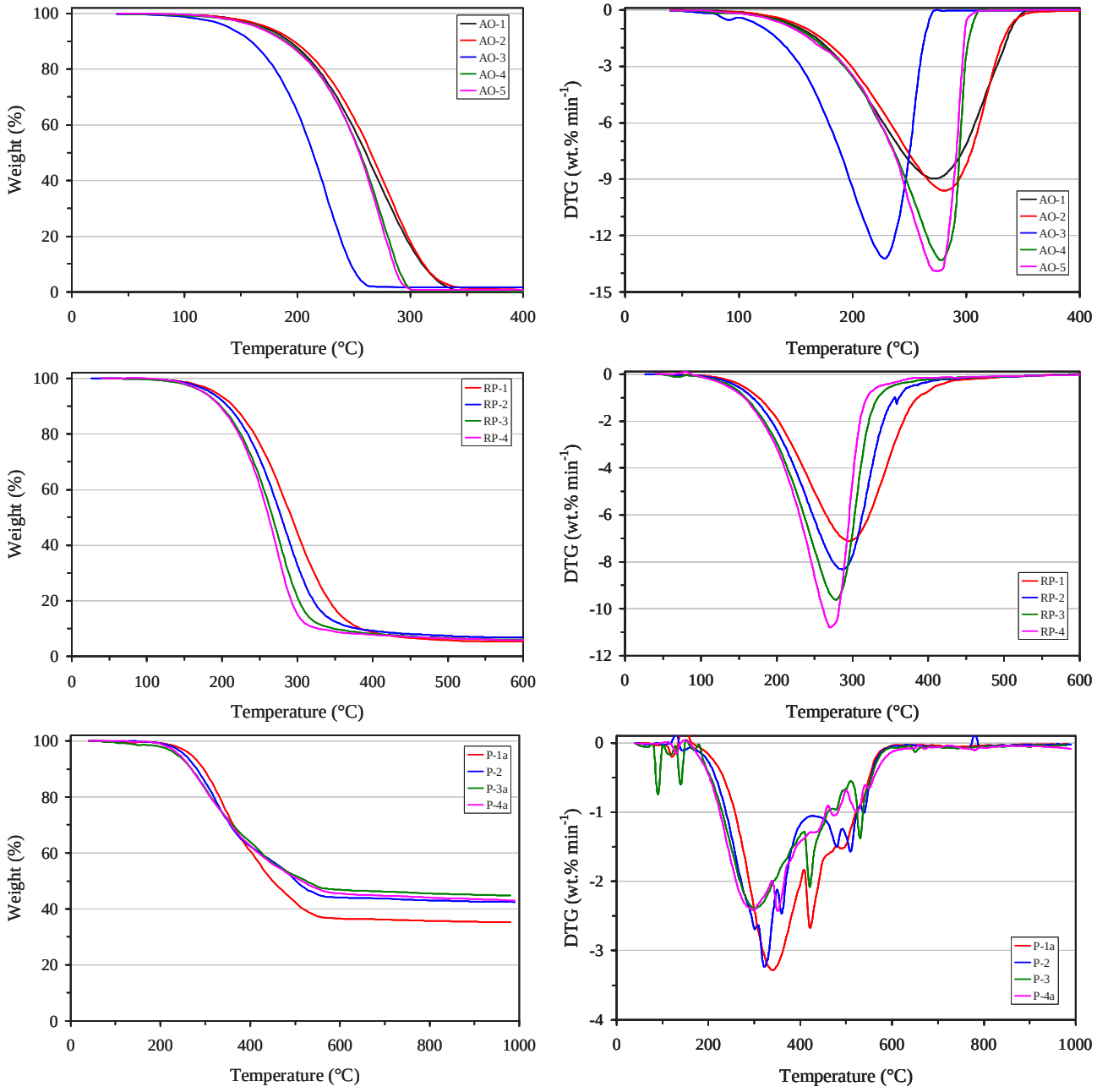

Figure 3.16. TG (left) and DTG (right) curves of the feedstocks, reaction products and pitches obtained in the 1st, 2nd, 3rd and 4th processing cycles of the anthracene oil.

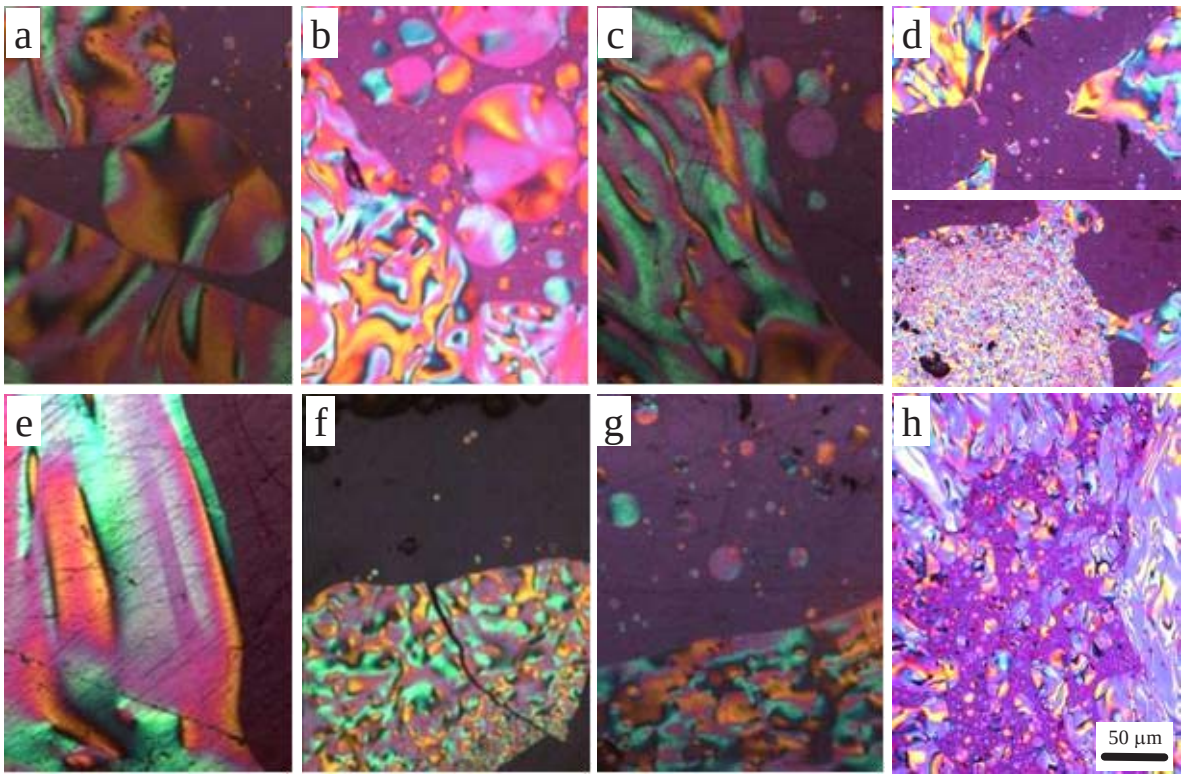

Figure 3.17. Optical microscopy of the pyrolysis products obtained from reaction products (a) RP-1, (b) RP-2 and (c) RP-3 and (d) RP-4 460 °C for 3 h under 5 bar and pitches (e) P-1a, (f) P-2 and (g) P-3a and (h) P-4a obtained at 440 °C for 3h.

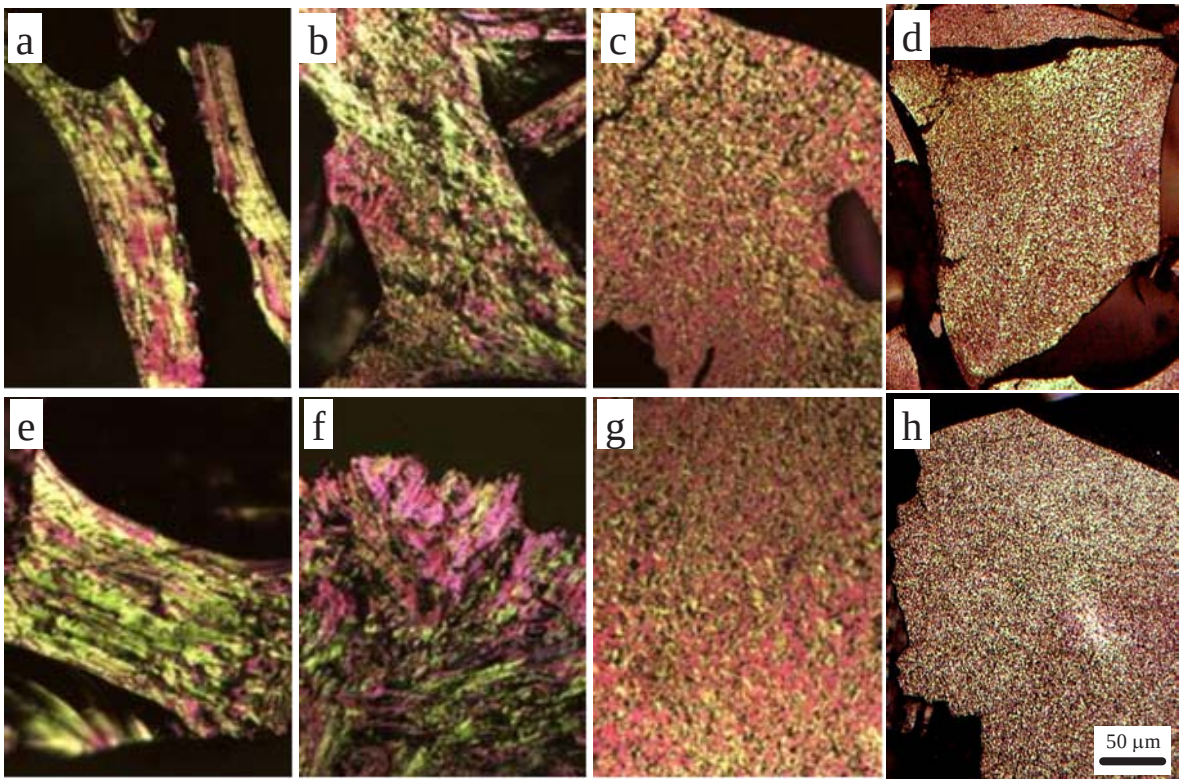

Figure 3.18. Optical microscopy of the cokes obtained from reaction products (a) RP-1, (b) RP-2 and (c) RP-3 and (d) RP-4 and pitches (e) P-1a, (f) P-2 and (g) P-3a and (h) P-4a obtained at 900 °C for 1h.

Task 3.3. Genotoxicity indices (INCAR-CSIC)

In connection with a previous study carried out by ICSTM (identification of single compounds by GC-MS), INCAR-CSIC has developed a methodology that is able to quantify the 16 PAHs listed by the EPA (American Environmental Protection Agency) as toxic pollutants. The detection limit was determined by constructing a calibration curve based on solutions of the 16 single PAHs used as external standards in different concentrations. Afterwards, the quantity of PAH in each sample is determined by using solutions of different concentrations and three internal standards (tridecane, heneicosane and triaconthane). Table 3.11 and Figure 3.19 summarize the results obtained. It is observed that all the distilled fractions present similar PAH compositions, phenanthrene being the most abundant compound followed by fluoranthene, anthracene, pyrene, fluorene and acenaphthene. It is, however, worth noting that the more condensed compounds (usually the more genotoxic compounds) such us chrysene and benzo[b]fluoranthene appear in lower proportions, as the severity of the treatment increases, possibly because of polymerization/condensation reactions during the thermal treatment. This tendency is also observed in the pitches, P-1 presenting a smaller amount of benzo[a]pyrene, indeno[1,2,3-c,d]pyrene, dibenzo[a,h]anthracene and benzo[g,h,i]perylene than P-2 and P-2 a lower amount than P-3 and P-4. Moreover, the total amount of 16-PAHs EPA in the pitches decreases from P-1 to P-3 (Table 3.11 and Figure 3.19). It is well known that, although all the compounds evaluated here are catalogued as toxics, the toxicity of each compound is different, the compounds of low molecular weight being generally less toxic. The benzo[a]pyrene equivalent (BaP-equivalent) is a useful tool commonly used to determine the toxicity of pitches. These values reflect the relative toxicity of each compound (expressed as the RPF factor) and therefore give a more accurate idea of the toxicity of the samples. The highest value was again obtained for P-1, the lowest corresponding to P-4 (Table 3.11 and Figure 3.19), which indicates that these pitches are less genotoxic than a typical coal-tar pitch (28,000-30,000 ppm of BaP-equivalent).

Similar results were obtained by IQNSA who adopted an alternative methodology based on liquid chromatography. As can be seen from Table 3.11, the carcinogenicity potential of the pitch was reduced n-fold.

Table 3.11. Genotoxicity of the feedstocks (distilled fractions) and anthracene oil-based pitches in ppm.

PAH	RPF	Feedstock ~ Distilled Fraction				Pitch			
		AO-1	AO-2	AO-3	AO-4	P-1a	P-2	P-3	P-4
Naphthalene	0.000	11,970	20,246	20,460	24,006	236	250	140	119
Acenaphtylene	0.000	559	809	169	450	91	140	70	3
Acenaphthene	0.000	56,429	61,272	30,391	11,730	291	299	130	62
Fluorene	0.000	45,701	59,936	48,593	27,000	183	586	450	1,660
Phenenthrene	0.000	158,071	232,460	184,988	204,660	3,094	6,590	8,440	14,029
Anthracene	0.000	33,381	48,025	49,690	41,360	1,783	3,290	580	3,147
Fluoranthene	0.034	106,819	125,936	88,848	35,170	35,830	42,920	46,880	48,932
Pyrene	0.000	91,528	89,530	58,948	47,940	35,920	40,710	24,720	37,791
Benzo[a]anthracene	0.033	3,810	3,255	6,485	1,520	32,550	27,270	19,800	8,417
Chrysene	0.260	19,700	16,062	4,472	2,680	21,580	29,920	9,780	11,332
Benzo[b]fluoranthene	0.100	13,305	5,054	1,142	60	21,550	14,710	120	3,182
Benzo[k]fluoranthene	0.000	4,553	1,433	96	140	35,070	7,150	840	1,457
Benzo[a]pyrene	**1.000**	**6,301**	**2,601**	**416**	**20**	**11,301**	**5,910**	**2,990**	**1,547**
Indeno[1,2,3-c,d]pyrene	0.100	2,002	411	89	40	15,310	890	300	714
Dibenzo[a,h]anthracene	1.400	388	90	167	80	2,590	170	170	446
Benzo[g,h,i]perylene	1.000	1,265	246	131	260	3,690	1,040	260	446
Total PAHs	-	555,782	667,369	495,085	397,116	221,069	181,845	115,670	133,284
BaP-equivalent	**-**	**18,700**	**12,500**	**5,300**	**2,430**	**31,100**	**18,900**	**8,300**	**3,250**

RPF, relative potency factor

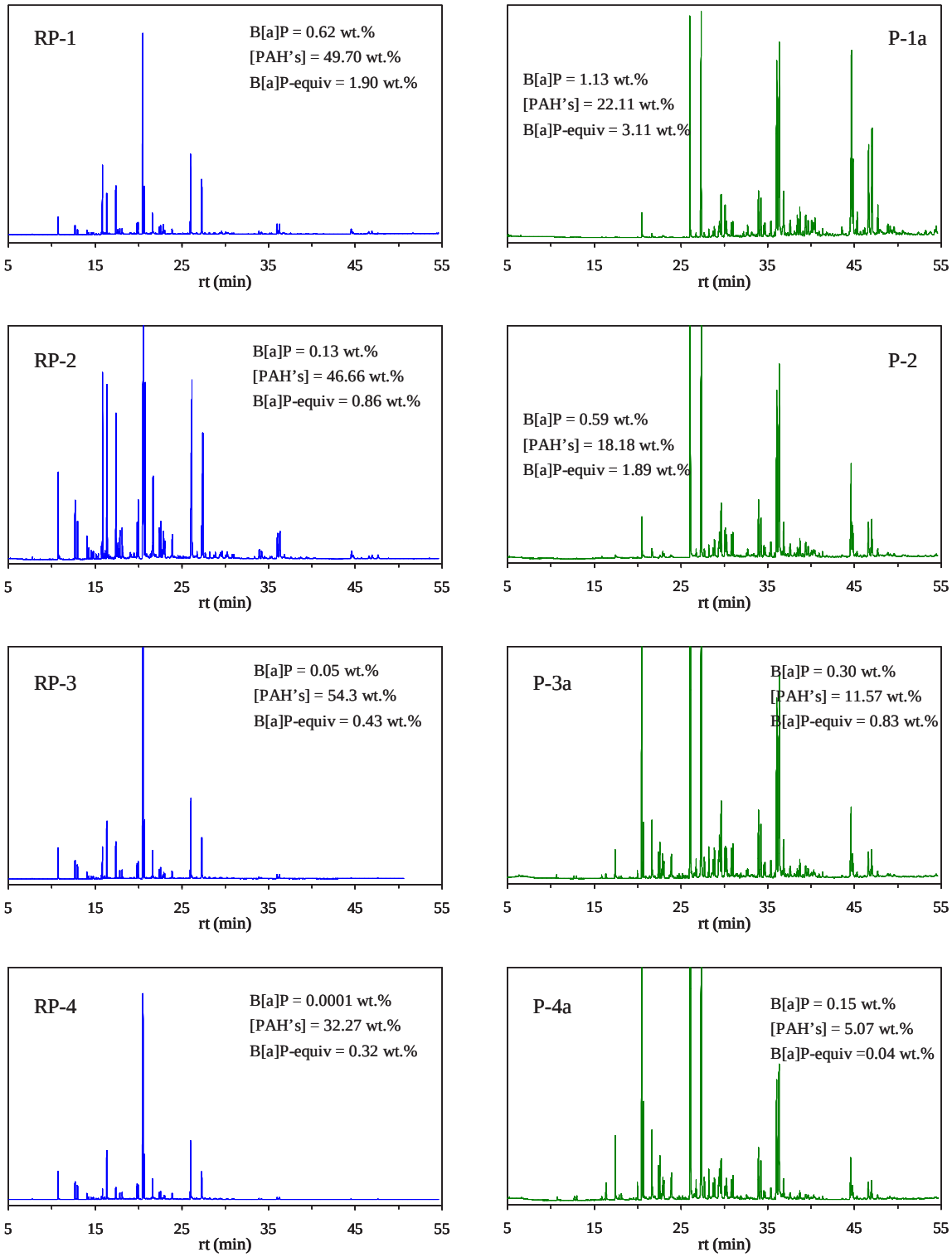

Figure 3.19. Genotoxicity of the reaction products (left) and pitches (right) determined by GC.

Work Package Conclusions

There were two main aims of this work. The first was to perform a detailed characterisation of the pitches produced from the "eco-pitch" process in terms of mass distribution and structural features. The second was to validate the procedure used to obtain this information; i.e. the use of planar-chromatography to aid the estimation of mass distributions. These data were then combined with data from NMR and EA to obtain average structural parameters. This method of characterisation was developed using a standard coal tar pitch (Cf. Ref 1 Chapter 7.0); the much larger sample set from the eco-pitch process provided a test of this approach, where the analyses were carried out in a more routine manner on samples of commercial interest.

Overall, the two aims seem to have been successfully achieved. Through the use of fractionation, differences amongst the pitches were detected that are not apparent from the analysis of the bulk samples. Through the combination and correlation of data from SEC, UV-F, LD-MS, NMR and EA, differences in mass and structure were found. The most important of these was the determination of changes in the amount of cata-condensed aromatic carbon and aromatic carbon substituted with aromatic groups. These parameters revealed a change in structure that could be related to the processing conditions and properties of the pitches. From this information basic reaction mechanisms were able to be inferred for the process.

Larger molecular sizes and larger polynuclear aromatic ring systems were observed in the pitch samples recovered from the later processing cycles, indicating that samples were getting progressively heavier with the increasing severity of the oxidative and thermal treatment steps. The most important differences found during the characterisation was in the amounts of cata-condensed aromatic carbon (Ccata) and aromatic carbon substituted with aromatic groups (Car-AS) detected in samples from different cycles of the process. Comparing these parameters revealed a change in structure that could be related to the processing conditions and properties of the pitches. From this information it was possible to infer basic reaction mechanisms for the process.

For the pitch produced from the first cycle of the process (P-1), a higher proportion of its carbon is in cata-condensed aromatic environments than the pitch from the fourth cycle. On the other hand, the pitch from the fourth cycle has the most Car-AS. This information suggests either a change in the reaction pathway for AO-1 to P-1 compared to AO-4 to P-4, or a progressive set of structural changes of the successive reactants (where reactant in each phase is different). P-1 is formed from condensation and ring closure reactions which lead to increasing sizes of aromatic clusters and P-4 more through cross-linking reactions that form biphenyl-like aromatic-aromatic single bonds. At the same time the P-4 sample contains molecules of the highest average molecule mass and may contain the largest fused aromatic ring systems. An example of the difference types of structures produced in the formation of P-1 and P-4 is presented in Figures 3.20 and 3.21 respectively.

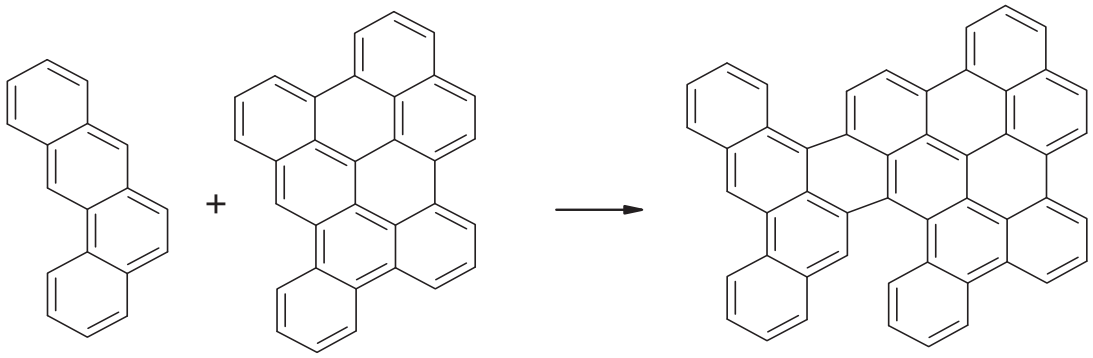

Figure 3.20. Simplified schematic example of the transformation of anthracene-oil AO-1 into pitch P-1.

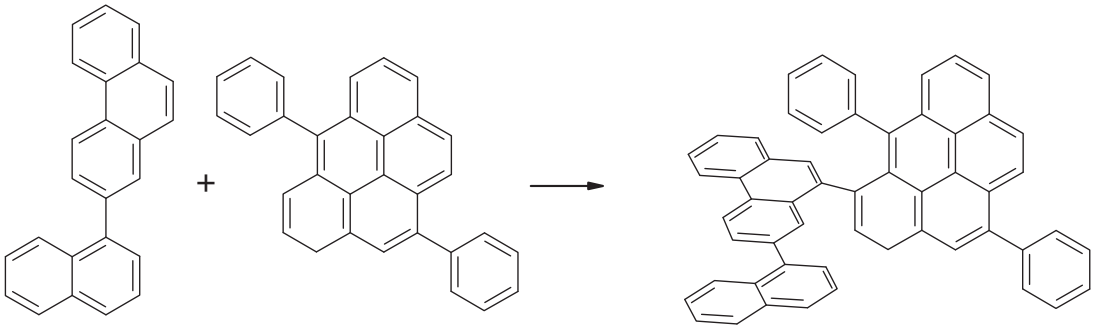

Figure 3.21. Simplified schematic example of the transformation of anthracene-oil AO-4 into pitch P-4.

Figures 3.20 and 3.21 are meant to show that the P-1 samples contain molecules that are more planar in geometry and that P-4 is more crossed-linked, with its fused aromatic ring systems possibly held in different planes to one-another. These conclusions on structure also match findings from independent work on the pyrolysis behaviour and ability of these pitches to generate mesophase and coke. That work was carried out at INCAR, Oviedo, Spain, and has been published[2] in conjugation with the work presented in Ref 1. Work regarding the mechanisms involved in the cross linking reactions between pitch and oxygen has been reported by other researchers[4,5].

The detailed characterisation of the pitch samples using the ASP method highlighted changes in structure and mass. The basic reaction mechanisms inferred from these studies correlate well with independent work on the same samples. In both sets of work similar conclusion were reached on the structural make-up of the pitches from different cycles of the process.

Upon pyrolysis, both the reaction products and the pitches gave rise to mesophase formation. However, “reaction products” require more severe reaction conditions to produce mesophase contents similar to those from the corresponding pitches. The effect of heat treatment on the pitch produced from the first cycle (P-1) showed that it more readily generated mesophase. On further heating, this mesophase led to coke with a flow-domain optical texture that is indicative of large areas of fused aromatic ring systems (i.e. in the form of pre-graphitic structures). The pitch from the fourth cycle generated lower quantities of mesophase; on further heating a coke that is less ordered and containing smaller regions, fused-aromatic-ring systems were produced that had a ‘mosaic’ optical texture.

After identification of the genotoxic compounds by mass spectrometry, these compounds were quantified in all the anthracene oil derivatives by gas chromatography. The results showed that the content in genotoxic compounds diminished with each anthracene oil processing cycle. Thus, the benzo[a]pyrene content in P-4 is ten times lower than P-1.

WORK PACKAGE 4. Feasibility of trial pitches for graphite electrode, pinstock and cathode preparation

The general objective of this work package was to test the possibility of using anthracene oil-based pitches in the preparation of graphite electrodes. Although a preliminary exhaustive characterization of the samples was made in work packages 2 and 3, WP-4 also includes a preliminary study of the pitches and the results are compared with those obtained for standard impregnating and binder coal-tar pitches. This is to facilitate the further understating of the role of the ecopitches in the preparation of the graphite electrodes. This work package was entirely responsibility of Carbone Savoie.

Task 4.0 : Preliminary characterization

A list of the different pitch samples supplied by IQNSA, at various steps of the process, either with a 90°C Mettler Softening Point (for impregnation application), or with a 110°C Mettler Softening Point (for binder application) is given in Table 4.1. We have received some samples in large quantities (4 tons) in order to be able to impregnate large blocks in Parma (GRAFTECH's central laboratory).

For the impregnation application, the analyses performed on the different samples are summarized in Table 4.2, and for the binder application in Table 4.3. Some samples come from the same production batch in IQNSA.

The evolution of pitch viscosity versus temperature and the thermogravimetrical analyses are given in the figures 4.1 to 4.4, for both 90°C and 110°C SP samples.

There is a large dispersion of characteristics, even for pitch samples processed at the same step, therefore it is difficult to see a significant effect of the process step. For 90°C SP samples, density and carbon yield decrease when the process step increases, and the same trend could be seen on 110°C SP samples. The only clear evolution that can be observed for both families of softening point, is the shift of the first peak of volatiles departure (seen on the thermogravimetric curves) towards lower temperatures when the process advances.

For 90°C SP samples, the Ecopitch is compared to a standard coal tar pitch produced by IQNSA, whereas for 110°C SP samples, the Ecopitch is compared to typical standard coal tar pitches, with a range of average characteristics. Generally speaking the Ecopitch is lower in density and carbon yield than standard coal tar pitches. Quinoleine insolubles or anthracene oil insolubles are very low for the Ecopitch, but the toluene insolubles are higher for the Ecopitch impregnating pitches compared to the reference, whereas it is the opposite for the Ecopitch binder pitches.

The viscosity versus temperature is either similar or higher for Ecopitch samples compared to the references, which is in accordance with the higher level of wetting temperature.
The TGA curves show that the first peak of volatiles departure is located at lower temperatures for Ecopitch than for standard coal tar pitches, and several small peaks can be observed instead of a large one, reflecting the presence of lighter structures.

Task 4.1 Electrode testing

No further work done during the last months, following GRAFTECH decision to stop.

Task 4.2 Simulation of pinstock PI

Same as Task 4.1.

Task 4.3 Large scale study

Same as Task 4.1.

Task 4.4 Evaluation of cathode block pitch impregnation

A subcontract has been signed between GRAFTECH and CARBONE SAVOIE in order that cathode blocks could be impregnated in Parma (GRAFTECH's central laboratory). After the poor results obtained during the impregnation of small electrode and pinstock samples with P1-B pitch (see tasks 4.1 and 4.2), it has been decided to try to study further processing steps, that would decrease the BaP content, and to perform trials on larger samples. At the end of task 4.1, P4-B had been selected and 4 tons of this pitch has been sent to Parma. Two graphitized cathode blocks 305 * 305 * 1778 mm have been impregnated, one with P4-B and one with IQNSA reference coal tar pitch (n° RC5032). The impregnation cycle comprises 6 hours under vaccum and 20 hours under pressure to fill the block porosity with the pitch. The weight of the blocks before impregnation was 200 kg, and the weight after impregnation was 214 and 216 kg for both blocks, giving a pickup of around 7 % for the two pitches. This pickup value is very low compared to values in industrial facilities (around 17%).

After impregnation, the two blocks have been rebaked in Parma before being shipped back to Carbone Savoie for analyses.

A slab has been taken at each block end, and the main physico-chemical characteristics have been determined on both ends, for both blocks. The results are given in Table 4.4. Compared to industrial impregnated products, the two blocks impregnated in Parma have been poorly impregnated: density is very low, porosity is very high, mechanical properties are much lower. Only the side B with the reference pitch presents characteristics reflecting the effect of impregnation, but for both sides A, the density and the porosity are at the level measured in the initial block before impregnation. A strong gradient in the block itself can observed, and clearly both sides B are partially or almost totally impregnated, whereas both sides A are almost not impregnated at all.

The weight loss per oxidation is very high for the side B with the reference pitch, and rather high for the side B with the Ecopitch P4-B, which confirms the presence of impregnation pitch (with a higher reactivity than the rest of the block). These high values compared to the oxidation level of industrial products, could be due to a low level of temperature during the rebaking treatment.

We cannot clearly distinguish any difference due to the impregnation pitch itself. Both pitches have the same aspect under optical microscope (see Figure 4.5). Even if the impregnation treatment has not been performed under representative conditions, we will conclude that the anthracene oil derivated pitch at the fourth step (P4-B) could be a potential candidate for the impregnation of the cathode blocks, with a lower PaH (and BaP) content.

In parallel to the study, the evaluation of the anthracene-oil derivated pitch as a potential binder pitch has been performed. From Task 4.1, P4-A pitch has been chosen, mainly because it leads to the highest decrease in PaH. Small artefacts of carbon cathode samples have been prepared with P4-A sample as a binder, and the final properties after baking have been determined and compared to the ones of reference samples made with a standard coal tar pitch. The size of the samples is 90 mm diameter and 150 mm height. The binder level has been first optimized to give the best properties, and it is higher with P4-A (+0.5%) than with the reference. The weight loss during baking is much higher for the samples with P4-A binder: 59 and 64%, compared to 43% with the reference pitch. This could be related to the lower carbon yield of the Ecopitch samples.

In relation to this high weight loss, the final properties of the carbon products are very low in density and mechanical strength (see Table 4.5).

Therefore we can conclude that the anthracene-oil derivated pitch, even if it would have a positive environnemental impact, could not be used as a binder in carbon cathodes. Would it be acceptable as a binder in the anode business? It could be interesting to consider, as the final properties required are different from the ones of cathodes, and as the tonnages involved are much higher.

Table 4.1. List of the different samples received, with their internal reference number.

Arrival date	Internal ref n° n° RC	IMPREGNATION PITCH 90°C Mettler	BINDER PITCH 110°C Mettler
28/11/2005	4829	P1b	
10/04/2006	4936		P2a
10/04/2006	4937		P4a
30/08/2006	5032	Nalon standard ref for Parma (4 tons)	
30/08/2006	5033	P1b for Parma (4 tons)	
06/12/2006	5136A		P3a
06/12/2006	5136B	P3b	
12/03/2007	5227	P4b (preliminary to the 4 tons sample)	
10/05/2007	5276		P3a
10/05/2007	5277		P4a
29/05/2007	5288	P4b (4 tons)	
05/11/2007	5386		P4a (3rd sample)

Table 4.2. Characteristics of the different 90°C SP samples (impregnation).

n° RC	Sample	CV (%)	FR (g/80mn)	QI (%)	TI (%)	C (%)	H (%)	N (%)	S (%)	C/H	density	FP (°C)	SP (°C)	Wetting T (°C)
4829	P1b	39,9	67	0,04	21,3						1,276	252	85,7	
5033	P1b (4 MT)	40,8	20 -11,5	1	24,4	94,26	4,83	0,85	-	1,63	1,277	258	86,3	
5136 B	P3b	41,9	19,6	0,8	21,9	90,13	4,6	0,87	0,97	1,63	1,274			115,5
5227	P4b	36,7	19	0,2		92,3	4,92	0,84	1,07	1,56	1,268	240	94,2	111,4
5288	P4b	38,8	19	0,9	21,4	91,86	4,95	-	-	1,54	1,263	230	92,1	111,3
5032	ref IQNSA	41,6	9,4	1,4	18,6	93,81	4,99	0,66	-	1,57	1,277	268	88	

FR : Filtration rate – FP : Flash Point – SP : Softening Point

Table 4.3. Characteristics of the different 110°C SP samples (binder).

n° RC	sample	CV (%)	density	Wetting T (°C)	C (%)	H (%)	N (%)	S (%)	C/H	TI	AOI (%)	C/H (AOI)
4936	P2	51,6		155	92,6	4,4	0,5	1,1	1,76	32,7	3,96	
5136A	P3a	48,1	1,29	146	92,8	4,5	1,0	0,97	1,7	29,5	3,63	
5276	P3a	47,0	1,276	151	91,6	4,7			1,63			3,72
4937	P4a	48,1		150,3	93,4	4,4	0,4	1,3	1,74	29,5	1,76	
5277	P4a	45,2	1,279	141	91,4	4,3			1,72	26,4	0,9	
5386	P4a	44,9	1,281	141,5	91,7	4,5			1,7	29,4	1,07	3,84
	ref	50-53	1,298-1,315	133-137	93,4	4,6	1,1	0,9	1,7-1,8	22-26	6-12	4 - 5,5

AOI : Anthracene oil insolubles (very close to QI content)

Table 4.4. Characteristics of the blocks impregnated with reference IQNSA pitch and with P4-B pitch. (WG : with-grain direction, AG : across-grain direction)

		RC5556 block		RC5557 block		industrial ref
		side A	side B	side A	side B	
	Impregnation pitch	std IQNSA (RC5032)		P4B (RC5288)		
Apparent hydrostatic density		1,636	1,714	1,645	1,67	1,76
Open porosity	(%)	20,4	15,6	19,5	18	14,2
Real density		2,191	2,174	2,192	2,189	2,175
Total porosity	(%)	25,4	21,1	25	23,7	19,2
Ash content	(%)	1,1	1,05	1,03	0,95	1,08
Electrical Resistivity WG	(µohm.m)	10,4	10,4	10,1	10	11,9
Electrical Resistivity AG		12,5	11,8	11,5	11,3	13,7
Young's modulus WG	(GPa)	7,9	9,8	7,8	9,4	10,6
Young's modulus AG		6,5	8,3	6,9	7,7	8,7
Flexural strength WG	(MPa)	14,8	19,3	15,2	18,1	20,5
Flexural strength AG		12	15,8	12,8	14,7	16,3
Crushing strength WG	(MPa)	29,9	36,6	28,8	34,8	39,4
Crushing strength AG		26,2	35,9	26,7	32,3	39,4
Thermal conductivity WG	(W/mK)	133	130	125	129	129
Thermal conductivity AG		108	112	115	117	99
CTE WG	(10-6/°C)	2,86	2,99	2,85	3,03	3,28
CTE AG		3,32	3,57	3,5	3,63	3,6
Air permeability WG	(nPerm)	2,5	1,4	2,3	1,8	2,6
Air permeability AG		1,6	1,7	3,1	1,9	1,7
oxidation	(%)	1,9	4,1	0,92	2,11	1,5

Table 4.5. Characteristics of the carbon artefacts made with a standard coal tar pitch as the binder, and with P4-A ecopitch as the binder

	Binder	std CTP	std CTP	P4a	P4a
Green density		1,681	1,686	1,661	1,664
Geo density after baking		1,515	1,503	1,432	1,419
Apparent hydrostatic density		1,517	1,509	1,443	1,425
Open porosity	(%)	23,8	24,3	27,8	28,7
Electrical Resistivity	(µohm.m)	24,8	25,3	31,3	34,5
Young's modulus	(GPa)	5,8	5,7	3,7	3,6
Flexural strength	(MPa)	8,3	7,3	4,0	3,8
Crushing strength	(MPa)	18,1	19,4	13,0	11,2
Thermal conductivity	(W/mK)	25,3	24,5	19,9	20,1
CTE	(10^{-6}/°C)	3,51	3,51	3,49	3,42
oxidation	(%)	1,3	1,7	1,4	2,0

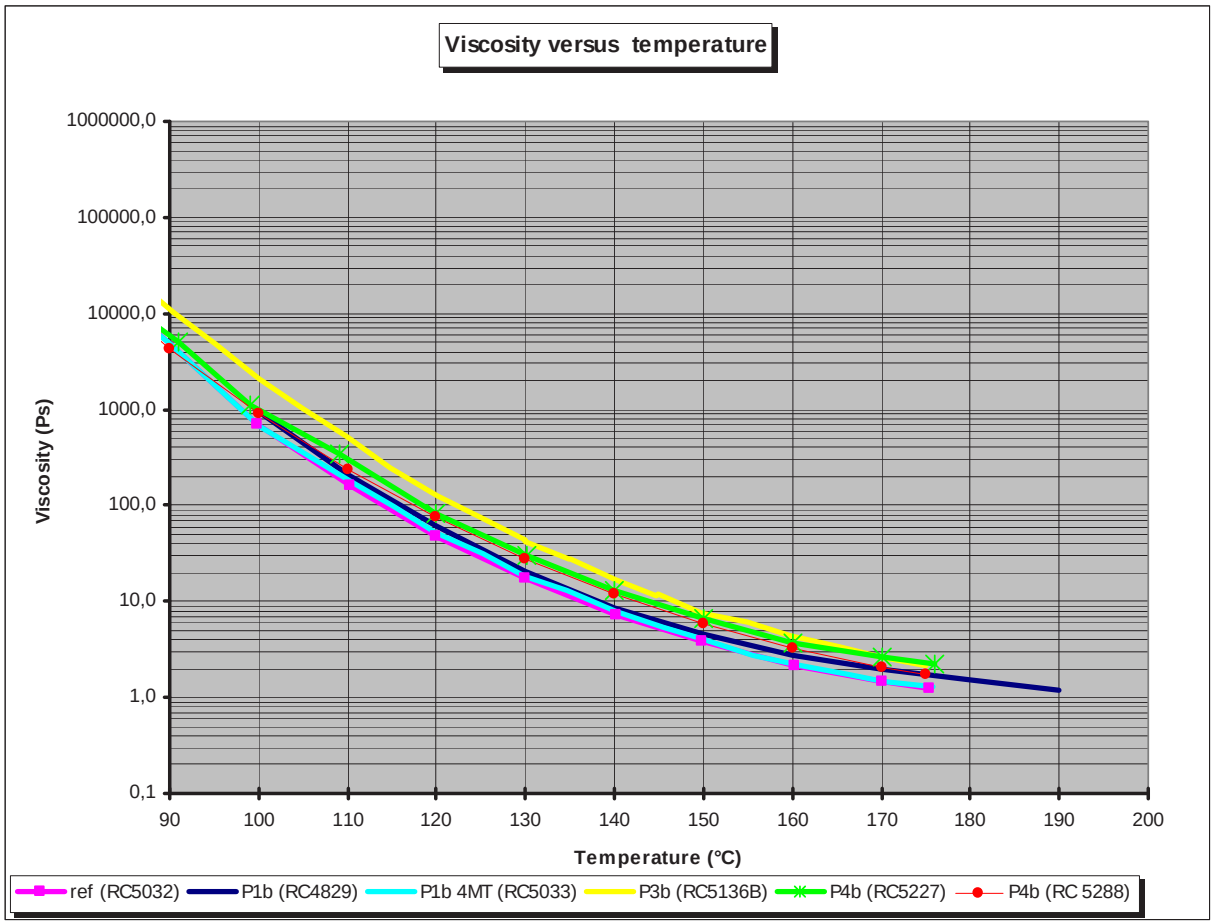

Figure 4.1. Viscosity versus temperature of the different 90°C SP samples.

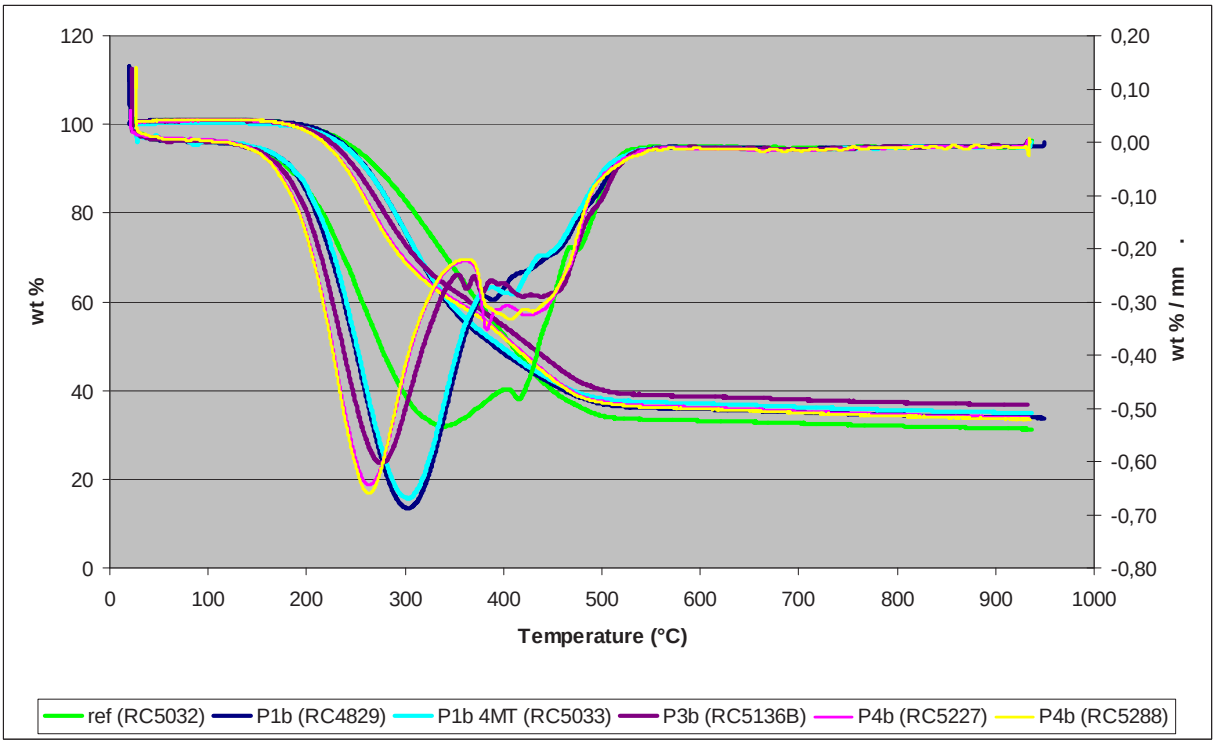

Figure 4.2. TGA curves of the different 90°C SP samples.

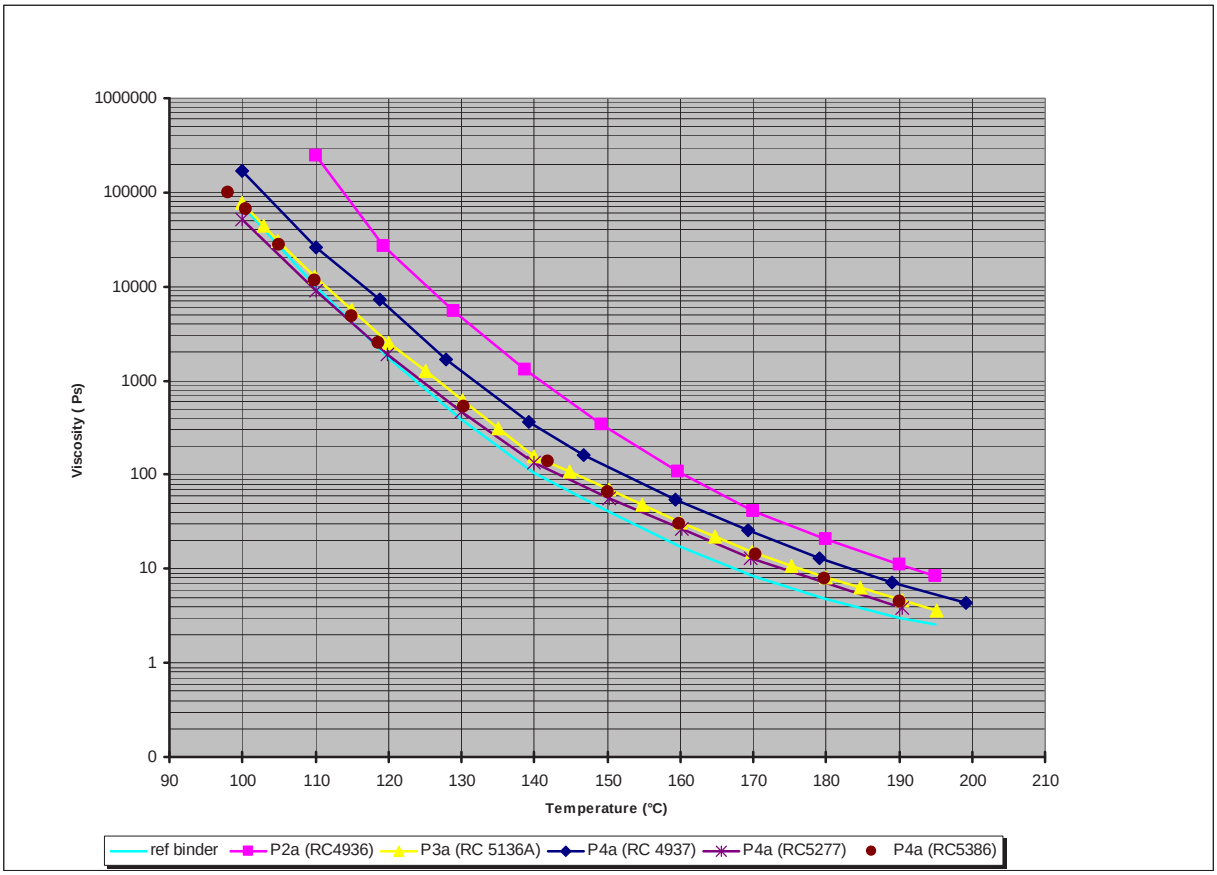

Figure 4.3. Viscosity versus temperature of the different 110°C SP samples.

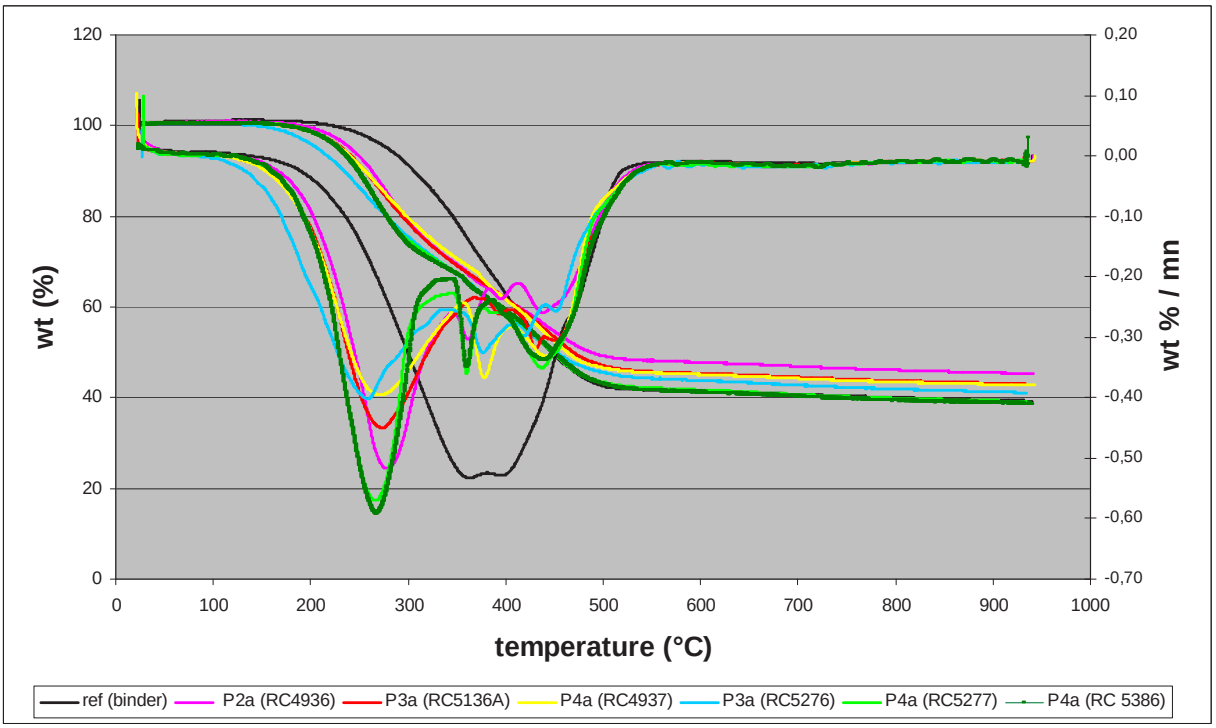

Figure 4.4. TGA curves of the different 110°C SP samples.

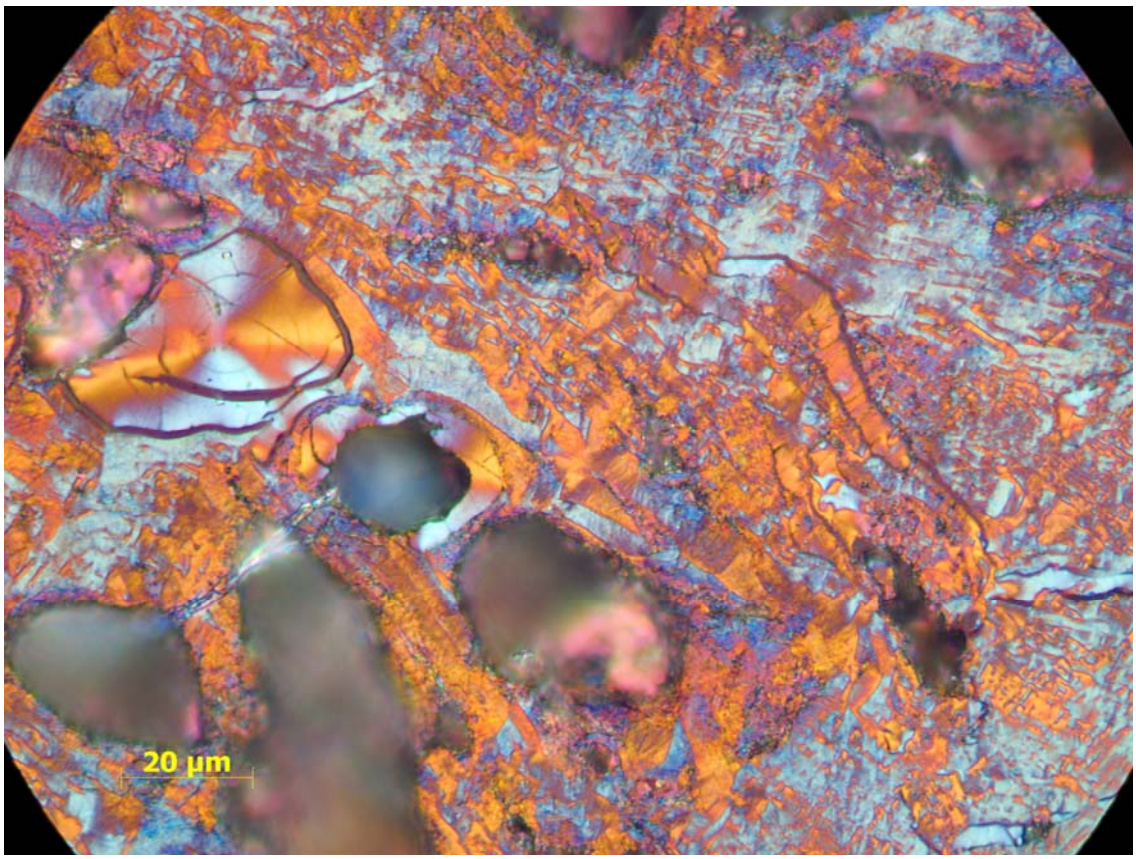

Figure 4.5. Observation under optical microscope of the block impregnated with standard IQNSA pitch.

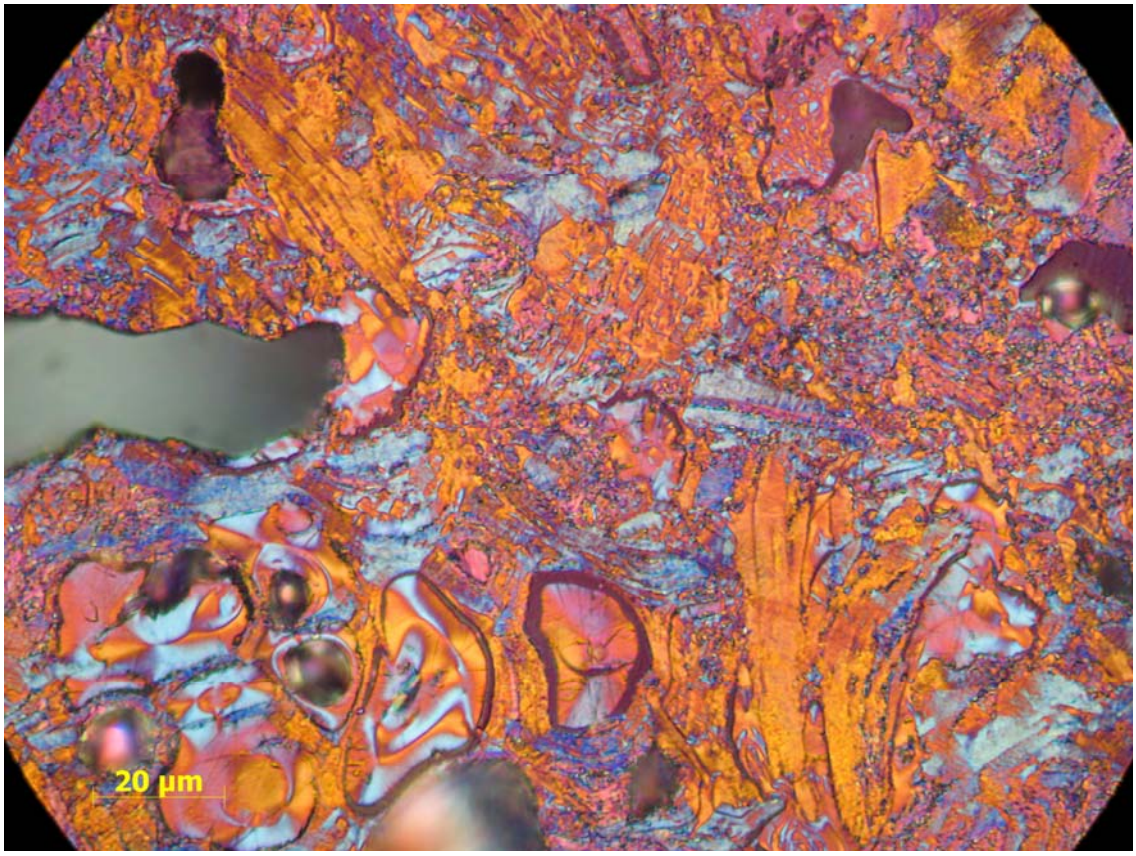

Figure 4.6. Observation under optical microscope of the block impregnated with P4-B Ecopitch.

Work Package conclusions

Carbone Savoie responsibilities inside the Ecopitch project, was to evaluate the possibility of the anthracene oil derivated pitch to be used an as impregnation pitch in electrodes, pinstocks and cathode materials. Due to industrial reorganization with Alcan taking over Carbone Savoie, the study has been done at the end on cathode products only, and the fourth step of process of the Ecopitch has proven to be a potential candidate for the impregnation of the cathode blocks with a lower PaH (and BaP) content.

Meanwhile the use of the Ecopitch as an alternative to standard coal tar pitch binders has been evaluated, but the application in cathode materials cannot be considered due to low final properties. The question of an application for anode materials is still open.

WORK PACKAGE 5. Preparation and testing of advanced carbon materials

The general objective of this work package was to carry out a prospective study of the feasibility of using anthracene oil derivatives to produce carbon fibres and mesophase-based materials. These activities were carried out by INCAR-CSIC and WUT.

Task 5.1 Carbon fibres

5.1.1. Carbon fibre precursors (INCAR-CSIC)

Two anthracene oil-based mesophases were used in this study: Meso-1 and Meso-2. The preparation procedure and the main characteristics of these mesophases were widely described in the WP-2 and WP-3. Briefly, Meso-1 was obtained from RP-1 by thermal treatment (with and without gaseous pressure) and subsequent sedimentation to concentrate the mesophase. Meso-2 was obtained using as raw materials the isotropic phase (Iso-1) generated during the preparation of Meso-1. Iso-1 was thermally treated and then sedimented to produce Meso-2.

All attempts to spin Meso-1 into fibres failed. A possible explanation for this could be the less control over the size of the pseudo-graphitic layers during the early stages of mesophase formation. Thus, the most reactive compounds in RP-1 would be able to develop a liquid crystal phase (mesophase) in the very early stages of the thermal treatment. This reactive mesophase could then mature into a highly polymerized mesophase during the whole thermal treatment. The small proportion of highly matured mesophase obtained together with the fresh mesophase formed at the end of the sedimentation process would contribute to a deterioration in the properties of the mesophase as a fibre precursor. It is worth noting that all other mesophases prepared in our previous work were tested and were found to exhibit the same behaviour. For this reason, a second mesophase (Meso-2) was prepared. This mesophase was successfully spun and then transformed into carbon fibres.

Figure 5.1. Fibre-maker equipment (left). In more detail, fibre spinning device (right) with spinnerets.

5.1.2 Carbon fibre preparation (INCAR-CSIC)

The carbon fibres were prepared following a three consecutive step procedure. This procedure involved: (i) the spinning of the mesophase into fibres, (ii) the stabilization of the green fibres and (iii) carbonization to obtain the final carbon fibres.

The spinning was performed by using a special apparatus consisting of a stainless steel reactor (spinning device) and a rotating spool (winding device), Figure 5.1. The reactor was equipped with a control pressure system, a thermocouple and a one-hole graphite exchangeable spinneret. Before extrusion, the mesophase was heated to a temperature slightly higher than its softening point (230 °C). Once the mesophase was sufficiently fluid, it was spun and directed to the rotating spool, where it was wound into fibres (green fibres). By this procedure, Meso-2 was spun into fibres with different diameters (Figure 5.2).

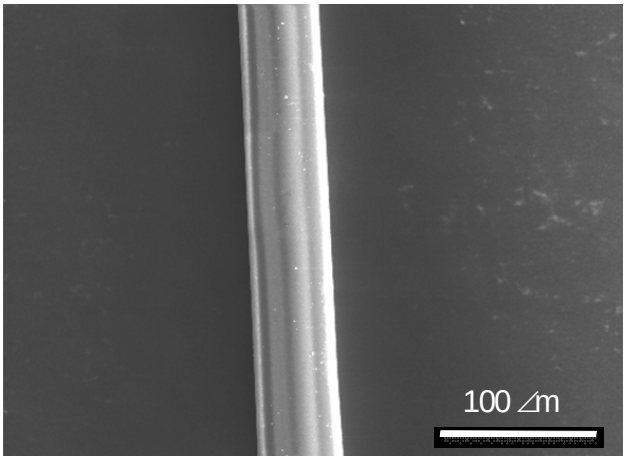

Figure 5.2. SEM micrograph of a green fibre obtained from Meso-2.

Stabilization of the green fibres in air before carbonization is necessary in order to reduce the fusibility of the fibre and so avoid its deformation during the subsequent carbonization. In this study, three different stabilization temperatures were used 220, 250 and 300 °C giving rise to 'SFibre 225', 'SFibre 250' and 'SFibre 300', respectively. Stabilization introduces oxygen functionalities at the surface of the fibre, producing a drastic change in the pyrolysis behaviour of the fibre (Figure 5.3). Thermogravimetric analysis of the samples showed that stabilization caused a significant reduction in weight loss when the temperature range of weight loss became shorter. It is worth noting the appearance of a small shoulder centered at ~ 700 °C, which was assigned to the decomposition of the oxygen functionalities introduced during stabilization.

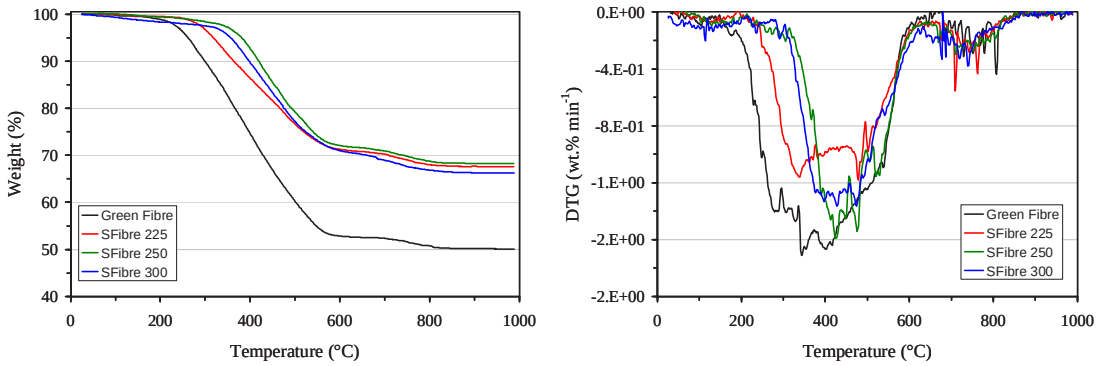

Figure 5.3. TG (left) and DTG (right) curves of the green and stabilized fibres obtained from Meso-2.

After stabilization, the fibres were carbonized in a horizontal tube furnace. The heating rate was increased at 10 ºC min^{-1} up to 1000 ºC and the residence time at this temperature was 1 h. The effect of temperature stabilization on the structure of the fibres carbonized to 1000 °C was apparent. Figure 5.4 shows the SEM micrographs of the carbon fibres obtained from Meso-2 stabilized at 225, 250 and 300 °C. Stabilization at 225 °C led to carbon fibres with a completely deteriorated structure. Damage caused by the release of volatiles was prominent (Figure 5.4a, position A) and the deteriorated carbon structure made it possible to observe the observation of the pseudo graphitic layers of the mesophase oriented along the spinning axis (Figure 5.4a, position B). Carbon fibres produced from the mesophase stabilized at 250 °C showed less deterioration than the previous one, but at the same time showed visible holes that had been produced during the release of volatiles (Figure 5.4b, position A). Finally, stabilization of the mesophase at 300 °C led to carbon fibres with a 'clean' surface, without any visible imperfections (Figure 5.4c). These results suggest that stabilization of mesophase at the highest possible temperature without allowing it to reach the point of combustion is one of the key challenges to avoid fibre surface imperfections, and therefore, to improve the properties of the final carbon fibre.

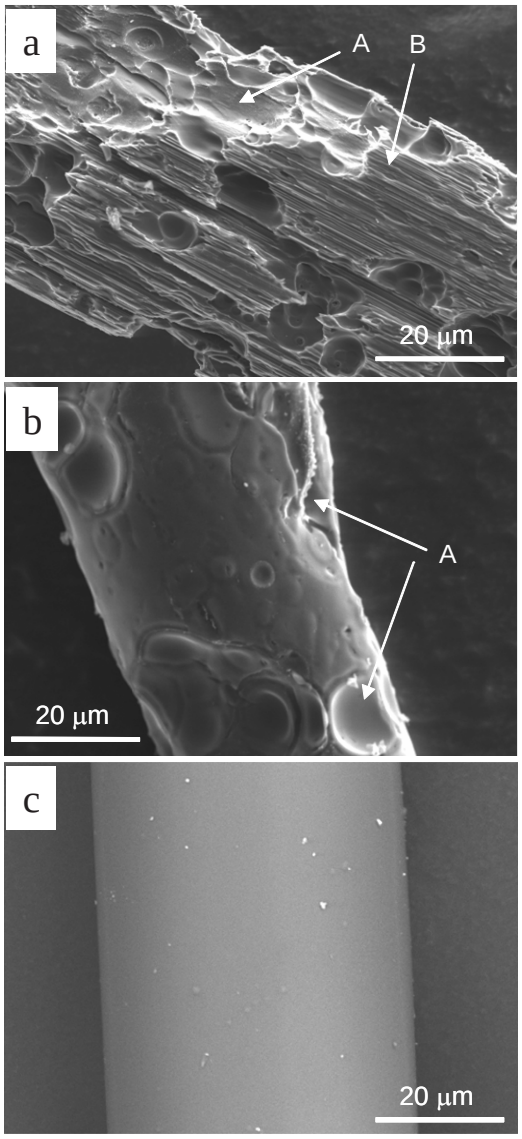

Figure 5.4. SEM micrograph of carbon fibres obtained from Meso-2 stabilized at (a) 225, (b) 250 and (c) 300 °C.

These promising results open the door for future investigation on the production of carbon/graphitic fibres from mesophase obtained from anthracene oil-based pitches. However, further studies must be carried out in order to elucidate crucial aspects related to carbon fibre preparation, especially those aspects related to the characteristics of the raw material. In this regard, studies aimed at obtaining a 'superb' mesophase with a reduction in the processing steps needed to produce the fibres described in the present project would be of great interest.

Task 5.2 Mesophase-based carbon materials

5.2.1. Evaluation of anthracene oil-derived pitches as precursors of carbon materials (WUT)
Pitches P-1, P-2, P-3 and P-4 used in the study were supplied by IQNSA. They derived from reaction products RP-1, RP-2, RP-3 and RP-4, respectively, which, in turn, were produced by thermal oxidative condensation of anthracene oils AO-1, AO-2, AO-3 and AO-4, respectively.

The specific objective of this preliminary part of study was to evaluate the suitability of pitches from different stages of anthracene oil processing as precursors for the graphitic and porous materials. The work included the determination of chemical composition and normalized properties of pitches and characterization of resultant cokes in terms of optical texture, graphitizability (HTT 2900^{o}C for 1 hour) and reactivity towards KOH and NaOH. The procedures applied to a given pitch were exactly the same to avoid any possible effect of the treatment variables on the parameters measured. The treatment with alkaline hydroxide was intended to compare the effect of activation agent (KOH or NaOH) and material origin on the porosity development. Based on the previous work [1], for the comparative activation study the physical mixture of a pitch semi-coke (HTT 520^{o}C, particle size 0.1-0.63 mm) and KOH/NaOH powder in 1:3 weight ratio was heat-treated at 800^{o}C for 1 h. The activations were performed in a nickel boat which was placed in a horizontal tubular quartz reactor under nitrogen flow.

Table 5.1. Characteristics of pitches P-1, P-2, P-3 and P-4

Determination		P-1	P-2	P-3	P-4
Softening point, SP (Mettler)	^{o}C	115	130	119	122
Toluene insolubles, TI	wt.%	23.8	34.6	30.1	30.9
Coking value, CV (Alcan)	wt.%	48.3	53.9	49.9	50.6
Elemental analysis (daf basis)	wt.%				
C		91.8	92.2	92.3	91.5
H		4.50	4.42	4.50	4.50
N		1.36	1.17	1.04	1.0
S		0.52	0.44	0.47	0.5
O $_{(diff)}$		1.8	1.7	1.7	2.5

Characteristics of the pitches are given in Table 5.1. Clearly, the pitches constitute one family. They all are practically QI free. The variations in toluene insoluble content (between 23.8 and 34.6%) and coking value (between 48.3 and 53.9%) should be attributed to differences in the softening point (between 115 and 130^{o}C) of the pitches due to various distillation cut off. Elemental composition is similar and typical of regular coal-tar pitches. The only meaningful difference lies in higher oxygen content of P-4 (2.5 vs. ~1.7 wt%), corresponding to more severe oxidation conditions.

Although flow type anisotropy predominates in the optical texture of cokes derived from P-1, P-2 and P-3, somewhat higher proportion of fine mosaics occurs in P-2 and P-3. P-4 derived coke, compared to those from pitches produced under milder oxidation conditions, is characterized by less developed anisotropy (medium and coarse mosaics), Figure 3.18 (WP-3). This correlates with enhanced oxygen content and proves that a partially cross linked system of limited ability to mesophase development is created on oxidative condensation of poorly reactive constituents of AO-4. Results of XRD analysis of materials graphitized at 2900^{o}C (Table 5.2) are very consistent with microscopic observations. P-1 derived graphite shows slightly better structural ordering than those from P-2, P-3 and P-4. The most pronounced difference is in the crystallite size, especially that of graphitic regions L_{112}. P-1 is, therefore, preferred as the precursor of graphitic carbons.

Porous texture of activated carbons derived from pitch semi-cokes was determined by N_2 adsorption at 77K (Table 5.3). In reaction with KOH under conditions used, all the pitch-cokes give ACs of extremely developed microporosity with a moderate weight loss. The worsening of structural arrangement from P-1 to P-4 cokes has a negligible effect on the porosity development on KOH activation. Reaction with NaOH, despite a considerably bigger weight loss, gives carbon with poorly developed porosity. Apparently, NaOH is an activated agent not suitable for the anisotropic precursors.

Table 5.2. Structural parameters of graphitic carbons prepared from P-1, P-2, P-3 and P-3 by heat-treatment at 2900°C for 1 hour

Determination		P-1	P-2	P-3	P-4
Interlayer spacing, d_{002}	nm	0.3364	0.3368	0.3369	0.3367
Apparent crystallite height, L_c	nm	47	37	41	34
Apparent crystallite diameter, L_a	nm	83	54	63	55
Size of graphitic regions, L_{112}	nm	14.4	11.5	11.9	9.8

Table 5.3. Porosity development in activated carbons produced using activation with KOH and NaOH of semi-cokes from P-1, P-2, P-3 and P-4 (800°C/1h, KOH(NaOH)/coke ratio 3:1)

Sample	Burn-off wt.%	S_{BET} m^2/g	V_T cm^3/g	V_{DR} cm^3/g	L_0 nm	V_{DR}/V_T
AP-1-520/800/3:1/KOH	22.9	2670	1.09	0.84	1.42	0.78
AP-2-520/800/3:1/KOH	21.2	2710	1.11	0.85	1.41	0.76
AP-3-520/800/3:1/KOH	22.6	2800	1.14	0.87	1.42	0.76
AP-4-520/800/3:1/KOH	21.6	2750	1.12	0.87	1.49	0.78
AP-1-520/800/3:1/NaOH	36.8	950	0.44	0.32	1.32	0.72
AP-2-520/800/3:1/NaOH	34.7	930	0.43	0.31	1.36	0.73
AP-3-520/800/3:1/NaOH	34.0	1015	0.47	0.34	1.31	0.72
AP-4-520/800/3:1/NaOH	35.6	780	0.36	0.26	1.32	0.73

S_{BET} – BET surface area
V_T - total pore volume
V_{DR} - micropore volume from Dubinin-Radushkevitch equation
L_0 - mean micropore width
V_{DR}/V_T – contribution of micropores to the total pore volume

Instead of porosity generation a complete disintegration of original particles occurs giving powder of particle size below 63 μm. In conclusion, only KOH is a suitable activation agent for the pitch derived carbons. P-1, P-2, P-3 and P-4 semi-cokes represent similar properties in terms of activation behaviour.

5.2.2. Synthesis of boron doped graphitic carbons for lithium-ion batteries (WUT)

High purity and structural perfection are primary requirements for the graphitic carbons to be used as an anode in the Li-ion battery. The interest in synthesis of boron doped graphites for Li-ion cells has twofold reasons. First, boron is well known as graphitization catalyst. Second, the presence of boron substituted for carbon in the lattice should, theoretically, result in the lithium storage in excess of stoichiometric LiC_6. The objective of our research was evaluation of suitability of anthracene oil derived graphitic carbon with superior properties as an electrode.

A series of pure and boronated graphites was synthesized from P-1 pitch using various heat-treatment routes. Raw materials for boronation were coke of 1000°C and graphitic carbon produced by coke heat-treatment and 2900°C. They were mixed with 2 wt% of nanopowder of boron, both crystalline (B_c) and amorphous (B_a), or boron carbide (B_4C) and annealed at 2300°C for 0.5 h under argon. Post-treatment in hydrogen at 700°C for 1 h was applied to remove any chemisorbed oxygen and to saturate possible dangling bonds. The flowsheet of preparation routes is given in Fig. 5.5.

5.2.3. Tailoring porosity development during KOH activation of pitch-derived carbons (WUT)

Specific applications of porous carbons as an electrode in the electric double layer capacitor or methane adsorbent require materials with well defined porous structure and surface chemistry. The literature concerning using pitch for preparation of activated carbons for these applications is relatively scarce [2,3]. This part of research has been focused on understanding factors which can be applied to control properties of AOP's derived activated carbons in terms of porosity development (N_2 sorption at 77 K), particle size distribution and surface properties (elemental composition, surface groups).

The effect of various variables can be summarized as follows:

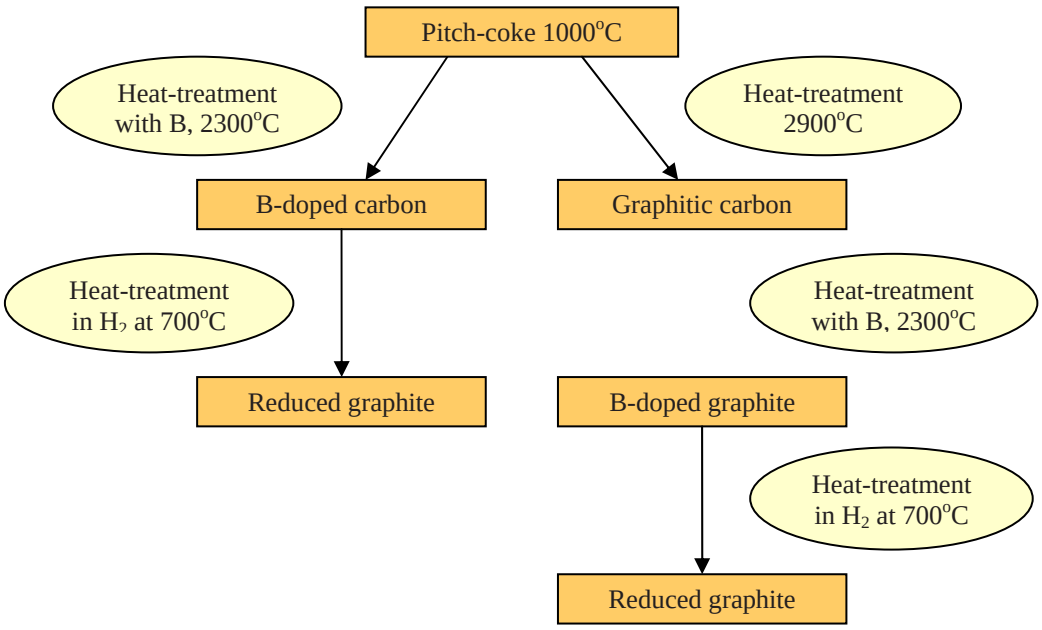

Fig. 5.5. Flowsheet of boron-doped graphite preparation routes used in the study.

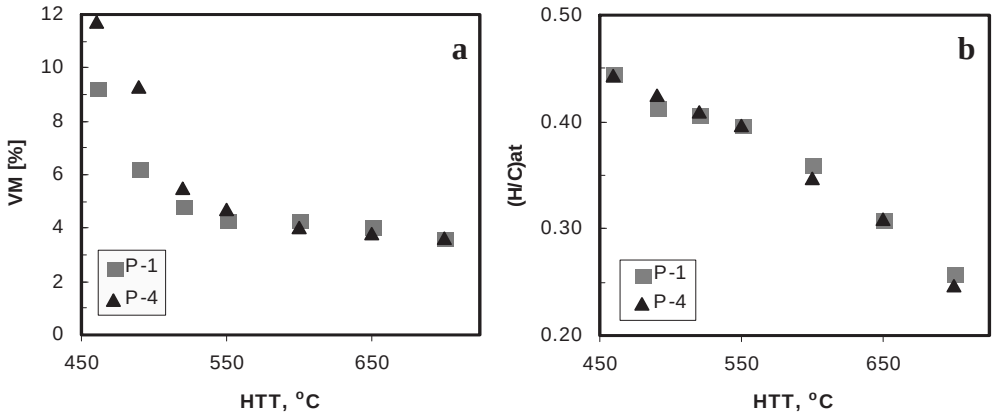

Fig. 5.6. Changes in the volatile matter content (a) and H/C atomic ratio (b) on the heat-treatment of pitches P1 and P4.

Structural organisation of precursor (optical texture)

As discussed in the chapter 5.2.1, the peculiarities in pitch semi-coke structure reflected by the optical texture varying from flow type (P-1) to medium/coarse mosaics (P-4) have a negligible effect on the activation behaviour. It has been demonstrated for P-1 that oxidation with nitric acid can be used to destroy pitch ability to mesophase formation. The semi-coke of near isotropic optical texture from the oxidized P-1 shows enhanced reactivity towards KOH compared to that from original P-1. For activation at 600°C the BET surface area increases from 2100 to 2430 m^2/g and at 700°C from 2460 to 2710 m^2/g.

Carbonization degree of precursor

A series of carbonaceous materials, mesophase pitches and semi-cokes, of varying carbonization degree was prepared by heat-treatment of P-1 and P-4 in the temperature range 460 – 700°C. The progress in carbonization with HTT resulted in the characteristic decrease in the volatile matter content VM and hydrogen to carbon ratio $(H/C)_{at}$, as presented in Fig. 5.6. The resultant mesophase pitches and semi-cokes were activated with KOH at 700 and 800°C for 1 hour using 3:1 KOH/precursor ratio. The reaction products were characterized using N_2 adsorption at 77 K and analysis of particle size distribution. The porous texture was characterized by BET surface area S_{BET}, total pore volume V_T,

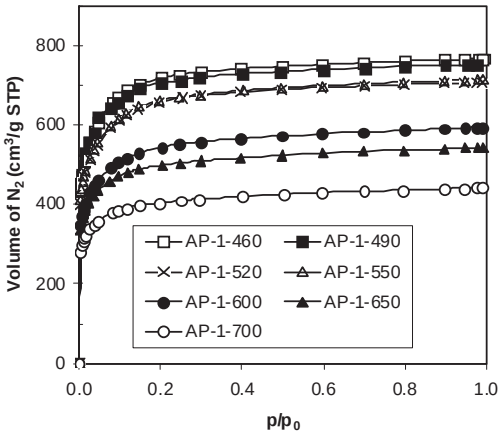

Fig. 5.7. N_2 adsorption isotherms for the series of activated carbons produced at 700°C from P-1 carbonization products.

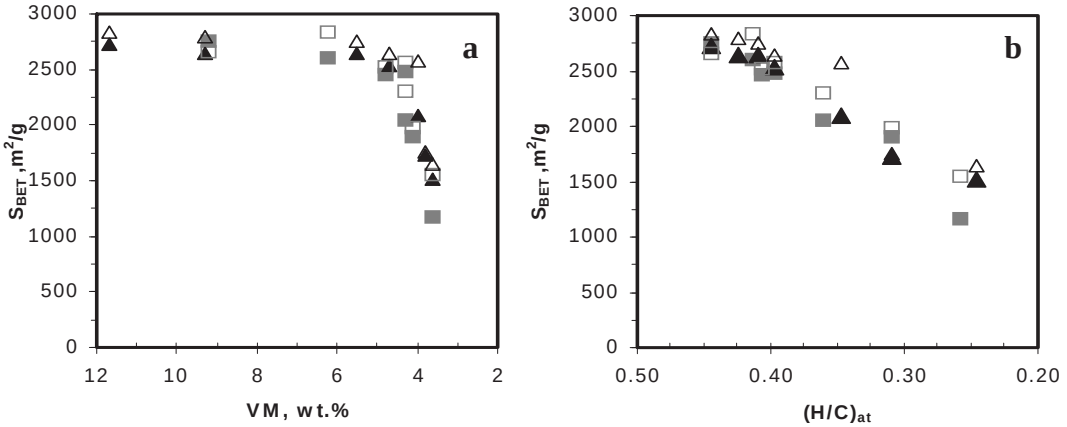

Fig. 5.8. Relation between BET surface area of KOH activated carbon derived from P-1 (■,□) and P-4 (▲,△) and the volatile matter content (a) and the H/C atomic ratio (b) for series of precursors derived from pitch P-1 and P-4. Open points - activation at 800°C, filled points - at 700°C.

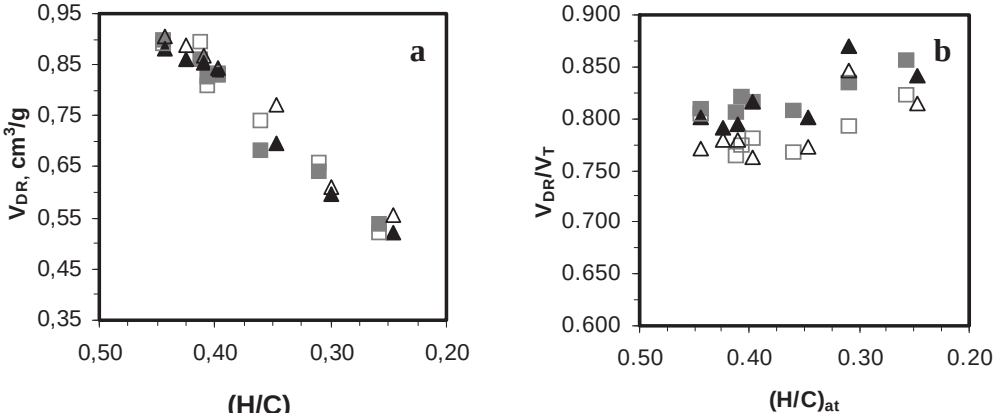

Fig. 5.9. Variation of microporosity parameters: micropore volume V_{DR} (a) and V_{DR}/V_T ratio (b) with carbonization degree $(H/C)_{at}$ for pitch derived carbons AP-1 (■,□) and AP-4 (▲,△)activated with KOH at 700°C and 800°C.

micropore volume V_{DR}, micropore volume contribution V_{DR}/V_T and mean micropore width L_0 based on N_2 adsorption isotherms.

Fig. 5.7 shows isotherms of N_2 adsorption at 77K for a series of P1 derived carbons which were activated at 700°C. The profile of isotherms clearly proves the microporous character of all materials

and decreasing nitrogen adsorption capacity with pitch HTT. The trend presented in Fig. 5.7 is representative of both pitches and the activation temperatures used.

The relation S_{BET} versus carbonization degree follows the same trend, which is different for VM and $(H/C)_{at}$, independent of the initial pitch and the activation temperature (Fig.5.8). In the case of VM, S_{BET} remains in the range of 2800-2500 m^2/g over a wide volatiles range from 12 to 4-5 wt% and decreases steeply to ~1500 m^2/g with further decrease in VM. The former range corresponds to the heat treatment between 460 and 550°C, i.e. to the stage of the mesophase formation and resolidification. The latter corresponds to the consolidation of semi-coke structure that is induced by hydrogen removal. For $(H/C)_{at}$ the relationship with S_{BET} is near linear. The behaviour suggests the importance of residual hydrogen for the porosity generation in the reaction with potassium hydroxide.

Fig. 5.9 illustrates the effect of carbonization degree of pitch, expressed as $(H/C)_{at}$, on the microporosity development during the activation at 700 and 800°C. The micropore volume V_{DR} decreases with carbonization progress from about 0.85 to about 0.50 cm^3/g with little effect of the activation temperature (Fig. 5.9a). Carbonization degree has a limited influence on the microporous nature of activated carbons produced from pitch derived precursors. V_{DR}/V_T ratio is between 0.75 and 0.9 and has a tendency to increase slightly with carbonization progress (Fig. 5.9b). The scattered points show decreasing micropore contribution as the activation temperature increases.

The reduction of propensity for porosity generation with pitch HTT is associated with enhanced disintegration of original coke particles as shown in Fig. 5.10.

The most relevant finding from this part of research is that the increase in pitch pretreatment temperature above 550°C results in a considerable reduction of porosity development however has a minor effect on pore size distribution in activated carbon.

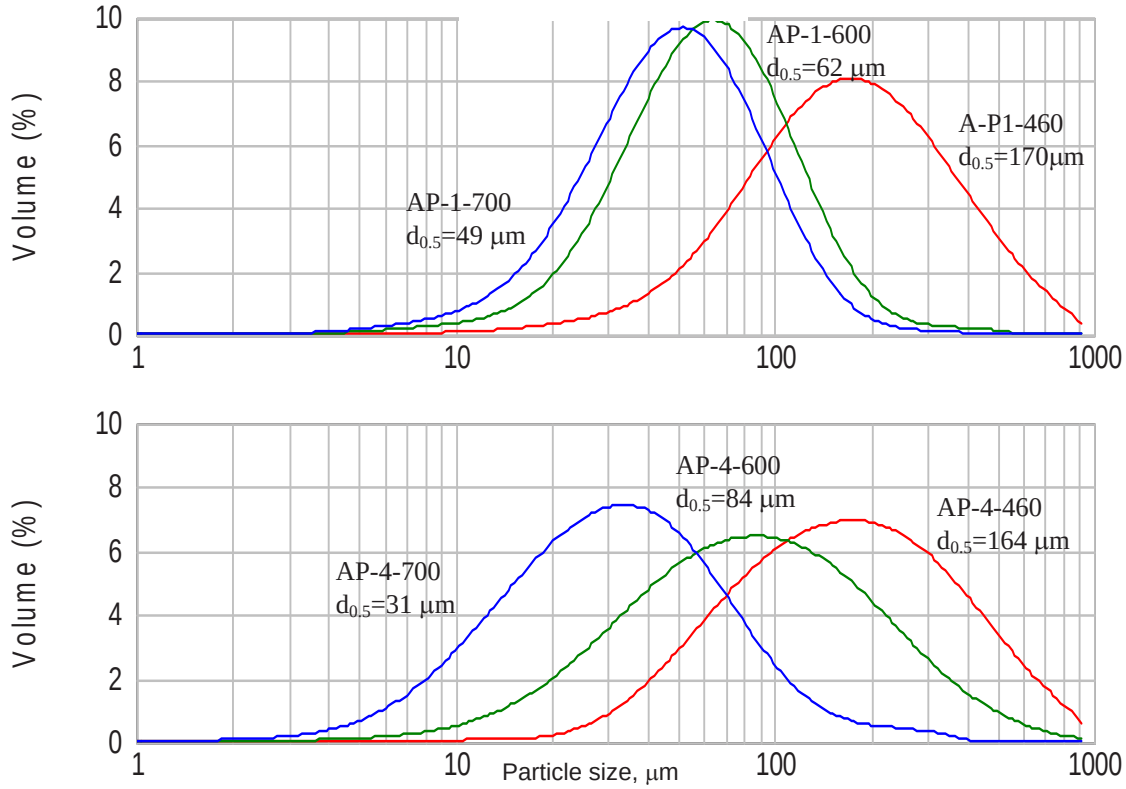

Fig. 5.10. Particle size distribution of KOH activated carbons (700°C) from P-1 and P-4 derived precursors of different carbonization degree.

Table 5.4. Effect of precursor particle size on the porosity development in KOH activated carbons produced from P-4 semi-coke at 700 and 750°C using KOH/coke ratio 2:1, 2.5:1 and 3:1

Sample	Burn-off wt%	S_{BET} m^2/g	V_T cm^3/g	V_{DR} cm^3/g	L_0 nm	V_{DR}/V_T
AP-4-520/700/2:1 – F1	12.1	1940	0.75	0.69	1.21	0.92
AP-4-520/700/2.5:1 – F1	14.7	2320	0.91	0.80	1.39	0.88
AP-4-520/700/3:1 – F1	18.0	2460	1.01	0.82	1.53	0.82
AP-4-520/700/2:1 – F2	10.9	1860	0.71	0.66	1.25	0.93
AP-4-520/700/2.5:1 – F2	14.3	2260	0.89	0.77	1.36	0.87
AP-4-520/700/3:1 – F2	18.0	2500	1.02	0.83	1.57	0.81
AP-4-520/750/2:1 – F1	14.2	2020	0.79	0.70	1.20	0.89
AP-4-520/750/2.5:1 – F1	17.2	2440	0.96	0.82	1.39	0.85
AP-4-520/750/3:1 – F1	20.1	2680	1.09	0.86	1.48	0.79
AP-4-520/750/2:1 – F2	13.7	1975	0.76	0.71	1.22	0.93
AP-4-520/750/2.5:1 – F2	17.3	2340	0.93	0.80	1.37	0.86
AP-4-520/750/3:1 – F2	20.9	2640	1.07	0.86	1.44	0.80

Precursor particle size and KOH/precursor ratio

To assess the effect of these two parameters on porosity development, the P-4 semi-coke samples of particle size in the range of 0.1-0.63 mm and 0.63–1.25 mm were activated at 700 and 750°C using KOH/coke ratio 3:1, 2.5:1 and 2:1. The porosity parameters calculated from N_2 adsorption isotherms, given in Table 5.4, show that increasing particle size practically has no effect on the porous texture characteristics. In contrast, the proportion of reagents is very essential for the control of both the surface area and pore size distribution of activated carbon. Narrowing of pores with a decrease of KOH/coke ratio from 3:1 to 2:1 has been confirmed by the evaluation of pore size distribution using DFT method (Fig. 5.11).

The reagent ratio is therefore a powerful parameter in the control of porous structure generated on KOH activation of pitch derived carbons.

Activation temperature

Increase in reaction temperature from 600 to 800°C results in a moderate enhancement of porosity development, i.e. in increase in pore volume and BET surface area and a widening of pores (Table 5.5). The change is more significant for the range of 600-700°C. Activation temperature is the major factor which controls surface chemistry of material. Activated carbon which is very rich in acidic oxygen groups: carboxylic, lactonic and phenolic is produced at 600°C. Increasing temperature results in significant reduction of total oxygen content and acidic functionalities (Table 5.6).

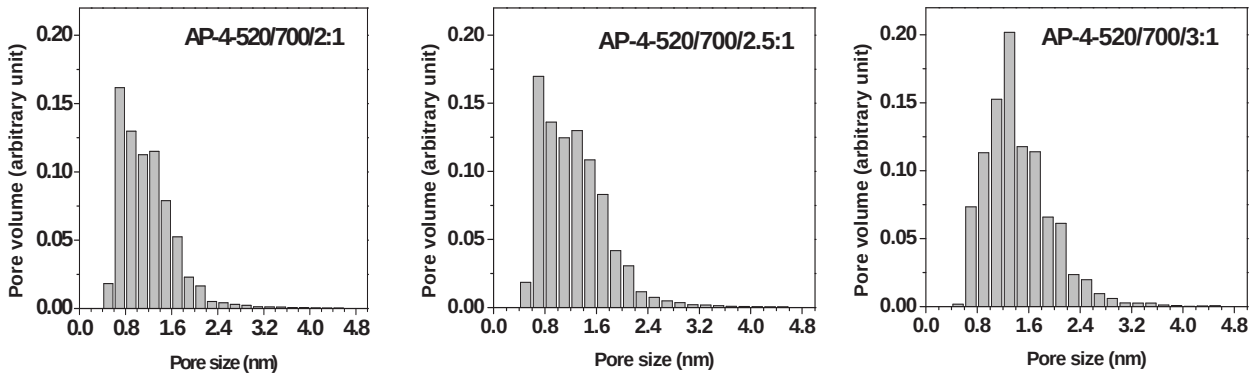

Fig. 5.11. Pore size distribution of activated carbons produced at 700°C using different KOH/P-4 semi-coke ratio.

Table 5.5. Porosity parameters of KOH activated carbons produced from P1 semi-cokes at different activation temperature, KOH/C-P1 3:1

Sample	Burn-off wt%	S_{BET} m^2/g	V_T cm^3/g	V_{DR} cm^3/g	L_0 Nm	V_{DR}/V_T
AP-1-520/600/3:1	14.6	2110	0.85	0.72	1.42	0.85
AP-1-520/700/3:1	19.9	2460	1.00	0.82	1.45	0.82
AP-1-520/800/3:1	22.9	2670	1.09	0.84	1.42	0.78

Table 5.6. Surface properties of KOH activated carbons produced from P1 semi-cokes at different activation temperature, KOH/C-P1 3:1

Sample	Oxygen content wt.%	Acidity Total	Carboxylic	Lactonic	Phenolic	Basicity meq/g	pH_{PZC}
			meq/g				
A-P1-520/600/3:1	13.5	2.48	0.78	0.69	1.00	0.54	3.6
A-P1-520/700/3:1	8.7	1.87	0.52	0.46	0.89	0.62	4.9
A-P1-520/800/3:1	6.4	1.29	0.22	0.31	0.76	0.72	6.8

5.2.3. Synthesis of nitrogen enriched porous carbons (WUT)

Nitrogen containing activated carbons with basic surface properties are attractive for several applications. Our interest in the synthesis of this category of porous carbon from anthracene oil pitches arises from the pseudocapacitance effect which is generated by nitrogen substituted for carbon in the graphene layer and contributes to enhancement of charge accumulated in the electric double layer [4,5]. Two routes were tested for synthesis of nitrogen enriched porous carbons from anthracene oil pitches:
- co-pyrolysis of the pitches with N-polymers followed by activation with steam and CO_2,
- ammonization of pitch-derived KOH activated carbons.

Co-pyrolysis of pitch with N-polymers

The polymers used as nitrogen carrier in co-pyrolysis with anthracene oil derived pitches were polyacrylonitrile (PAN) and various forms of melamine (M). N-containing activated carbons were prepared at a laboratory scale according to the procedure used in previous work [6]. It comprises hot mixing of pitch with a given N-polymer followed by carbonization at 850^{o}C and activation with steam at 800^{o}C or CO_2 at 850^{o}C up to 50 wt% burn-off.

Due to high yield and suitable properties of carbonization residue PAN is an attractive precursor of carbonaceous materials. Blending with pitch has a practical purpose, to produce an advanced material while keeping the cost of raw material in a reasonable limit. Pitches P-1, P-2 and P-4 were blended with PAN in the weight ratio of 60:40. Pure PAN powder was used as reference material. All the pitches have superior ability to disperse/dissolve PAN, as evidenced by homogeneous isotropic appearance with few fine mosaic intrusions in the chars produced. Nitrogen content in the chars from blends is in the range of 8.7-9.3%, i.e. lower than in PAN char (16.6%) but still quite satisfactory.

N_2 adsorption isotherms (Fig. 5.12) show microporous character of all activated carbons. It is interesting to note that at 50 wt% burn-off, CO_2 is more efficient in terms of porosity development for PAN char while steam for blend derived char. Steam activated carbons from polymer and blend derived chars show very similar total nitrogen adsorption capacity, however distinctly higher adsorption at a low relative pressure indicates more microporous character of the former carbon. Porosity parameters calculated from the adsorption data (Table 5.7) are consistent with isotherm profiles. We conclude that the selection of pitch, P-1, P-2 or P-4, has no essential influence on the nitrogen content and porous texture of activated carbons. Some peculiarities can be related to the varying contribution of pitch derived material to the blend char due to different coking value of a given pitch. For all blends activation with steam leads to a better developed porosity but a lower nitrogen content (3.8-4.4 vs. 5.5-5.9 wt%) than activation with CO_2. This can be related to exceptionally high resistivity of blend chars to gasification with CO_2.

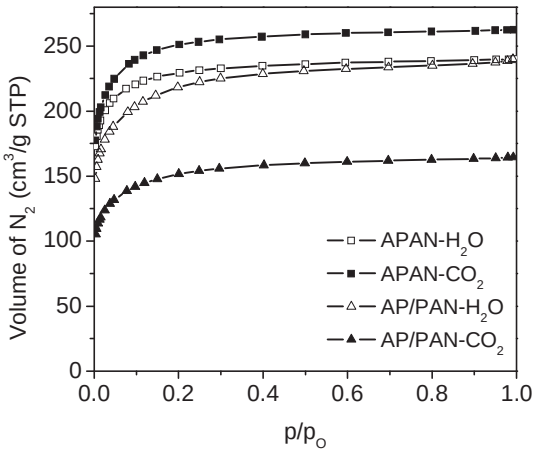

Fig. 5.12. N_2 adsorption isotherms of steam and CO_2 activated carbons from PAN and pitch/PAN blend.

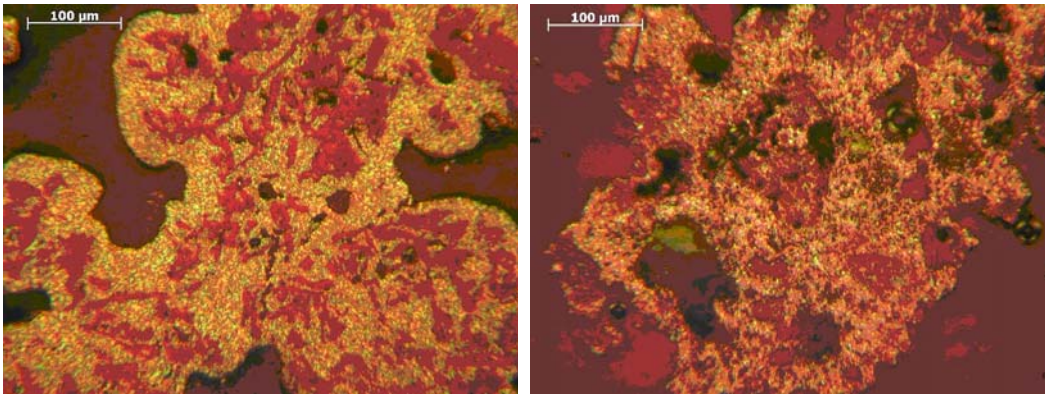

Fig. 5.13. The optical texture of chars from P-1/MF (a) and P-1/Mox (b) blends.

Table 5.7. Porosity parameters of nitrogen enriched steam and CO_2 activated carbons from pitch/PAN blends calculated from N_2 adsorption isotherms at 77K

Sample	N content wt%	S_{BET} m^2/g	V_T cm^3/g	V_{DR} cm^3/g	V_{DR}/V_T	L_0 Nm
APAN-H_2O	6.77	880	0.34	0.31	0.90	0.94
APAN-CO_2	7.99	960	0.37	0.33	0.88	1.03
AP-1/PAN-H_2O	4.39	810	0.34	0.28	0.82	1.13
AP-1/PAN-CO_2	5.47	690	0.29	0.23	0.80	1.17
AP-2/PAN-H_2O	3.96	770	0.33	0.26	0.80	1.12
AP-2/PAN-CO_2	5.59	585	0.26	0.21	0.81	1.21
AP-4/PAN-H_2O	3.83	905	0.38	0.31	0.81	1.15
AP-4/PAN-CO_2	5.93	545	0.23	0.19	0.82	1.12

The interest in melamine as a precursor of nitrogen enriched carbon is due to very high nitrogen content and low price, however an exceptional thermal stability causes that a direct production of char on the polymer heat-treatment is impossible. The problem could be overcome, in part, by using melamine-formaldehyde resin (MF) and a special preparation procedure [7,8]. In our study co-treatment with pitch is considered as an alternative way to prepare N-carbons using melamine as nitrogen carrier. The oxidation of melamine and resin with air under suitable condition was performed to increase the interaction of oxidized forms of polymers (Mox and MFox) with pitch constituents on co-treatment. To prepare activated carbons pitch P-1 was blended with different forms of melamine (M, Mox, MF,

MFox) in the weight ratio of 50:50. The miscibility of these polymers with P-1 is rather poor so their dispersing/dissolving in pitch matrix is not as easy as in the case of PAN. Despite applying prolonged mixing of components at elevated temperature (250°C) the resultant chars have heterogeneous appearance in the micrometer scale. Polarized light optical microscopy shows the texture of mosaics with several isotropic intrusions (Fig. 5.13). The suitability of pre-oxidation is confirmed by enhanced nitrogen content and porosity development of resultant activated carbon (Table 5.8). Oxidized melamine (Mox) appeared to be the most promising nitrogen carrier. P-1/Mox char of nitrogen content ~ 12.7 wt% is produced with a satisfactory enough yield of 35 wt%. Activation of the char with H_2O and CO_2 gives typically microporous carbon with a moderate BET surface area of 670-700 m^2/g and nitrogen content of 4.2 and 6.2 wt%, respectively. In contrast, activation P-1/MFox char gives material of similar nitrogen content but with very poor porosity development.

Table 5.8. Porosity parameters of nitrogen enriched steam and CO_2 activated carbons from P-1/melamine and P-1/melamine resin blends calculated from N_2 adsorption isotherms at 77K

Sample	N content wt%	S_{BET} m^2/g	V_T cm^3/g	V_{DR} cm^3/g	V_{DR}/V_T	L_0 nm
AP-1/M-H_2O	2.18	548	0.25	0.20	0.80	1.04
AP-1/M-CO_2	3.13	276	0.12	0.10	0.83	1.18
AP-1/Mox-H_2O	4.25	701	0.32	0.25	0.78	1.10
AP-1/Mox-CO_2	6.17	668	0.31	0.24	0.77	1.14
AP-1/MF-H_2O	2.85	193	0.10	0.07	0.70	1.22
AP-1/MF-CO_2	3.81	12	0.01	0.00	n.d.	n.d.
AP-1/MFox-H_2O	4.26	311	0.14	0.12	0.81	1.29
AP-1/MFox-CO_2	5.85	18	0.01	0.00	n.d.	n.d

Table 5.9. Heteroatoms content and porosity development of KOH activated carbons from P-1 semi-coke (700°C/1h, KOH/ coke ratio 3:1) before and after ammonization at 450°C and 700°C

Sample	N content wt%	O content wt%	S_{BET} m^2/g	V_T cm^3/g	V_{DR} cm^3/g	V_{DR}/V_T
AP-1-520/700	0.3	6.7	2480	1.02	0.83	0.82
AP-1-520/700-N450	3.2	3.5	2430	0.99	0.79	0.79
AP-1-520/700-N700	3.5	2.0	2230	0.91	0.70	0.77
AP-1-700/700	0.3	6.8	1540	0.63	0.54	0.86
AP-1-700/700-N450	2.8	2.5	1290	0.45	0.40	0.88
AP-1-700/700-N700	4.4	1.7	1010	0.39	0.35	0.90

Synthesis of N-carbons by ammonization of KOH activation products

The treatment of lignocellulose origin materials with ammonia at elevated temperature (ammonization) has been reported as a possible way of producing activated carbons containing nitrogen surface groups [9]. It has been therefore anticipated that ammonization of high surface area and oxygen rich KOH activated carbons can be an efficient way for producing materials with enhanced charge accumulation.
Activated carbons used for the ammonization were AP-1-520/700 and AP-1-700/700 which were produced from P-1 pre-treated at 520 and 700°C, respectively, by activation at 700°C for 1h using 3:1 KOH/coke ratio. The activated carbons differ in terms of porosity development (S_{BET}= 2480 m^2/g, and 1560 m^2g) but show a comparable high oxygen content (6.7 wt.%), occurring mostly in the form of acidic groups (Table 5.9). Treatments with ammonia were carried out in a quartz fluidized-bed reactor. After tests at different temperatures in the range of 300-750°C, the ammonizations at 450°C and 700°C for 1 h were selected as optimal in terms of nitrogen bonding. In fact only moderate amount of nitrogen, varying between 2.8 and 4.4 wt%, could be incorporated into porous carbon structure. Moreover, no essential effect of porosity development on nitrogen trapping could be noticed from elemental analysis data (Table 5.9). However, N1s XPS spectra (Fig. 5.14, Table 5.10) demonstrate clearly different distribution of nitrogen forms in materials produced at 450 and 700°C. The low temperature treatment gives activated carbon rich in functionalities like amides, imides, nitriles and lactams (peak centered at ~399.7 eV) and N-oxides (peak at ~404 eV), while pyridinic and pyrrolic/pyridonic functionalities,

responsible for peaks at 398.7 and 400.3 eV, respectively, are the most abundant forms in that ammoxidized at 700°C.

Table 5.10. Distribution of surface nitrogen forms in KOH activated carbons from P-1 semi-coke after ammonization at 450°C and 700°C based on N1s XPS spectra

Sample	N content at%	N-6 %	N-C/N-5 %	N-Q %	N-X %
AP-1-520/700-N450	5.5	25.7	45.9	14.3	14.1
AP-1-520/700-N700	5.3	44.8	35.0	12.7	7.5

N-6 – pyridinic N
N-C – N in amides, imides, nitriles and lactams
N-5 – pyridonic/pyrrolic nitrogen
N-Q – quaternary N
N-X - N-oxides

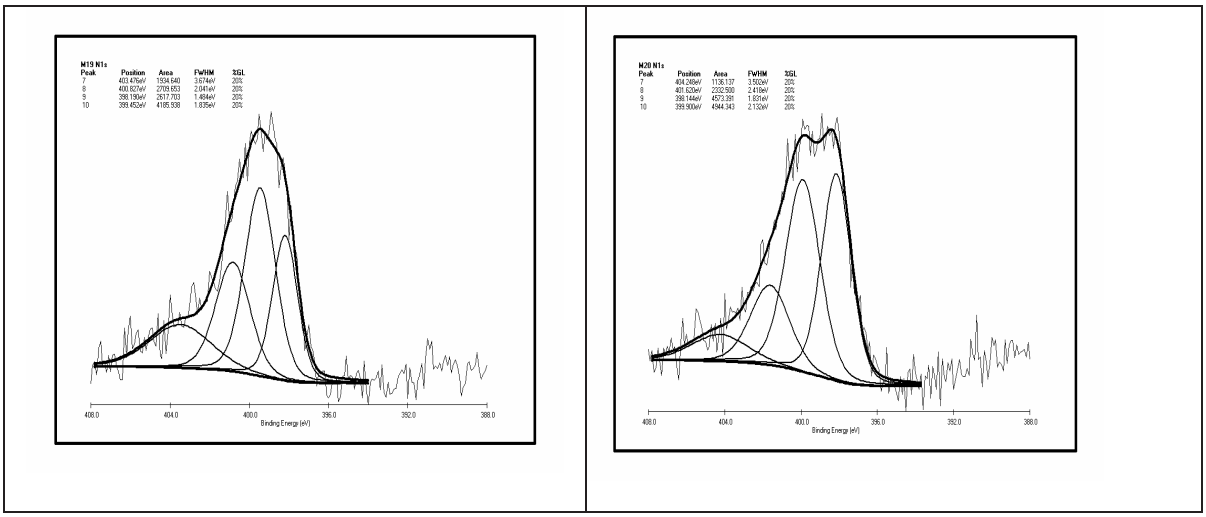

Fig. 5.14. N1s spectra of AP1-520/700-N450 (a) and AP1-520/700-N700 (b).

To find out factors which control nitrogen trapping during ammonizations we performed the treatments at comparable conditions, 700°C for 1 h, for a series of materials of different particle size and porosity development which were produced from pitch P-1. They included nonporous coke powder of HTT 700°C and average particle size of 30 μm and activated carbons AP-1-520/700 and AP-1-700/700 of S_{BET} = 2480 and 1540 m^2/g, respectively. The samples of activated carbon were used "as received", i.e. of wide particle size distribution and average size of 200 and 52 μm and as the size fraction of 63-100 μm with average particle size of 95 and 85 μm (Fig. 5.15). Ammonizations gave materials with nitrogen content in the range of 3.5-5.8 wt%. It is interesting that there is no correlation with porosity development, instead, a clear effect of particle size is observed. The highest nitrogen content (5.8 wt%) was obtained for pitch coke with the smallest average particle size of 30 μm. However, at best 4.4 wt.% of nitrogen could be introduced by the treatment under the same conditions of any of the activated carbons. The results suggest therefore that under conditions used the nitrogen enrichment occurs preferentially on the outer surface of particles with little reaction on pore surface.

5.2.4. Monolithic adsorbents for methane storage from KOH activated pitch cokes (WUT)

Methane is a supercritical gas under ambient conditions so can be adsorbed effectively in micropores only. This implies that a high performance adsorbent system should consist of particles of highly microporous activated carbon which are packed as tightly as possible to reduce interparticle voids [10]. This part of work is an attempt at preparing high packing density monolithic carbon adsorbent using activated carbon powder produced by KOH activation of anthracene oil derived pitch coke.

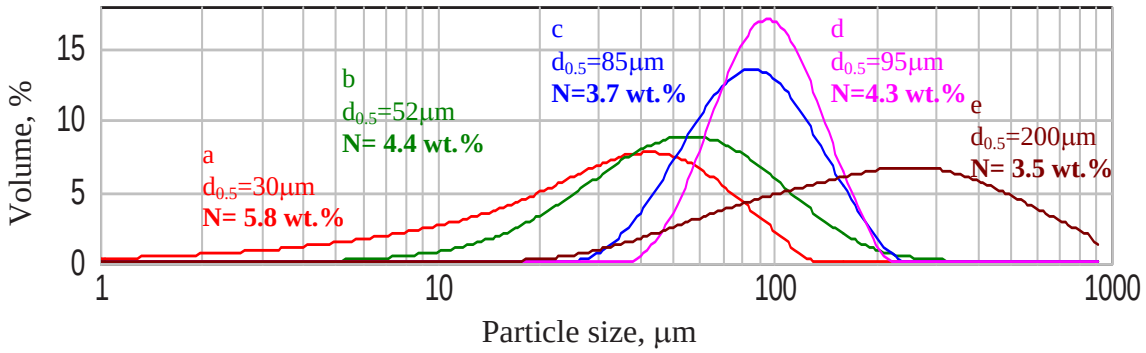

Fig. 5.15. Effect of particle size on nitrogen up-take during ammonization at 700°C of coke powder (a) and KOH activated carbons of BET surface area of ~1500 m^2/g (b, c) and ~ 2500 m^2/g produced from P-1 pitch.

Based on the results presented in the chapter 5.2.2 the semi-coke from P-4 was selected as raw material for activation. New system with chamber type nickel reactor was constructed to allow activation of about 20 g of precursor in a single batch. The activation variables used were: KOH/semi-coke ratio 3:1, semi-coke particle size 0.1-0.63 mm, activation temperature 750°C for 1 h, nitrogen flow 30 dm^3/h. The portion of 60 g of activated carbon was produced in a few runs with an average burn-off of 21.6 wt% and a good repeatability.

Porosity characteristics of the powdered material:

S_{BET} = 2550 m^2/g, V_T = 1.07 cm^3/g, V_{DR} = 0.86 cm^3/g, L_0 = 1.26 nm, V_{DR}/V_T = 0.80.

The powder was compacted in a heated mould into disc-shaped monoliths of 18 mm diameter and 7-10 mm height using polyfurfuryl alcohol (PFA) and phenolformaldehyde resin of novolac type (NOV) as a binder. Forming conditions were optimized so to get discs of high density and good mechanical strength using a minimum proportion of binder. The conditions used were: pressure - 40 MPa, mould temperature - 160°C, activated carbon to binder ratio - 2:1. The final stage of activated carbon monolith preparation was baking under nitrogen at 900°C for 1 h with a programmed heating rate. The series of monoliths, four discs each, which are produced in that way are M-AP-4/-PFA and M-AP-4/NOV. An additional series M-AP-4/PFA-H was prepared by post-treatment of M-AP-4/-PFA under hydrogen at 700°C for 1 hour to induce hydrophobic character of surface.

5.2.5. Anthracene oil-derived pitches as precursors for needle coke (INCAR-CSIC)

The feasibility of using anthracene oil derivatives to produce needle coke was investigated by INCAR-CSIC. The reaction product from the first cycle of anthracene oil processing (RP-1) was tested as a potential precursor for preparing this type of materials. The carbonizations were performed in the temperature range of 450 and 460 °C, at residence times of 7 and 25 h and gaseous pressures (nitrogen) of 1-5 bar. The results showed that cokes with different degrees of microstructure orientation can be obtained. Although light pitch components are one of the most important factors responsible for the orientation of the microstructure, the release of volatiles must be controlled in order to improve the process yield and coke microstructure. It was found that using pressures above 5 bar led to anisotropic cokes with poorly orientated microstructures (Figure 5.16, cokes C1, C2 and C3). On the other hand, the use of pressures below 5 bar led to very poor carbonization yields (Table 5.11, cokes C1,C2 and C3). For these reasons a variable nitrogen pressure was employed. In a first approach, carbonization was carried out under 5 bar, which was later reduced to 1 bar. By this procedure, light components evolved in the first step of carbonization and then in the second step, they were removed, favouring the orientation of the microstructures. Carbonization temperature and residence time were critical factors that determined the yield of the process, the orientation of the microstructures and the conversion of the raw material into coke. In fact, lower temperatures and longer residences times led to a complete conversion of the raw materials, giving rise to cokes with a well oriented structure and acceptable yields (Figure 5.16, cokes C4, C5 and C6). It was observed that the increase in residence time was more selective and effective when it was applied in the second carbonization step (under 1 bar of pressure). This first approach demonstrated the feasibility of using the raw material (reaction product RP-1) and this particular procedure to obtain ‘needle cokes’.

Table 5.11. Experimental conditions for the preparation of needle cokes from the reaction product RP-1.

Sample	Treatment	Yield (wt.%)
C1	460ºC, 2h, 5bar + 450ºC, 5h, 1bar	25.8
C2	460ºC, 2h, 5bar + 460ºC, 6h, 1bar + 450ºC, 12h	27.0
C3	450ºC, 3h, 5bar + 450ºC, 6h, 1bar + 450ºC, 12h	27.2
C4	450ºC, 8.5h, 5bar + 450ºC, 12h, 1bar	31.6
C5	450ºC, 3h, 5bar + 450ºC, 17h, 1bar	30.4
C6	450ºC, 8.5h, 5bar + 460ºC, 17h, 1bar	28.4

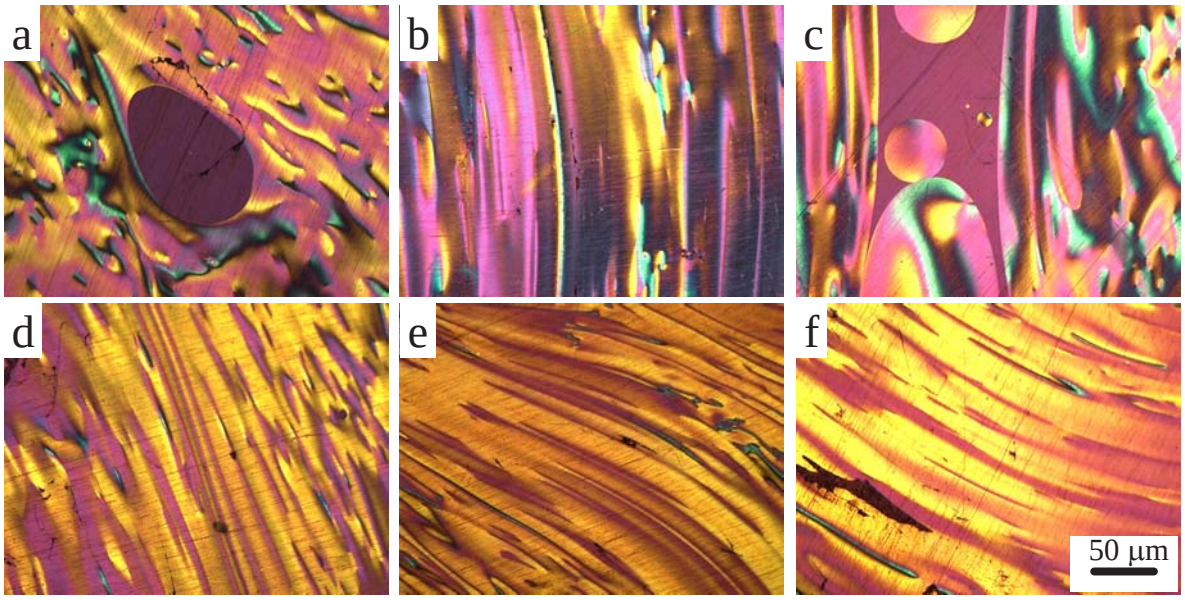

Figure 5.16. Optical microscopy of the cokes (a) C-1, (b) C-2, (c) C-3, (d) C-4, (e) C-5 and (f) C-6 obtained from the reaction product RP-1 under different experimental conditions (*see Table 5.11*)

Task 5.3. Testing of carbon materials

Carbon materials produced from anthracene oil derived pitches in the preceding task were tested in terms of applicability for anode material in litium-ion batteries, electrode in electrochemical capacitors and monolithic methane adsorbents, as appropriate.

Table 5.12. Structural parameters of graphitic carbons from P-1

Sample	d_{002} *nm*	L_c *nm*	L_a *nm*	L_{112} *nm*
P-1-2300	0.3385	33	52	4.2
P-1-2300B_a	0.3371	43	61	10.5
P-1-2900	0.3364	47	83	14.4
P-1-2900/B_c-2300	0.3357	52	60	12.2
P-1-2900/ B_4C-2300	0.3357	47	52	11.8
P-1-3100	0.3366	56	94	17.1

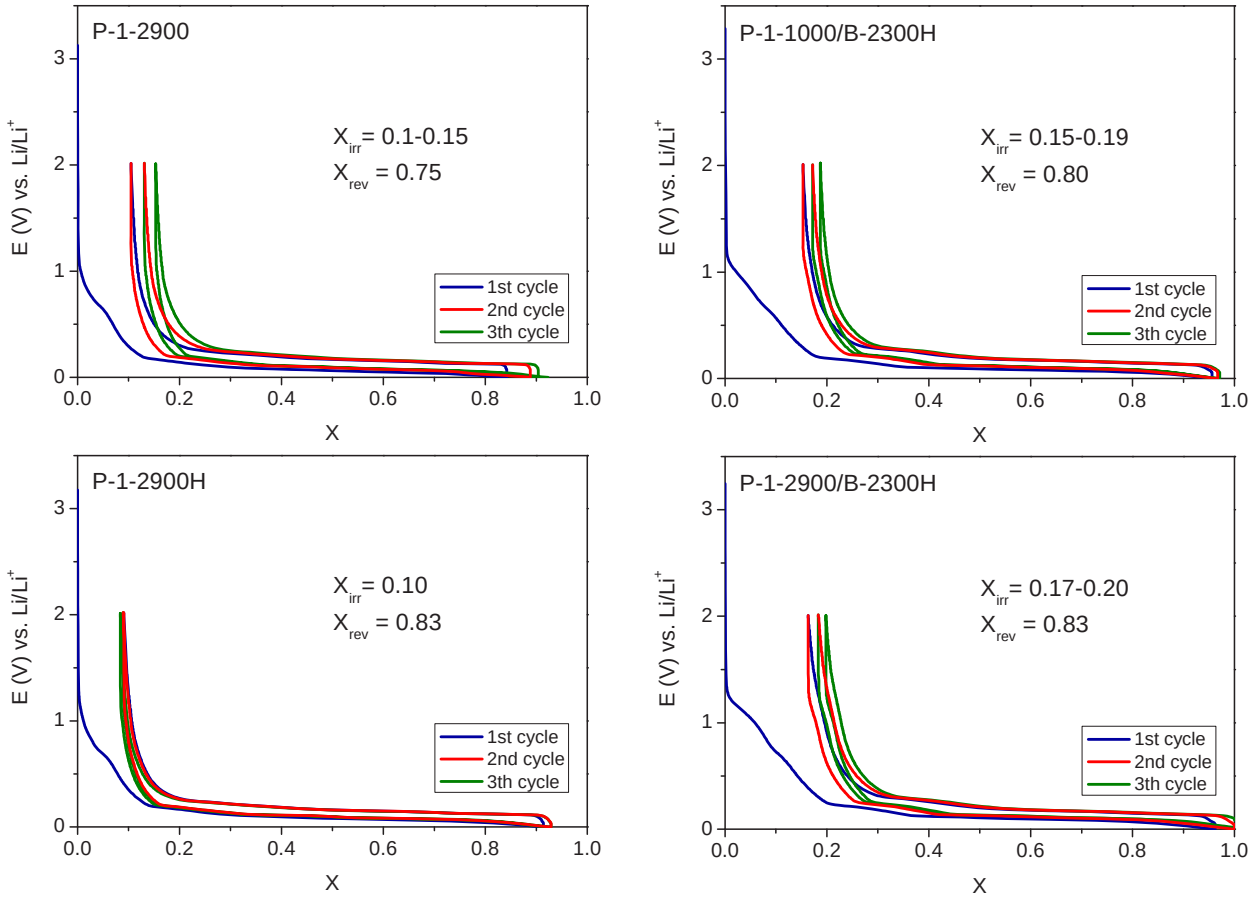

5.17. Galvanostatic lithium insertion/deinsertion for undoped and boron doped P-1 derived graphites

5.3.1. Lithium insertion in boronated carbons and graphites (WUT)

The study on boronated carbons were intended to get improved electrode material for Li-ion cells. Twofold effects of boron doping were anticipated: to improve structural ordering of graphitic material and to facilitate lithium charging/discharging. The former was assessed using XRD analysis, the latter by monitoring electrochemical Li intercalation/deintercalation on pellets prepared by mixing 85% of carbon, 5% of acetylene black and 10% of PVDF and mounted in a Li/carbon cell. Voltammetry and galvanostatic experiments were performed using a multichannel potentiostat/galvanostat Mac Pile. Results of XRD analysis of selected samples are given in Table 5.12. Fig. 5.17 shows galvanostatic charge/discharge profiles for some materials studied. The most relevant finding of the study can be summarized as follows. Boron, independent of form used, is very effective catalyst of P-1 coke graphitization on heat-treatment at 2300^{o}C. When added to graphitic carbon boron induces a slight

improvement of structural ordering which has been established by preceding heat-treatment at 2900°C, but the final effect is inferior to that of heat-treatment at 3100°C without boron. Boron seems to have no positive effect on lithium insertion, whatever the procedure is used (treatment with boron of pitch-coke or graphite). For all the graphitized materials lithium insertion/deinsertion occurs within a narrow potential range (0-0.5 V) with reversible capacitance X_{rev} between 0.75 and 0.83. Post-treatment of graphitic materials in hydrogen at 700°C has a profitable effect on lithium insertion/deinsertion. This is reflected mostly by the formation of stable passivating layer at first cycle and a decrease in irreversible capacity. Graphite produced by heat-treatment at 2900°C followed by treatment in hydrogen gives most promising electrochemical characteristics - high reversible capacity X_{rev} =0.83 and the lowest irreversible capacity X_{irr} = 0.10.

5.3.2. Evaluation of electric capacitance properties of anthracene oil derived porous carbons (WUT)
The objective of this part of the study was to explore the ways for using anthracene oil derived pitches as precursor of porous carbons of improved performance of charge accumulation in electric capacitor. In general, this can be done by optimizing porosity characteristics and modification surface properties to induce pseudocapacitance effect. Hence, the materials selected for testing as electrode in capacitor system can be classified in two groups. First, activated carbons of tailored porous texture by varying pitch pretreatment temperature and reagent ratio. Second, activated carbons enriched in nitrogen which were prepared in task 5.2.3 using different procedures.

The electrochemical behaviour was assessed using two-electrode capacitor assembled in Swagelok system with pellets of comparable mass around 10 mg. Capacitance measurements were performed in 1 M H_2SO_4 and 6 M KOH as an electrolyte using voltammetry at the scan rates from 1 to 100 mV/s, galvanostatic charge/discharge under current load from 0.2 to 20 A and impedance spectroscopy in the frequency range from 100 kHz to 1 mHz.

Table 5.13. Porosity parameters and capacitance values of KOH activated carbons estimated by voltammetry and galvanostatic techniques

Sample	S_{BET}	L_0	V_{DR}/V_T	Voltammetry at 1 mV/s		Galvanostatic at 0.5 A/h		ESR at 1kHz
				C_G	C_S	C_G	C_S	
	m^2/g	nm		F/g	$\mu F/cm^2$	F/g	$\mu F/cm^2$	Ω/cm^2
AP-4/520/700/2:1	1940	1.21	0.92	267	13.8	253	13.0	0.74
AP-4/520/700/2.5:1	2320	1.39	0.88	285	12.3	282	12.2	0.96
AP-4/520/700/3:1	2460	1.53	0.82	274	11.1	261	10.6	0.59
AP-4/600/700/3:1	2090	1.33	0.80	250	12.0	244	11.7	0.69
AP-4/650/700/3:1	1730	1.23	0.87	251	14.5	242	14.0	0.38
AP-4/700/700/3:1	1560	1.21	0.84	221	14.2	217	14.2	0.53

Effect of porous texture on charge accumulation in the electric double layer
This part of study was focused on elucidating the effect of surface area and pore size distribution on the electric double layer capacitance. Activated carbons selected for electrochemical measurements were prepared from P-4 pitch using various pre-treatment temperature (520-700°C) and KOH/coke ratio (from 2:1 to 3:1), while the activation temperature and time were fixed at 700°C and 1h. The samples are listed in Table 5.13 together with most essential porosity characteristics and electric capacitance data.

At a moderate scan rate (1 mV/s) or current load (0.5 A/h) the gravimetric capacitance C_G (F/g) is very satisfactory for most of the materials, in the range of 240-290 F/g. The activated carbons of relatively lower S_{BET} and narrower pores show high surface capacitance C_S, about 14 $\mu F/cm^2$, which is calculated in relation to the unit of BET surface area. The decrease of capacitance with increasing current load is typical behaviour (Fig. 5.18). Surprisingly good performance at high current load of AP-4/650/700 and AP-4/700/700 can be related to a better conductivity as suggested by a lower equivalent series resistance (ESR). Voltammetry characteristics (Fig. 5.19) present for all the activated carbons a regular rectangular shape at scan rate of voltage up to 20 mV/s. Further increase in the scan rate results in aggravation of the characteristics which occurs to the least extent in AP-4/650/700 and AP-4/700/700.

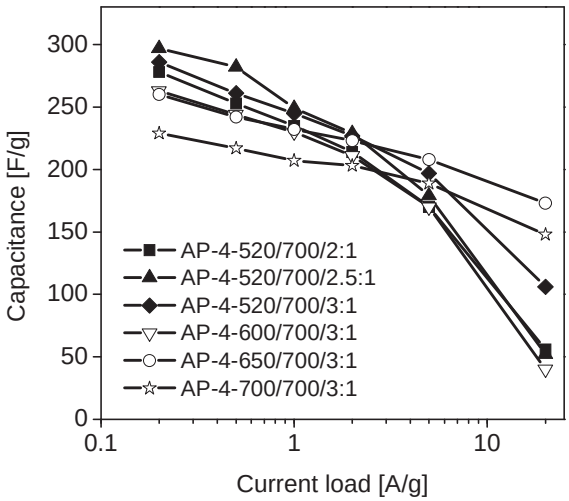

Fig. 5.18. Variation of electric capacitance with current load for a series of KOH activated carbons derived from P-4 pitch.

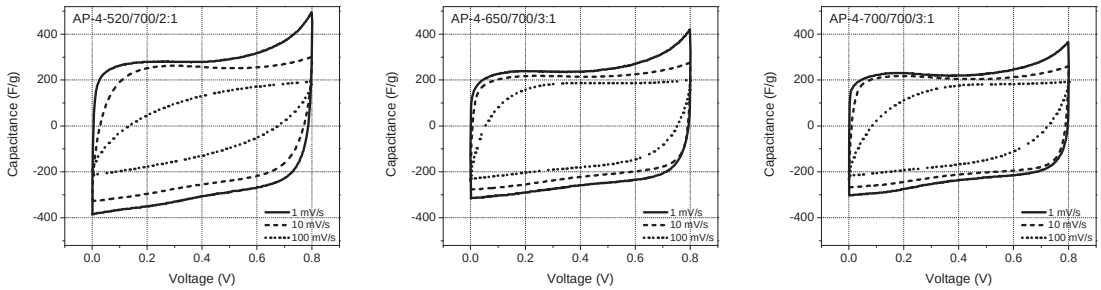

Fig. 5.19. Voltammetry characteristics of a capacitor built from the selected KOH activated carbons at different scan rates of voltage. Electrolytic solution: 1M H_2SO_4.

This observation suggests that increasing pre-treatment temperature contributes to a better performance of activated carbon, possibly due to reduced resistivity.

Nitrogen enriched pitch-derived activated carbons as an electrode of supercapacitor

Anhracene oil derived porous carbons tested in this part of research as electrode material for supercapacitor were produced by steam and CO_2 activation of pitch/N-polymer blends and by ammonization of KOH activated carbons.

Nitrogen enriched activated carbons from pitch/PAN and pitch/melamine blends used for electrochemical measurements are listed in Table 5.14 together with most essential physicochemical characteristics and capacitance data in 1M H_2SO_4. Activated carbons from N-polymer/pitch blends represent materials of moderate or poor porosity development, however some of them show quite interesting electrochemical properties. This category includes steam activated carbon from a blend with PAN (AP/PAN-H_2O) and steam and CO_2 activated carbons from blend with oxidized melamine (AP-1/Mox-H_2O, AP-1/Mox-CO_2) which are distinguishable by a higher porosity development (S_{BET} 670-820 m^2/g) compared to the others. For these materials the gravimetric capacitance C_G measured at low scan rate of 1 mV/s or current load of 0.5 A/h is between 120 and 130 F/g and the corresponding surface capacitance approaches as high value as 20 μF/g. The superior capacitance has to be attributed, at least in part, to the pseudocapacitance effect generated by nitrogen and oxygen functionalities. In fact, surface capacitance increases for the carbons along with nitrogen and oxygen contents. In principle, the performance of steam and CO_2 activated carbons from the blend of P-1 and Mox can be considered as similar to that of steam activated PAN.

Table 5.14. Porosity parameters, heteroatoms content and capacitance values in 1M H_2SO_4 of nitrogen enriched activated carbons from pitch/PAN and pitch/melamine blends

Sample	S_{BET}	V_{DR}/V_T	N	O	Voltammetry at 1 mV/s		Galvanostatic at 0.5 A/h	
	M^2/g	nm	wt%	wt%	C_G F/g	C_S $\mu F/cm^2$	C_G F/g	C_S $\mu F/cm^2$
APAN-H_2O	880	0.90	6.77	5.36	168	19.1	151	17.2
APAN-CO_2	960	0.88	7.99	4.07	145	15.1	136	14.2
AP/PAN-H_2O	820	0.82	4.06	3.56	131	16.0	120	14.6
AP/PAN-CO_2	570	0.83	5.85	3.18	83	14.6	71	12.5
AP-1/M-H_2O	548	0.80	2.18	6.80	79	14.4	60	10.9
AP-1/M-CO_2	276	0.83	3.13	3.23	38	13.8	34	12.3
AP-1/Mox-H_2O	701	0.78	4.25	6.79	133	19.0	116	16.6
AP-1/Mox-CO_2	668	0.77	6.17	5.50	135	20.2	114	17.0

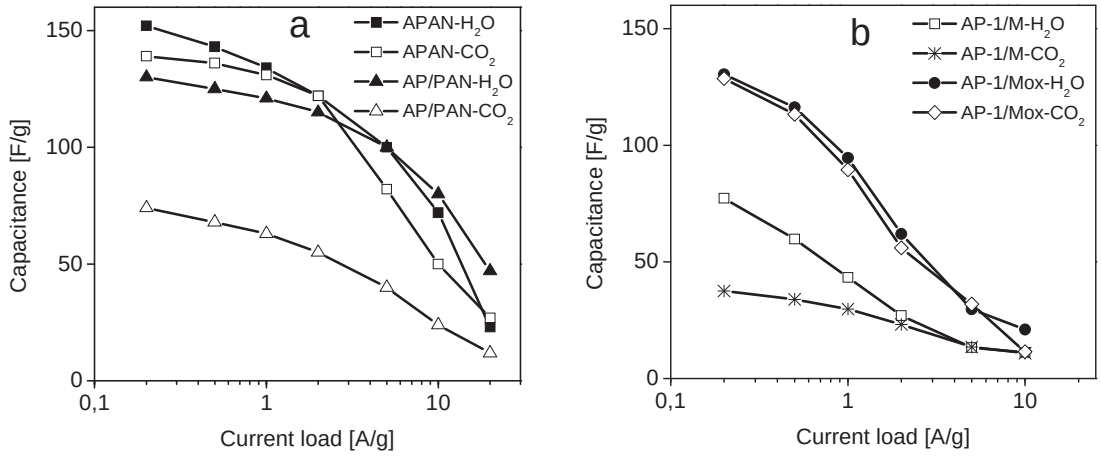

Fig. 5.20. Variation of electric capacitance with current load for steam and CO_2 activated carbons derived from the blends of pitch with N-polymers.

The second group of N-activated carbons produced is characterized by poor electrochemical properties as indicated by low C_G, in the range of 70-80 F/g. This group comprises activated carbons from P-1/M blend and CO_2 activated from P/PAN blend. In general, these activated carbons are inferior to the former in terms of porosity development (S_{BET} 270-570 m^2/g), but their surface capacitance is also lower. This is despite quite high nitrogen content, e.g. in CO_2 activated carbon from P/PAN blend.

The reasons for such a big difference in the electric capacitance of activated carbons classified into these groups are not clear from their porous texture characteristics and elemental composition.

Fig. 5.20 shows the variation in capacitance with an increase in current load up to 20 A for the nitrogen enriched activated carbons. In general, the materials are not well adapted to work at high current load. Their performance is significantly worse than porous materials presented in the preceding section. Most dramatic capacitance fading occurs for the activated carbons derived from pitch/melamine blend.

Activated carbon AP-1-520/700, which was prepared by the activation of P-1 semi-coke at 700°C using 3:1 KOH/carbon ratio was used as the starting material to study the effect of ammonization at 450°C and 700°C on electrochemical properties. Nitrogen enriched carbons AP-1-520/700-N450 and AP-1-520/700-N700 were then heat-treated under nitrogen and hydrogen at 700°C to follow changes in surface chemistry and possible contribution of different functionalities to the electric capacitance.

Table 5.15. Electrochemical properties of N-containing materials in 6MKOH and 1M H_2SO_4

Sample	Electrolyte	S_{BET}	N	O	Voltammetry C_G, F/g		Galvanostatic at 0.2 A/h	
					2 mV/s	50 mV/s	C_G F/g	C_S $\mu F/cm^2$
		m^2/g	wt%	wt%				
AP-1-520/700	H_2SO_4	2480	0.3	6.9	262	187	270	10.7
	KOH				299	242	302	12.0
AP-1-520/700-N450	H_2SO_4	2430	3.2	3.5	244	164	249	10.2
	KOH				269	209	272	11.2
AP-1-520/700-N450/I	H_2SO_4	2440	2.4	3.4	241	157	245	10.0
	KOH				256	152	258	10.5
AP-1-520/700-N450/H	H_2SO_4	2150	0.8	1.9	214	131	217	9.9
	KOH				237	182	240	11.0
AP-1-520/700-N700	H_2SO_4	2230	3.5	2.0	213	173	216	9.7
	KOH				226	175	230	10.3
AP-1-520/700-N700/H	KOH	2580	1.9	1.6	233	179	235	9.0

Table 5.15 contains most essential data on porosity, surface chemistry and electric capacitance measured in 6M KOH and 1 M H_2SO_4 for a series of activated carbons prepared in that way.

Ammonization at 450°C results in reduction of oxygen by about 3.5 wt% which is replaced by equivalent amount of nitrogen. At 700°C the removal of oxygen is even deeper. The post-treatment induces essential changes to the surface chemistry of activated carbon treated with ammonia at 450°C. Most noticeable is a partial removal of unstable nitrogen functionalities (amides, lactams and imides) or their conversion to more stable pyrrolic and pyridinic forms which occur together with further reduction of oxygen groups. When the post-treatment occurs under hydrogen the chemical modification is distinctly more extensive and associated with the reduction of porosity development. For AP-1-520/700-N700 the post-treatment under hydrogen induces limited changes to surface chemistry but a considerable increase in surface area should be noticed. The observed effects of post-treatment are related to different mechanism of ammonization. At relatively mild conditions (<500°C) predominates the reaction of ammonia with acidic groups at a higher temperature (>500°C) that is etching of carbon material.

Data in Table 5.15 show a noticeable reduction of capacitance both the calculated as gravimetric C_G and surface C_S after ammonization with a minor effect of further treatment. The reason of such a behaviour is alteration of chemical structure of surface. Removal of oxygen groups reduces the pseudocapacitance contribution, the effect being in a part only compensated by nitrogen generated pseudocapacitance. Fig. 5.21 shows clearly the variation of gravimetric capacitance in relation with oxygen and nitrogen contents in the material.

In summary, our study demonstrates that anthracene oil derived pitch can be successfully used as precursor of porous carbon suitable for electric capacitor. High gravimetric electric capacitance and a good behaviour under high current load discriminate KOH activated carbon of BET surface area in the range of 1500-2000 m^2/g which is produced from pitch coke pre-treated about 650°C in terms of performance as electrode material. Amongst the routes tested for producing nitrogen enriched activated carbons the most promising seems to be co-pyrolysis of pitch with melamine which was previously activated by oxidation. However, further study is required to fully assess the feasibility of the process and electrochemical properties of resultant material.

5.3.3. Performance of monolithic methane adsorbents from pitch derived activated carbons (WUT)

Monoliths made of activated carbon powder from P-4 semi-coke activation using polyfurfuryl alcohol (PFA) and novolac resin (NOV) as a binder were assessed in terms of porous texture and methane adsorption capacity under elevated pressure. N_2 adsorption at 77K was applied to characterize porosity in the range of micro- and mesopores, mercury porosimetry under pressure up to 400 MPa was used to characterize mesopores above 3.6 nm and macropores up to 14 μm. The methane storage capacity under

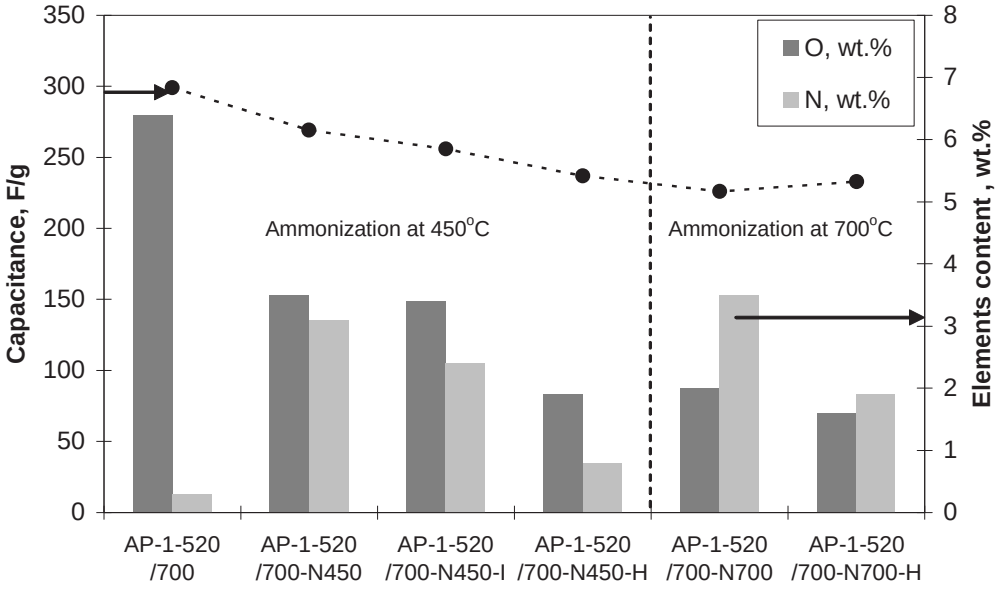

Fig. 5.21. Relationship between electrochemical properties and nitrogen/oxygen content in parent and ammonized materials.

pressure up to 6.5 MPa was determined using volumetric adsorption system with 9 cm^3 sample chamber [11].

Compared to the activated carbon powder the monoliths have BET surface area S_{BET}, total pore volume V_T and micropore volume V_{DR} reduced by about 40% (Table 5.16). This is due to both the presence of binder derived coke and micropore blockage. PFA binder gives slightly more porous monolith than NOV binder. Hydrogen treatment allows recover a small part of blocked porosity.

Table 5.16. Porosity parameters of activated carbon powder and monoliths produced thereof

Sample	S_{BET} m^2/g	V_T cm^3/g	V_{DR} cm^3/g	L_0 nm	V_{DR}/V_T
AP-4/520/750	2550	1.07	0.86	1.26	0.80
M-AP-4/PFA	1470	0.60	0.51	1.24	0.85
M-AP-4/PFA-H	1540	0.64	0.51	1.29	0.80
M-AP-4/NOV	1450	0.58	0.47	1.15	0.81

Mercury porosimetry shows bimodal pore size distribution (Fig. 5.22). Clearly, most of pore volume constitute interparticle voids of size above 500 nm. The pore size distribution in this region seems to depend to a certain extent on the binder used. The effect of post-treatment in hydrogen is an increase in pore volume V_T which is associated with reduction of density measured at 0.1 MPa, d_b. The values of bulk density d_b, measured at 0.1 MPa, and apparent density d_a, measured at 400 MPa, were used to calculate contributions of fractions: carbon skeleton F_C, micropores F_μ and interparticle voids F_V to the unit volume [10]. The highest contribution of F_μ (0.304) and the lowest of F_V (0.400) point to M-AP-4/PFA as the monolith of superior porous texture (Table 5.17).

The characteristics of methane uptake at elevated pressure (Fig. 5.23) demonstrate an essential difference in the performance of monolith. M-AP-4/PFA-H made using PFA as a binder and heat-treated under hudrogen is distinguishable clearly by the highest both the gravimetric adsorption expressed in mmol/g and volumetric storage capacity V/V. At 3.5 MPa the respective values amount to 10.2 mmol/g and 131 V/V (Table 5.18). This rather unexpected result seems to suggest a relevance of surface chemistry on the methane uptake under elevated pressure.

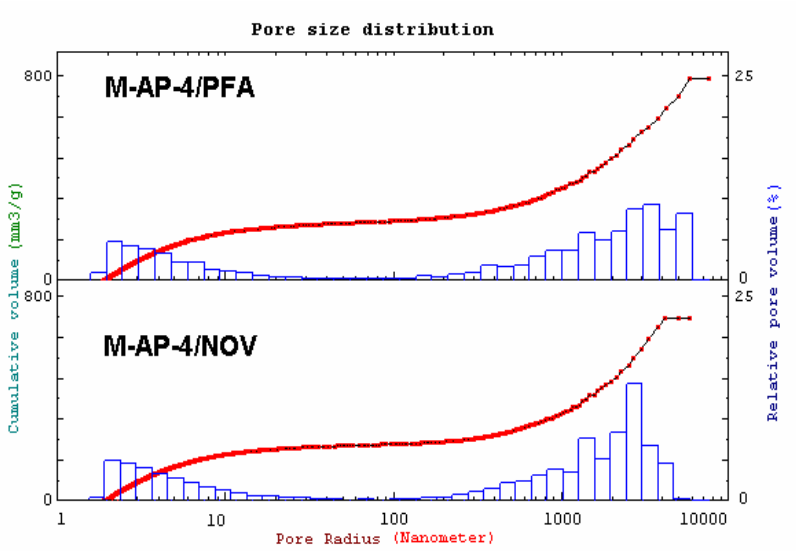

Fig. 5.22. Pore size distribution of monolits made of made of KOH activated carbon powder and polymeric binder measured using mercury porosimetry under pressure up to 400 MPa.

Table 5.17. Mercury porosimetry characteristics of monoliths

Sample	V_T cm^3/g	$V_{<50\ nm}$ cm^3/g	$V_{>50\ nm}$ cm^3/g	d_b g/cm^3	d_a g/cm^3	F_C	F_μ	F_V
M-AP-4/PFA	0.642	0.080	0.562	0.622	1.037	0.296	0.304	0.400
M-AP-4/PFA-H	0.724	0.109	0.615	0.591	1.065	0.281	0.274	0.445
M-AP-4/NOV	0.672	0.076	0.596	0.644	1.136	0.307	0.260	0.433

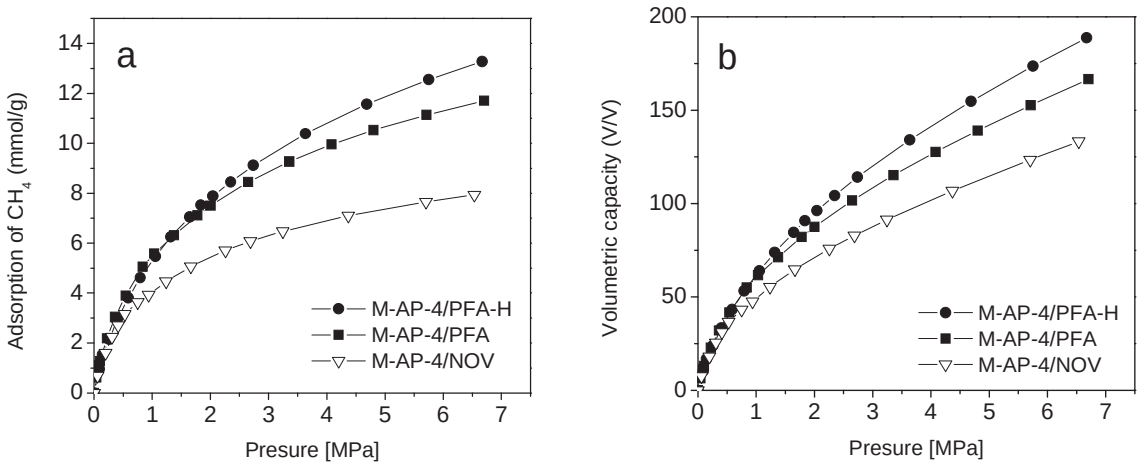

Fig. 5.23. Gravimetric adsorption capacity (mmol/g) and volumetric storage capacity (V/V) of methane on monoliths made of KOH activated carbon powder and polymeric binder under pressure up to 7 MPa.

The results got in the project reveal feasibility of using KOH activated carbon produced from anthracene oil derived pitch for moulding monolithic gas adsorbents. It seems that optimization of porosity of powder material and moulding condition and using a post-treatment to unblock a part of microporosity can enhance the volumetric storage capacity to the level required for application.

Table 5.18. Gravimetric adsorption capacity and volumetric storage capacity of methane on monoliths made of KOH activated carbon measured under pressure 3.5 MPa

Sample	Gravimetric adsorption capacity mmol/g	Volumetric storage capacity V/V
M-AP-4/PFA	9.4	118
M-AP-4/PFA-H	10.2	131
M-AP-4/NOV	7.1	96

References

1. Kierzek K, Gryglewicz G, Machnikowski J. Some factors influencing porosity development during KOH activation of various precursors, Karbo 2004;49:47-51.
2. Mora E, Blanco C, Pajares JA, Santamaría, Menéndez R. Chemical activation of carbon mesophase pitches. Journal of Colloid and Interface Science 2006;298:341-347.
3. Chunlan L, Shaoping X, Yixiong G, Shuqin L, Changhou L. Effect of pre-carbonization of petroleum cokes on chemical activation process with KOH. Carbon 2005;43:2295-2301.
4. Lota G, Grzyb B, Machnikowska H, Machnikowski J, Frąckowiak E. Effect of nitrogen in carbon electrode on the supercapacitor performance, Chem. Phys. Letters 2005;404:53-58.
5. Jurewicz K, Babel K, Ziolkowski A, Wachowska H. Electrochim.Acta. Ammoxidation of active carbons for improvement of supercapacitor characteristics 2003;48:1491-1498.
6. Machnikowski J. Grzyb B, Machnikowska H, Weber JV. Surface chemistry of porous carbons from N-polymers and their blends with pitch. Microporous and Mesoporous Materials 2005;82:113-120.
7. Hulicova D, Yamashita J, Soneda Y, Hatori H, Kodama M. Supercapacitors prepared from melamine-based carbon, Chem. Mat. 2005;17:1241-1247.
8. Li W, Chen D, Li Z, Shi Y, Wan Y, Huang J, Yang J, Zhao D, Jiang Z. Nitrogen enriched mesoporous carbon spheres obtained by a facile method and its application for electrochemical capacitor, Electrochemistry Communications 2007;9:569-573.
9. Boudou J. P. Surface chemistry of a viscose-based activated carbon cloth modified by treatment with ammonia and steam, Carbon 2003;41:1955-1963.
10. Cook TL, Komodromos C, Quinn DF, Ragan S. Adsorbent storage for natural gas vehicles. In Carbon Materials for Advanced Technologies, p.269-302. Ed. T.D.Burchell, Pergamon, New York 1999.
11. Czepirski L, Holda S, Łaciak B, Wojcikowski M. Apparatus for investigation of adsorption equilibria and kinetics at elevated pressure, Ads. Sci. Technol. 1996;14:77-82.

Work Package conclusions

The anthracene oil derivatives prepared in this work were shown to have great flexibility for producing different types of carbon materials. Thus, carbon fibres can be prepared from the reaction product obtained during the first cycle of anthracene oil processing (RP-1) in a simple but feasible procedure. However, a deeper study is required in order to reduce the multiple and complex steps involved in the preparation of the anthracene oil-based mesophase.

This study of mesophase-based carbons produced from the anthracene oil derived pitches reveals attractive properties for advanced applications in the emerging area of energy storage. In particular, P-1 is preferred to produce graphitic carbons with a high structural ordering and an interesting electrochemical lithium insertion/deinsertion behaviour, which is a primary requirement for Li-ion cell anodes. Activation of pitch derived carbons with KOH under adapted conditions can be used to obtain microporous carbons with a tailored porous texture. The resultant materials showed very a satisfactory capacitance when tested as electrode in an electric supercapacitor and methane adsorbent. In terms of possible applications this new category of carbonaceous precursors can be considered as fully competitive to the pitches derived from purified (QI-free) coal tar. Moreover, their high aromaticity and high capacity to generate cokes with a preferential optical texture of domains makes anthracene oil

derivatives excellent candidates for the preparation of cokes with a highly oriented microstructure, especially in the case of RP-1.

WORK PACKAGE 6. Modelling the process and scaling up the production of anthracene oil based pitches

This Work Package was developed by INETI in close collaboration with IQNSA.

6.1. Experimental Work

In the starting phase of this Workpackage, 3 samples of anthracene oil, anthracene oil reaction product and anthracene oil pitch were analysed. All these materials were supplied by R&D Department of Industrial Quimica del Nalon, S.A.

As there are no standard procedures for elemental analysis of anthracene oil, anthracene oil derived products and anthracene oil pitch, standard procedures for coal or for fuel oil were used for these analysis. In Table 6.1 the analytical methods used are shown. The results of samples elemental analysis are presented in Table 6.2. The values obtained show that no great changes were detected in elemental analysis of anthracene oil and anthracene oil derived products.

Table 6.1 Analytical methods.

Elemental Analysis	**Method**	**Notes**
Carbon Content (% w)	ASTM D 5373 (for coal) ASTM D 5291 (for fuel oil)	CHN Equipment
Hydrogen Cont. (% w)	ASTM D 5373 (for coal) ASTM D 5291 (for fuel oil)	CHN Equipment
Sulphur Content (% w)	ASTM D 4239 (for coal) ASTM D 1552 (for fuel oil)	CS Equipment
Nitrogen Content (% w)	ASTM D 5373 (for coal) ASTM D 5291 (for fuel oil)	CHN Equipment

Table 6.2 Anthracene oil and anthracene oil based pitch elemental analysis.

Elemental Analysis	Anthracene Oil Reaction Product Ref. RP1	Anthracene Oil Ref. AO1	Anthracene Oil Pitch Ref. P-1a
Carbon (% w/w)	92.1	91.9	92.9
Hydrogen (% w/w)	5.3	5.6	4.3
Sulphur (% w/w)	0.5	0.6	0.6
Nitrogen (% w/w)	1.0	0.9	1.3

A literature survey was undertaken to update the information concerning pitch production from anthracene oil [1 – 7]. This survey was also used to define experimental procedures of pitch production from anthracene oil. The main characteristics are presented in Table 6.3.

The results obtained by INCAR group have shown that polymerisation of anthracene oil by air-blowing could be a suitable process with potential industrial applications [1]. The polymerisation found to be influenced by processing variables, which are not independent of each other. The mass of anthracene oil fed to the reactor influences the reaction rate by modifying the air diffusion rate. Temperature and reaction time have an important effect on the composition and pyrolysis behaviour of the resultant products. High temperature (325ºC) and small air-flow, 60 l/(h Kg, appear to give rise to products with potential industrial applications as precursors of graphitizable carbons and allowed to obtain yields of about 90 wt% [1].

Table 6.3 Summary of experimental conditions from literature survey.

Experimental Conditions		**Remarks**
Reaction Temperature	250, 275 e 300 ºC	Sampling at 5 and 10 h The results suggest that air-blowing could be a suitable process for the conversion of anthracene oil into carbon precursors with potential industrial applications. Reference [1]
Reaction time	15h	
Air Flow Rate	112 l/(h Kg)	
Anthracene Oil (AO)	200 / 500 / 1000 g.	
Stirring Speed	100 rpm	
Pressure	atmospheric	
Reactor type	500 ml glass reactor	
Reaction Temperature	250, 300ºC e 325 ºC	Sampling at 0.5, 1, 2, 3, 4 and 5 h Anthracene oil treatment with $AlCl_3$ led to pitch-like materials, being temperature and $AlCl_3$ concentration the controlling parameters. The reaction is rapid with yields about 90 wt % of the oil. $AlCl_3$ catalyzes the polymerization during carbonization and accelerates the pyrolysis. Reference [2]
Reaction time	6h	
Nitrogen Flow Rate	80 ml/min at 5 ºC/min	
Anthracene Oil (AO)	continuous feeding	
Stirring Speed	100 rpm	
Pressure	atmospheric	
Catalyst	$AlCl_3$ (5, 8, 10 wt %)	
Reactor type	500 ml glass reactor	
Reaction Temperature	300 ºC	Structure and composition of products from the reaction of anthracene oil with $AlCl_3$ were examined by Size-exclusion chromatography. Reference [3]
Reaction time	2 h	
Catalyst	$AlCl_3$ (10 wt %)	
Reactor type		
Reaction Temperature	250, 275 e 300ºC	Sampling in treatment with air, at 5 and 10 h. Sampling in treatment with S, analysis at different times between 5 and 90 min Anthracene oil was treated with air or with sulphur. Air-blowing caused condensation reactions, thereby producing large molecules. Reference [4]
Air Flow Rate	112 l / (h kg)	
Sampling		
Sulphur	5, 7.5, 10, 20% (w/w)	
Reaction time	Treat. with air: 15 h Treat. with S: 120 min	
Reaction Temperature	250,275 and 300 ºC	Sampling at5, 10, 40 and 90 min Anthracene oil readily reacts with sulphur, the initial concentration of sulphur being the main controlling parameter of the reaction. The amount of sulphur incorporated into the reaction products determined the optical texture of the resultant cokes. Reference [5]
Reaction time	120 min.	
Anthracene Oil (AO)	500 g	
Catalyst	Sulphur 5, 10, 20% wt	
Nitrogen Flow Rate	80 l/(h.Kg) at 5 ºC/min	
Reactor type	500 ml glass reactor	

		Remarks
Reaction Temperature	300 ºC	Thermal polymerisation of AO with: S, or $AlCl_3$ or air. With S and with air, polymerization involved a low number of AO components, which selectively reacted to form intermediate and large polymers. $AlCl_3$ led to a wider polymerization and a product with more oligomers of intermediate size. Reference [6]
Reaction time	2 h	
Catalyst	[$AlCl_3$]=10 wt %	
Sulphur	10% wt	
Air Flow Rate	120 l/(h.Kg)	
Pressure	0.5 MPa	
Reaction Temperature	350 - 400 ºC	Thermal treatment of products obtained from the air-blowing of anthracene oil improved their quality, as it caused the polymerization of the heavy and the light components, the decomposition of the peroxy and carboxylic functionalities, release of H_2O and CO_2 and the formation of new C-C bonds. Reference [7]
Reaction time	3 – 8 h	
Catalyst	[$AlCl_3$]=10 wt %	
Anthracene Oil (AO)	500 g	
Air Flow Rate	120 l/(h.Kg)	
Pressure	1 MPa	
Reactor type	Cylindrical stainless steel reactor, 270mm height and 95 mm i.d.	

6.1.1. Experimental Installations

Experiments at atmospheric pressure

Experimental work was started under batch conditions at atmospheric pressure with air-blowing and without adding any catalyst. The work studied the influence of different process variables.
The designed reactor consists in cylindrical stainless steel vessel with two different diameters. The above part has a height of 208 mm and is 159 mm in diameter; the below part has a 325 mm height and 77.9 mm in diameter. The schematic representation of the reactor design is presented in Figure 6.1. Photos of the installation and the reactor are presented in Figures 6.2. Both the thermocouple and the plastic tubes that correspond to the refrigeration system are visible. At the top of the image is visible the air-blowing tube.

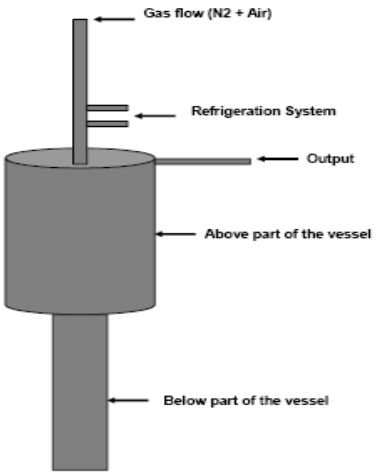

Figure 6.1 Schematic representation of the reactor design.

The anthracene oil was placed on the lower part of the vessel. Then an air-blowing tube was injected Air and N_2 into the reactor, directly to the oil (AO). The air-blowing was carried out under atmospheric pressure. The temperature was monitored by two thermocouples, one inserted into the lower part of the

reactor (temperature of the anthracene oil), and the other monitoring the temperature in the above part of the reactor.

Figure 6.2 INETI lab-scale experimental installation.

Experiments under pressure

Studies carried out previously by IQNSA in collaboration with INCAR-CSIC had shown that operating at a pressure of 10 bar was enough to prevent the massive devolatilization of the sample. So it was decided to do some experimental work under pressure. Some studies were carried out in an autoclave installation changing the pressure and reaction time used.

The used autoclave was adapted from an equipment already existing in INETI, that could operate under a 10 bar pressure in a steady, controlled state. The experimental work was carried out in a 5.5 dm3 autoclave, built of Hastelloy C276, by Parr Instruments. The Autoclave characteristics are present in Table 6.4. The maximum pressure and temperature conditions that this autoclave can operate are 450ºC e 340 bar.

Table 6.4 Autoclave characteristics.

Volume (dm^3)	Height (cm)	Diameter (cm)	Height/Diameter Ratio
5.5	38.5	14	2.8

In Figures 6.3 and 6.4 are presented photos of the overall view of the autoclave installation and of the cooling and stirring system.

Figure 6.3 Autoclave for pressurized experimental runs.

Figure 6.4 Cooling and stirring system

For monitoring each test run, the autoclave was connected to a PID programmable controller, which indicates the oven temperature, the autoclave pressure and temperature and also allows the control of the temperature inside the reactor. The data acquisition system is linked to a PC. This system allowed the supervision of the autoclave and the compilation of all the data in a file, thus enabling the plots and all the calculations to be carried out subsequently.

The autoclave cover is constituted by several valves and accessories:

- thermocouple,
- turbine stirring system, Figure 6.4,
- cooling system which allows the introduction of water or air inside the autoclave, Figure 6.4,
- Pressure indicator with a Bourbon tube which allows to measure the pressure inside the reactor,
- Two valves for the entrance and exit of the gas. The exit valve was connected to a back pressure regulator which was linked to a condensate vessel,
- Safety rupture disc.

The sealing of the autoclave is guaranteed by a Gasket, flex graphite which fits between the cover and the body of the Autoclave. The Autoclave is connected to a Parr controller model 4843, constituted by a digital controller of temperature with proportional, integral and derivative share (PID). This controller allows the adjustment of the temperature acting either in the interior of the reactor, by the introduction of water in the cooling coil, and in the oven, controlling its heating. The controller also allows the acquisition of data, therefore it has an interface that allows the linking to a computer. Thus, it is possible the register of the temperature inside the Autoclave, as well as of the levels of heating and cooling of the system. The controller has three indicating modules, one of the pressure in the interior of the reactor, one of the temperature of the oven and another one of the agitation speed. The pressure is presented with a resolution of 1 psi and a 10 precision of psi. The temperature values have a resolution of 1ºC and a precision of 2ºC.

6.1.2. Technical Procedure

Experiments at atmospheric pressure

The reactor was first loaded with anthracene oil. The anthracene oil was placed on the below part of the vessel. Afterwards, it was heated in N_2 atmosphere and kept at the desired temperature value during the reaction time previously defined. The temperature was continuously monitored by two thermocouples. The air-blowing tube injected air and N_2 into the reactor, directly into the oil (AO). The air-blowing was carried out under atmospheric pressure. The installation was operated in batch, it worked for periods of eight hours or more according to the desired conditions. At the end of this period, the heating was stopped, the reactor was cooled to room temperature and opened to collect the produced pitch.

Experiments under pressure

The autoclave was first loaded with anthracene oil. Then, the autoclave was pressurised to a preset value with air. Afterwards, it was heated and kept at the desired temperature value during the reaction time previously settled. During the runs the pressure was kept at the preset value by opening a back pressure regulator every time the pressure became higher than the established value. This valve was connected to a condensation vessel to condensate the gaseous compounds produced during the devolatization of the anthracene oil (AO). At the end of this period, the autoclave was cooled to room temperature and opened.

6.1.3. Results and Discussion

Experiments at atmospheric pressure

In Table 6.4 are presented the experimental conditions used in AO conversion into solid derived AO products. Solid derived AO products were analysed to determined elemental analysis, these results are presented in Table 6.5. Carbon and hydrogen contents are lower than those presented in Table 6.2.
The softening points of some of the samples are presented in Table 6.6.

Table 6.5 Range of experimental conditions tested (1).

Run	Reaction time (h)	Temperature (ºC)	AO Volume (ml)	N_2 Feeding: (l/min)	Air Feeding: (l/min)
004.007	5	390	130	3.5	1.6
025.007	5	420	210	3.5	1.6
023.008	7	300	74	3.5	1.6
001.009	7	275	70	3.5	1.6
006.009	7	325	70	3.5	1.6
012.009	2	300	70	3.5	1.6
013.009	3	325	70	3.5	1.6
018.009	7	300	70	3.5	0.13
020.009	10	300	70	3.5	0.13
021.009	10	250	70	3.5	0.13

Table 6.6 Elemental analysis of anthracene oil solid derived products.

Run	Elemental Analysis			
	C (% w)	H (% w)	N (% w)	S (% w)
004.007	90.0	3.4	1.4	0.43
025.007	88.2	3.2	1.5	0.42
023.008	85.9	4.9	1.7	0.53
031.008	92.9	4.5	1.4	0.46
001.009	90.8	4.0	1.6	
006.009	90.8	4.0	1.6	0.52
012.009	91.2	4.9	1.4	0.60
013.009	89.2	3.9	1.4	0.50
018.009	89.4	5.4	1.2	0.52
020.009	92.5	4.4	1.5	0.53

Table 6.7 Anthracene oil and anthracene oil based pitch softening point.

Run	Softening Point (ºC)
Anthracene Oil Reaction Product Ref. RP1	123.4
012.009	40.3
013.009	89.2
018.009	50.8
020.009	130.7

Some samples were studied by scanning electron microscopy (SEM) with X-ray microanalysis by energy dispersive spectrometry (EDS) associated. A high resolution Philips XL 30 FEG/EDAX NX scanning electron microscope was used. Before to SEM/EDS studies, the samples were coated with a thin gold film using an ion sputter JLC 1100, in order to obtain the conductivity needed to SEM observations. The obtained results are presented in Appendix 1 Figures A6.1 to A6.6.

A second set of experimental runs was made, as presented in Table 6.8. The properties of the obtained anthracene oil based pitches like softening point and toluene insolubles are presented in Table 6.9, together with the elemental composition.

Table 6.8 Range of experimental conditions tested (2).

Run	Temperature (ºC)	Reaction time (h)	N_2 Feeding (g/min)	Air Feeding (g/min)
8	275	12	1.04	0.15
9	275	10	1.04	0.15
10	275	10	1.04	0.15
11	275	9	1.04	0.15
12	275	10	1.04	0.30
13	275	12	1.04	0.30
14	275	11	1.04	0.30
15	275	10	1.04	0.22
16	275	11	1.04	0.37
-		**Pitch received**	-	-

As it can be observed in Table 6.9, the experiments that led to pitches with softening points closer to the pitch received from Nolan are Run 13 and Run 14, both done at temperature of 275ºC, with 1.04 g/min of N2 and 0.30 g/min of air. However, Run 13 was done during 12h, while Run 13 lasted 11h. With the exception of the values obtained for Run 12 and Run 13, toluene insoluble values are similar and within the expected range. The elemental analysis of the anthracene oil based pitches are presented in Table 6.9. Similar values were obtained for all the pitches obtained, which were similar to those obtained from the received pitch. However, pitch obtained by Run 13 seems to present an elemental analysis more similar to the received pitch than the pitch obtained by Run 14.

Table 6.9 Pitch elemental analysis, softening point and toluene insolubles.

Run	Reaction time (h)	Softening Point (ºC)	Toluene Insoluble. (%)	C (%)	H (%)	N (%)	S (%)
8	12	146	26.0	90.4	4.6	1.3	0.57
9	10	166	28.4	90.0	4.5	1.3	0.52
10	10	160	28.3	88.8	4.5	1.3	0.51
11	9	pastes	-	92.0	5.1	1.1	0.66
12	10	88	9.0	90.6	4.9	1.3	0.68
13	12	134	16.2	90.8	4.6	1.3	0.59
14	11	110	29.7	89.6	4.8	1.4	0.67
15	10	pastes	-	91.5	5.0	1.3	0.70
16	11	161	25.0	90.4	4.6	1.4	0.57
-	**Pitch received**	120	22.8	89.1	4.6	1.3	0.55

Experiments under pressure

These experiments have been made with moderately high temperature (250-300ºC) and moderate pressures (1-10 bars) in a cylindrical vessel during 2 to 6 hours. It was not possible to use longer residence times due to the exit gas valve getting clogged which disabled the maintenance of the pre-set value of the pressure.

It was varied the pressure inside the autoclave and the residence time, maintaining the volume of AO used constant (300 ml). The pressure in autoclave was controlled by a back pressure regulator which opened when the pressure was higher than pretended. The experimental conditions are presented in Table 6.10.

Table 6.10 Range of experimental conditions tested.

Run	Reaction time (h)	Pressure (bar)	Temperature (ºC)	AO Volume (ml)	N_2 Feed: (l/min)	Air Feed: (l/min)
001.001	3	1	250	300	♦	♦
001.002	6	1	250	300	♦	♦
001.003	5	5	250	300	♦	♦
001.004	3	6	250	300	♦	♦
001.005	2	10	250	300	♦	♦

The gas feeding, nitrogen and air flow aren't accounted, they was the necessary to guaranty the pressure pretended in vessel reactor.

During the experiments, there were some technical problems which disabled the possibility of using this installation to produce pitch like material. Some of these problems are described below.

- It was observed a modification of the AO physical proprieties in contact with atmospheric air when it was transferred to the reactors vessel and this could not guarantee the AO used in all the runs had the same characteristics. It was observed an increase in the viscosity of the oil.
- It was not possible to determine the air flow introduced in the reactor during the experiments, because the flow meter could not work at pressures above 1 bar and as the pressure inside the autoclave was always higher a back flush was observed to occur.
- When the pressure was higher than the set value the back pressure regulator opened and instead of gaseous compounds leaving the reactor it was observed the presence of a liquid fraction which caused the clogging of the valve. The valve had to be cleaned in all runs what raised the possibility of occurring leaks.
- The pressure reducer of the air bottle only allowed maintaining the pressure of the autoclave below 15 bar.

Figure 6.5 Liquid with high viscosity obtained in the experiments.

When the experimental runs were over the autoclave was opened and it was observed that there was no formation of a solid fraction pitch like derived of AO, but it was detected the presence of a yellow substance that, provably, was PAHs vapours (especially crystallized anthracene). The product obtained was a high viscosity liquid as can be seen in Figure 6.5. This system needed profound changes to be able to be used in the AO reactions with air, so it was decided not to continue using the autoclave and the work only at atmospheric pressure as planned in the project proposal will be carried out.

6.2. Process Modelling

The principal objective of this task is to simulate the existing industrial unit to verify the influence of the main process operational parameters with the objective of introducing new data from lab studies and to optimise the existing process.

In the industrial scale installation, Anthracene Oil is sprayed into a large scale tubular reactor, controlling temperature, pressure, air ratio and residence time (flow rate). The range of experimental conditions is presented in Table 6.11.

The principal objective of this task is to simulate the existing industrial unit to verify the influence of the main process operational parameters with the objective of introducing new data from lab studies and to optimise the existing process.
The main problems of the industrial installation are:

- Pitch quality decreases with increasing yield
- The reactor blocks after 50/60 days operation that means high maintenance cost

Table 6.11 Global characteristics of industrial scale installation.

Temperature	**250-255 ºC (300-305 ºC)**
Inlet pressure	**10-11 bar**
Outlet pressure	**2.5-3 bar**
Air ratio	**0.18 kg / kg of AO**
Flow rate	**300-900 kg/hour**

To assist INETI in this modelling, IQNSA studied several parameters involved in the process and the principal conclusions reached are:

- Determinations of heat flow during the reaction evidence that the process is exothermic. This exothermicity contributes with ~ 30 °C to the reaction temperature.
- An increasing temperature has the influence to increase the pitch yield but also promotes a vapour phase reaction that generates small solid carbon particles that are deposited in the reactor walls and pipes, blocking the system.
- Increasing air ratio also improves pitch yield but in this case the oxygen is not completely consumed and the plant works in not safety conditions.
- Increasing the pitch yield in just one-stage produces higher molecular weight molecules, as can be seen under size exclusion chromatography, getting lower wettability and filterability properties.
- Pressure has to be maximized to keep anthracene oil in a liquid phase. In that sense the selected pressure is the maximum pilot plant working pressure.
- The mass balance of the reaction have been evaluated and the approximate stoichiometry is as follows:

$$2.023\ C_{17.26}H_{12.88} + 1.256\ O_2 \rightarrow C_{34.91}H_{21.03} + 2.511\ H_2O$$

  This stoichiometry was verified with the consumption of oxygen and water generation.

- The reaction velocity is very fast (< 5 seconds). This conclusion indicates that an inline reactor based on static mixers may be optimal for the process.

- The oxygen introduced in the reactor is mainly eliminated as H_2O, and in less extent in CO_2 and CO.

IQNSA contribution was also dealt with a deeply characterization of the products AO1 and RP1 to provide INETI enough data for process simulation and modelling (WP-6). The supplied data includes,

- Distillation profile (average boiling point and volatility)
- Average molecular weight and molecular weight distribution
- Density and its variation with temperature
- Heat capacity and its variation with temperature
- Thermal conductivity and its variation with temperature
- Latent heat of vaporization at the boiling point and its variation with temperature
- Vapour pressure as a function of temperature using Clausius-Claypeyron equation
- Reaction exothermic behaviour
- Viscosity and its variation with temperature
- Detailed composition

6.2.1. Design and optimization of the computational grids

The modelling work was made in "Fluent", a modelling software package that uses an user developed real scale 3-dimensional grid, where the most realistically possible physical model is applied. With the right data, it is possible to have detailed simulations of the physical characteristics of mixing flow inside the equipment. Chemical reactions can be included in an additional computational phase allowing a better description of all the mass and energy changes inside the reactor.

Five atomizer models are available in "Fluent" to predict the spray characteristics from knowledge of global parameters such as nozzle type and liquid flow rate. Each model includes physical atomizer parameters, such as orifice diameter and mass flow rate, to calculate initial droplet size distribution, velocities, and positions.

To develop a detailed model of the process it was necessary to have a detailed knowledge of the existing system. In addition to the known operating characteristics of the air-blowing process some additional physical and technical data were necessary.

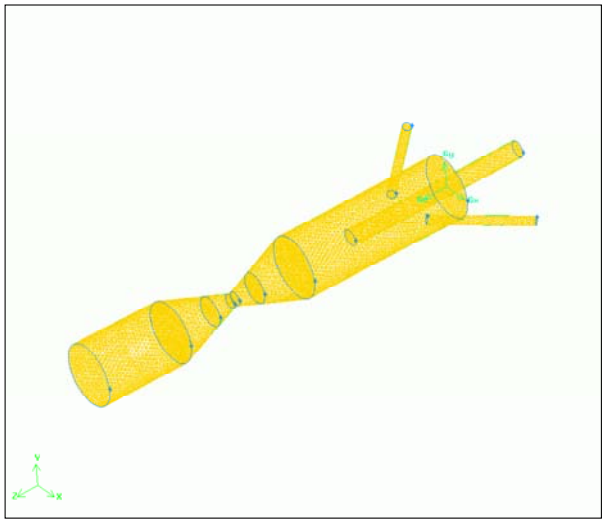

Figure 6.6 Isometric view of the developed gridline (wireframe view of the 3-Dimensional model).

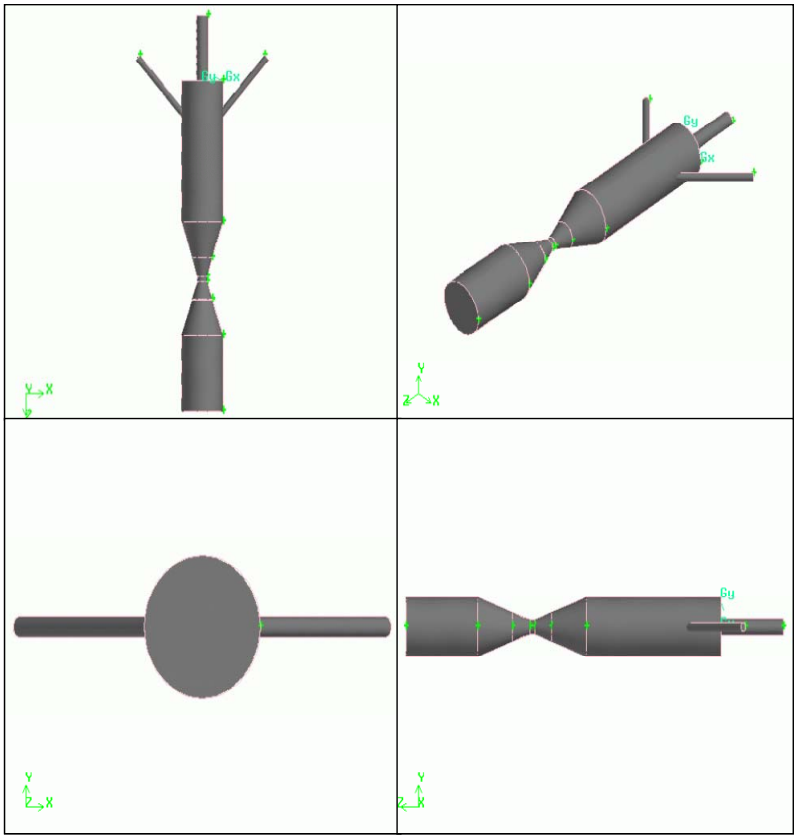

Figure 6.7 Four external views of the 3-Dimensional model.

With some detailed information obtained from the reactor specifications, a 3D wire-frame model of the injector section was developed using the required 3D graphics software. A sample of some of the obtained images is presented in Figures 6.6 and 6.7.

To the developed grid was applied a model of the atomizer known as the “Plain-Orifice Atomizer Model”. However, regardless of this designation, there is nothing simple about the physics of the internal nozzle flow and the external atomization. In the plain-orifice atomizer model in “Fluent”, the liquid is accelerated through a nozzle, forms a liquid jet and then breaks up to form droplets. The internal regime determines the velocity at the orifice exit, as well as the initial droplet size and the angle of droplet dispersion. A large number of parameters needs to be adjusted to evaluate the turbulence characteristics of the fluid flows, the will affect the droplet formation in the injector.

With the developed 3D Grid, some preliminary simulations were made to evaluate the fluid flow inside the injector section, using two test fluids with different properties. Some of these preliminary results are presented in Figures 6.8 and 6.9.

The preliminary work done on the 3-dimensional model of the initial section of the reactor, allowed for a first approach of the effects of the dimensions of the grid on calculations. The grid, as initially designed, included a large number of cell volumes, of more than 150 000, which could allow for a more refined modelling of the process but that has shown to be too large to achieve adequate results in acceptable computational times.

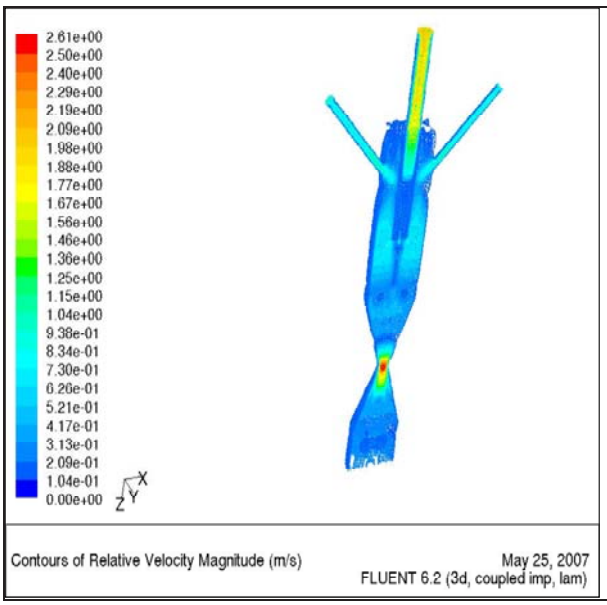

Figure 6.8 Preliminary visualization of Velocity Magnitude Contours

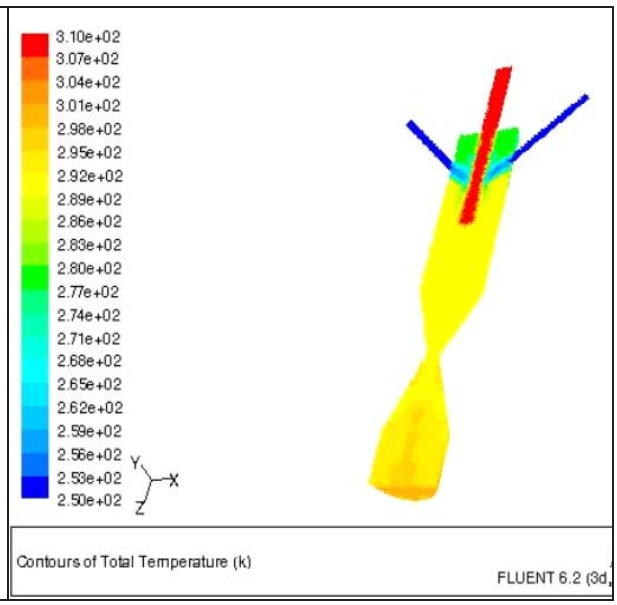

Figure 6.9 Preliminary visualization of Temperature Contours

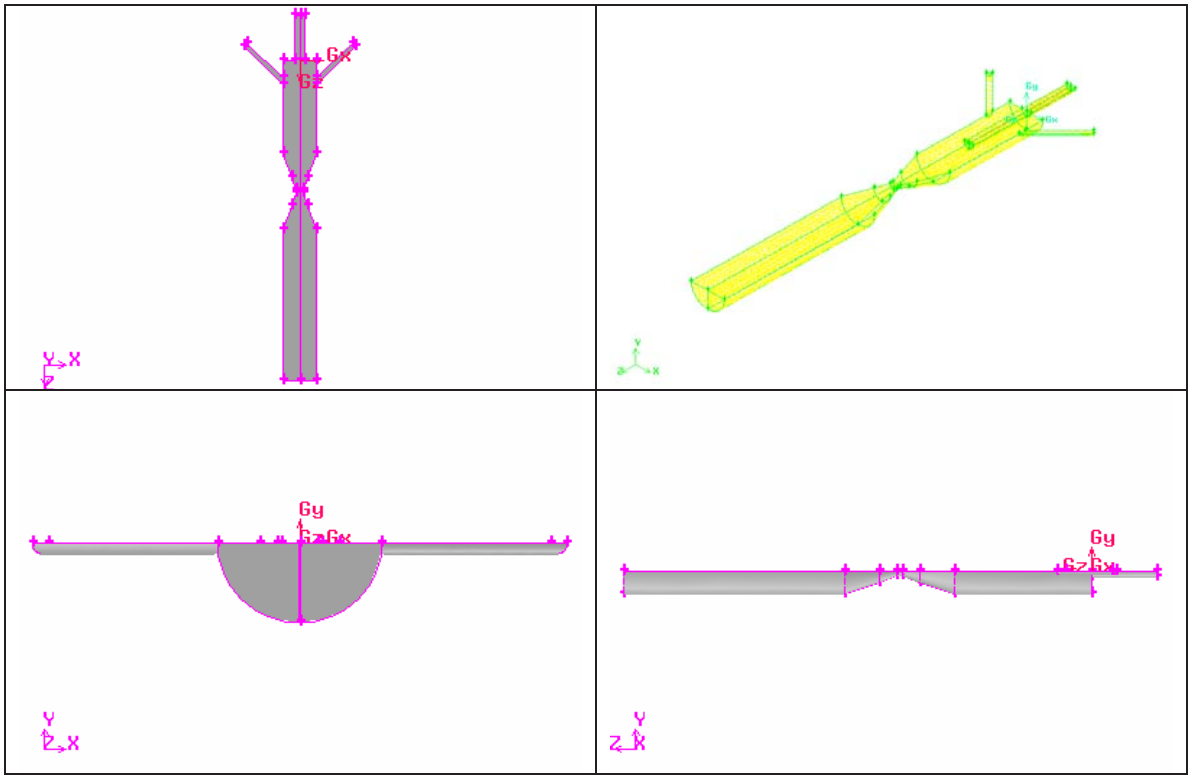

Figure 6.10 Four external views of the optimized 3-Dimensional model (shaded and wireframe view).

In this phase the grid was completely redesigned and optimized, to reduce the number of cell volumes of the 3-dimensional grid, decreasing simultaneously the calculation times and smoothing the progress of the model development. The size of the object was extended to enable a better understanding of the physical and chemical effects that occur after the narrowest point, as the initial size had proven in preliminary tests to be too short. This new grid is presented in Figure 6.10.

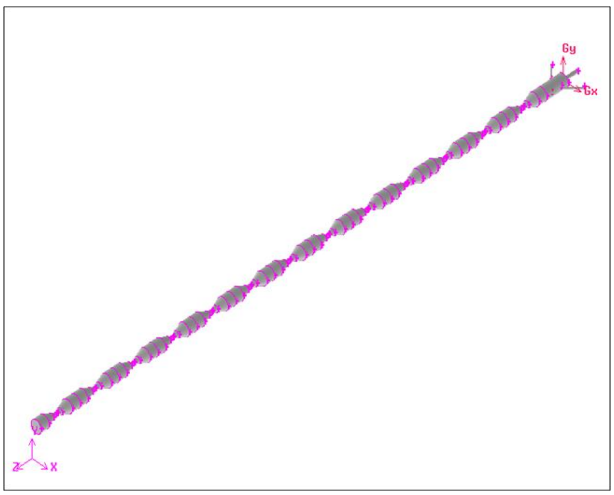

Figure 6.11 Shaded view of the full reactor first quarter

The 3-dimensional object was then used to create a new computational grid. The number of created cell volumes was 20.155, corresponding to a reduction of 13.1% on the number of cell volumes with resultant benefits on calculation times. A large part of the reduction of the 3-dimensional computational grid size was achieved by the introduction of symmetry planes that reflect the overlaying geometry. Some special attention should was made the injector, adjusting its dimensions to get a better representation of the real equipment.

The real dimensions of the reactor are still too large as the real proportions correspond to a tubular structure of more than 40 segments. An attempt was made of the simulation of the real dimensions of this structure, thank to the modular characteristics of the 3-D design software used. A visualization of approximately one quarter of the full reactor is presented in Figure 6.11.

6.2.2. Evaluation and optimization of process chemical and physical data

To develop a detailed model of the process it was necessary to have a detailed knowledge of the existing system. It was somewhat difficult to have correct values for the experimental operation characteristics of the air-blowing process. Besides currently known properties of the system, reactants and products, some additional physical and technical data were required for the model.

The chosen reaction to model the process involved a direct reaction between anthracene oil and oxygen, with liberation of water as shown in equation (1).

$$AO1 + O_2 \rightarrow RP1 + H_2O \qquad (1)$$

It was necessary to define these new chemical substances in “Fluent” with a complete assessment of their properties. Some of the chosen calculation models to evaluate these properties were given by the project partners,

Equation (2) was used to determine the density as function of temperature:

$$d_T = d_R + (T_R - T) * b \qquad (2)$$

$$10^5 * b = 162.7 - 86.3 * d_{20}$$

d_{AO1} = 1.092 g/cc (@85 ºC) d_{RP1} = 1.108 g/cc (@114 ºC)

b_{A01} = 65 b_{RP1}= 62

Equation (3) was used to determine the heat capacity for pitches as function of temperature and density at 20ºC of each species:

$$Cp = (3.665/d_{20}) - 1.729 + 0.00389 * T \qquad (3)$$

Equation (4) was used to determine the latent heat of vaporization as function of density and boiling point (T_b) of each species:

$L = d_{20} * (486.1 – 0.599\ T_b)$ (4)

$L_T = L * [3-(2\ T/T_b)]^{0.38}$ To adjust for the real temperature.

Equation (5) was used to determine the vapour pressure as function of temperature for both species:

$\log P = A – B/T$ (5)

A=5.7028; B= 3389 for both A01 and RP1

S are presented in Table 6.12. The system considers SI Units for all properties.

Table 6.12 Evaluation of the properties for the new chemical substances.

Chemical Formula	Undefined: Two model compounds were chosen. A01 ➔ $C_{18}H_{22}$ RP1 ➔ $C_{36}H_{42}$ *These species will be further optimized*
Molecular Weight (kg/mol)	Values corresponding to the chosen species.
Density (kg/m3)	Temperature dependent equation (1)
Viscosity (kg/m.s)	*Unknown (estimated from model compounds data)*
Specific Heat Capacity (J/kg.K)	Temperature dependent equation (2)
Binary Diffusivity (m2/s)	*Unknown* *(fluent defaults are used to estimate this property)*
Thermal Conductivity (W/m.K)	*Unknown (estimated from model compounds data)*
Latent Heat (J/kg)	Temperature dependent equation (3)
Vaporization Temperature (K)	*Unknown (estimated from available data)*
Boiling Point (K)	613.15 K for AO1 621.15 K for RP1
Saturation Vapor Pressure (Pa)	Temperature dependent equation (4)

The species presented in table 6.3 were chosen to represent a better chemical relationship while defining their conversion reaction, which was changed into equations (6) or (7):

$2\ AO1 + ½\ O_2 \rightarrow RP1 + H_2O$ (6)

$2\ C_{18}H_{22} + ½\ O_2 \rightarrow C_{36}H_{42} + H_2O$ (7)

To define this chemical reaction, it was used an Arrhenius based model, being necessary to determine the parameters presented in Table 6.13. These parameters will still need to be further refined to achieve a better representation of the underlying equipment behaviour.

Table 6.13 Evaluation of the parameters for the chemical reaction.

Formation Enthalpy (J/mol)	*Unknown (estimated from model compounds data)*
Activation Energy (J/mol)	*Unknown (estimated and optimized in the next phase)*
Pre-Exponential Factor ()	*Unknown (estimated and optimized in the next phase)*

6.2.3. Results obtained with the available data

With the developed 3-dimensional grid as presented in Figure 6.10, and with the data evaluation methods summarized in Table 6.13, some simulation tests were carried out using Fluent that allowed assessing the reliability of the designed grid and the properties that were used.

In Figure 6.12 are presented the cell volumes inside the reactor model. The smallest cell volumes, according to the grid design that was made, are found in the injector and the initial section of the reactor, while the larger volumes are located in the final sections.

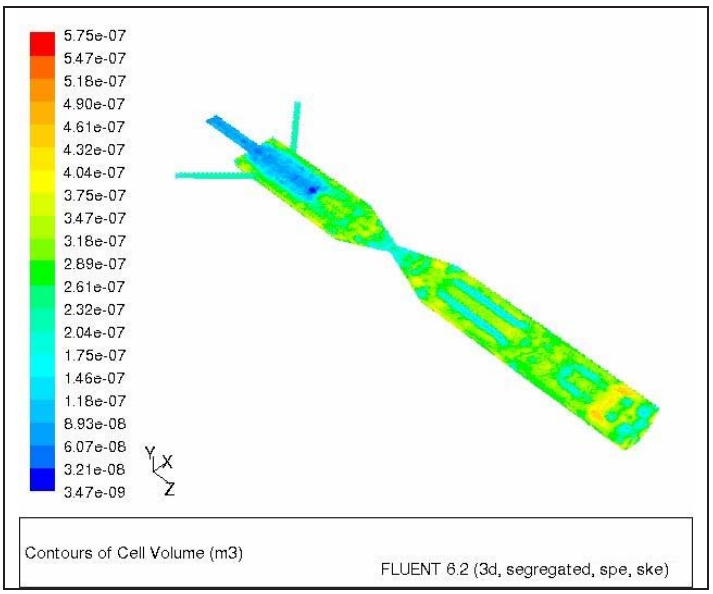

Figure 6.12 Representation of the cell volume size distribution inside the reactor (m^3)

The model was initialized based on an axial inlet of the anthracene oil, while through the lateral inlets was defined a flow of air. Accordingly to the physical model, these flows are thoroughly mixed and will react due to the defined reaction. The conditions inside the reactor are a result of the models defined in "Fluent" and of the initial conditions of the inlets. The conditions inside each cell will result from all the mass and energy inputs and outputs that connect it with the neighbouring cells.
The computing system then follows through a long series of calculations, where every physical and chemical parameter of each cell defined in the 3-dimensional domain is calculated. After every computer iteration of the physical domain the parameters inside each cell will change as they will be affected by the conditions of their 3-dimensional neighbours. Mass and energy balances are evaluated for each cell and for the entire domain.

In the initial iterations the associated deviations for all these mass and energy balances is unavoidably large. If the initially given conditions are physically sound, the computing system will however converge into a stabilized solution where all the mass and energy balances deviations are minimized. The number of iterations required for this stabilization is an unknown factor that will depend on very different parameters and even on the initial characteristics and dimensions of the 3-dimensional grid.
The model was initialized in "Fluent" and a large number of simulations were required to ensure that the physical model was adequate to represent the desired real equipment. A second phase included the definition of the chemical reaction (7), followed for another large number of iterations until the model gave stabilized results.

The obtained results are evaluated on base of physical parameters like the evaluation of temperature distribution and the fluid flow inside the equipment, with related parameters like pressure and density. A second phase includes the chemical aspects of the model, which result from the defined chemical reaction, reaction data and other input conditions that were defined. Among these chemical related parameters we will have distribution of the mass or molar fractions of each species, the distribution of diffusion coefficients and some energy related parameters like the enthalpy, kinetic energy and thermal conductivity.

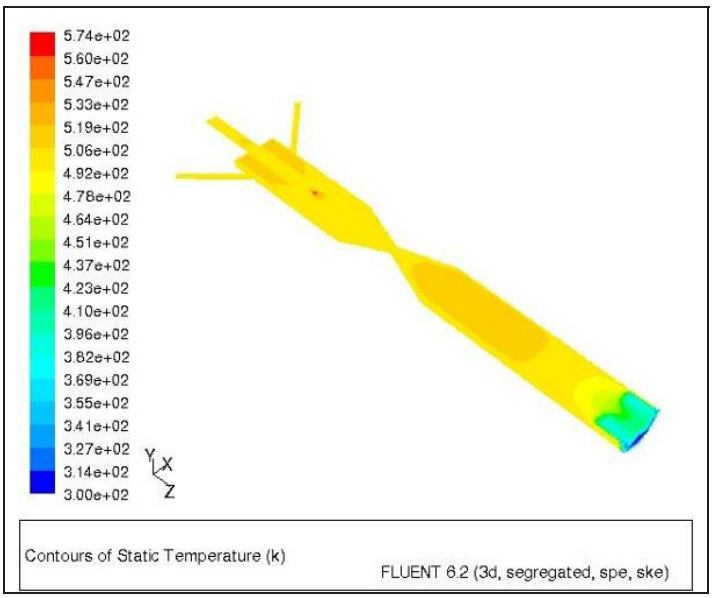

Figure 6.13 Visualization of the temperature inside the reactor (m^3)

In Figure 6.13 are presented the contours of temperature profile inside the equipment. The accuracy of the temperature distribution is rather difficult to evaluate as real temperature data values are not available for comparison. There is an increase of temperature as the considered reaction is exothermic. It is also important to highlight that the maximum temperature, resulting from the underlying model was found from the cells located in the neighbourhood of the injection point.

The mixing of the input flows and the geometry of the injector section cause a large increase of the flow velocity, especially in the initial section, near the injection point. The velocity distribution inside the equipment is shown in the Figure 6.14. The region of higher velocities located n the injector is of special interest for the full development of flow. In the Figure 6.15 is presented the vorticity magnitude, which represents the intensity of rotation of the flowing fluid mixture, and reflects the rotation of the fluid that results from geometry of the inlets.

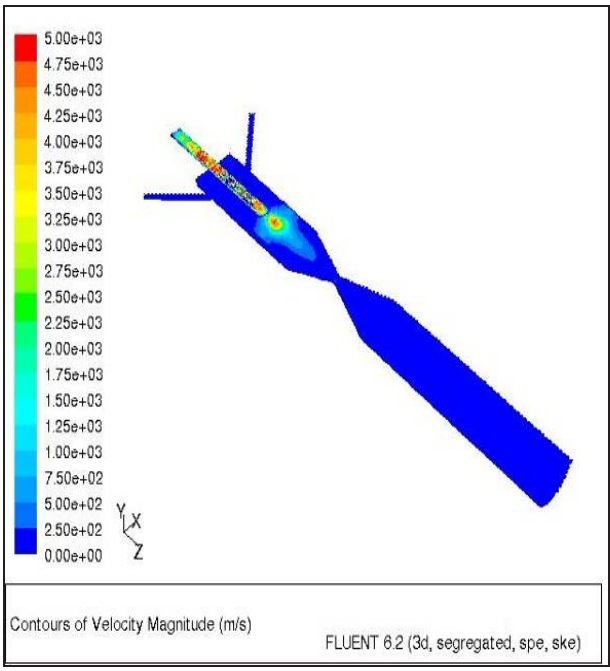

Figure 6.14 Visualization of the velocity magnitude (m/s)

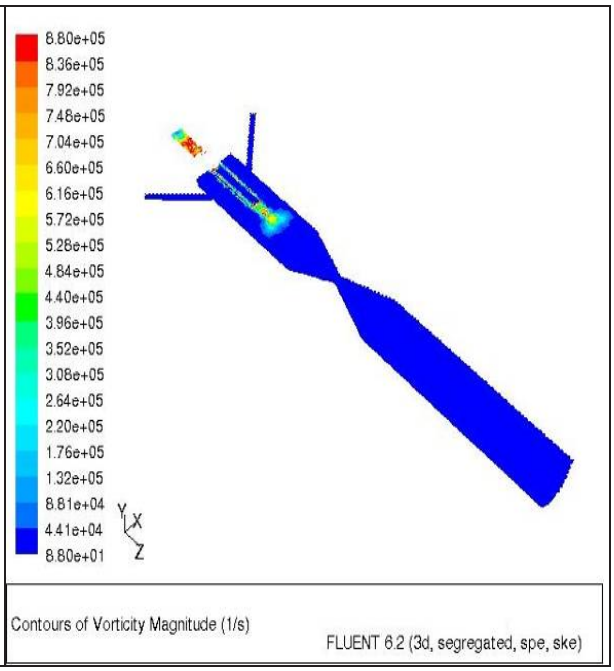

Figure 6.15 Visualization of vorticity magnitude (1/s)

In Figure 6.16 are presented the contours of static pressure inside the equipment. These values are not very high except the observation that the injector design caused a pressure increase in the inlet tube of the anthracene oil.

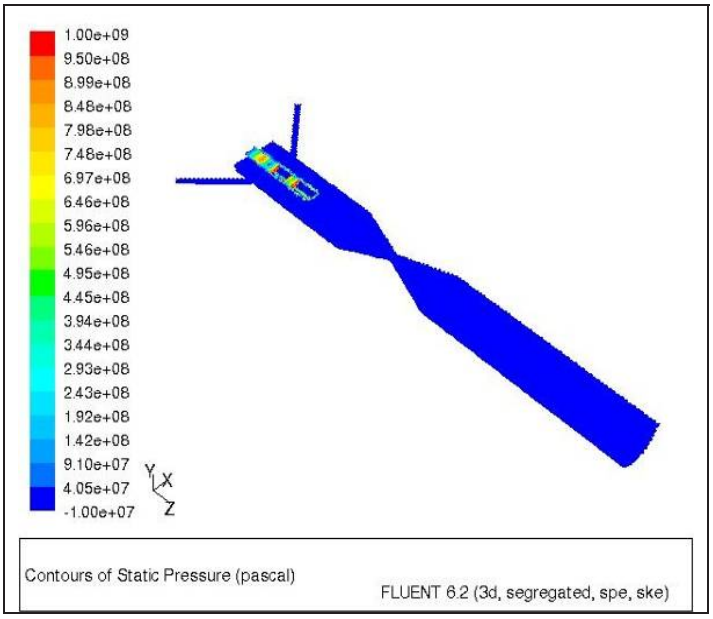

Figure 6.16 Visualization of the static pressure contours (Pascal)

The rate contours for the defined reaction is presented in Figure 6.17, and agrees fairly well with the temperature profile presented previously. There is a maximum in the reaction rate that is related with the temperature maximum and velocity maximum found in Figures 6.13 and 6.14.

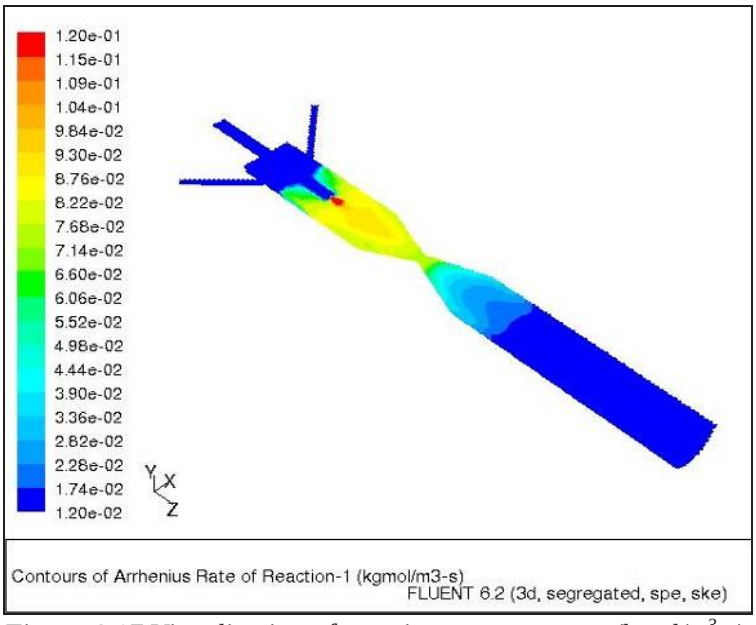

Figure 6.17 Visualization of reaction rate contours (kmol/m^3·s).

With the defined reaction between A01 and oxygen, several concentration profiles were created and are presented in Figures 6.17 to 6.22. The molar fraction contours for A01 and RP1, represent fairly the conversion, which results from the defined reaction. According with available data it is clear the conversion between these two species inside the reactor. In Figure 6.18 A01 molar fraction decreases continuously while it is converted to RP1 as it can be seen on Figure 6.19.

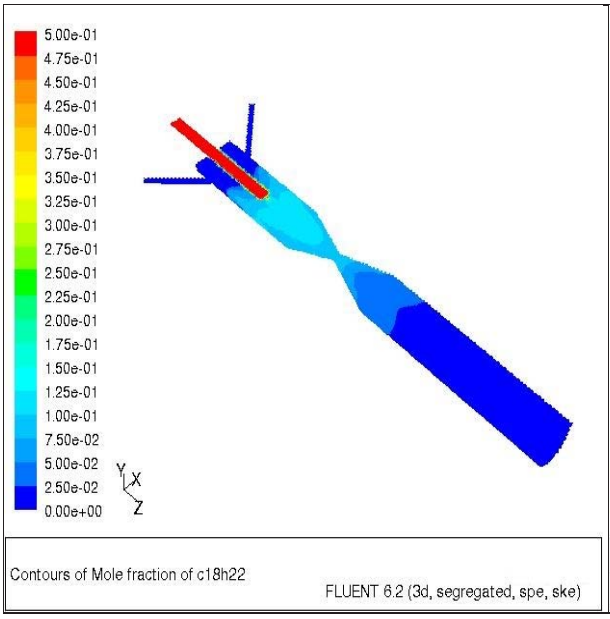

Figure 6.18 Visualization of molar fraction contours of A01.

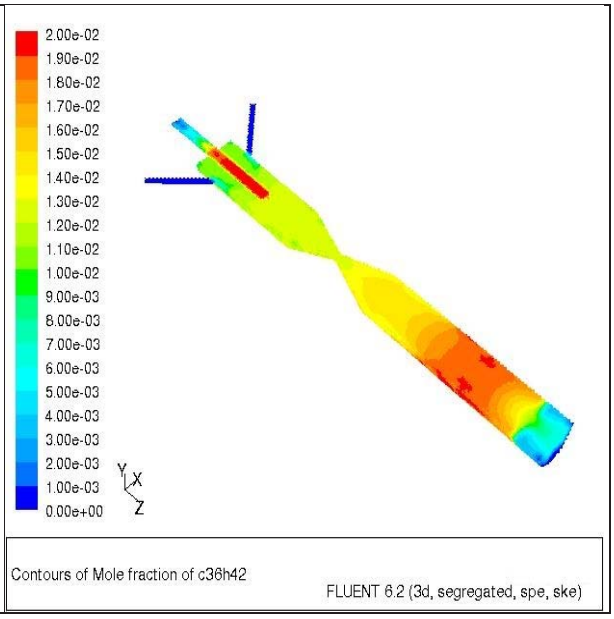

Figure 6.19 Visualization of molar fraction contours of RP1.

With the defined reaction between A01 and oxygen, several concentration profiles were created and are presented in Figures 6.18 to 6.22. The molar fraction contours for A01 and RP1, represent fairly the conversion, which results from the defined reaction. According with available data it is clear the conversion between these two species inside the reactor. In Figure 6.18 A01 molar fraction decreases

The molar fractions of the other species inside the reactor also result from the defined reaction. In Figures 6.20 and 6.21 it is possible to visualize the evolutions of O_2 and H_2O inside the reactor, with the conversion between themselves.

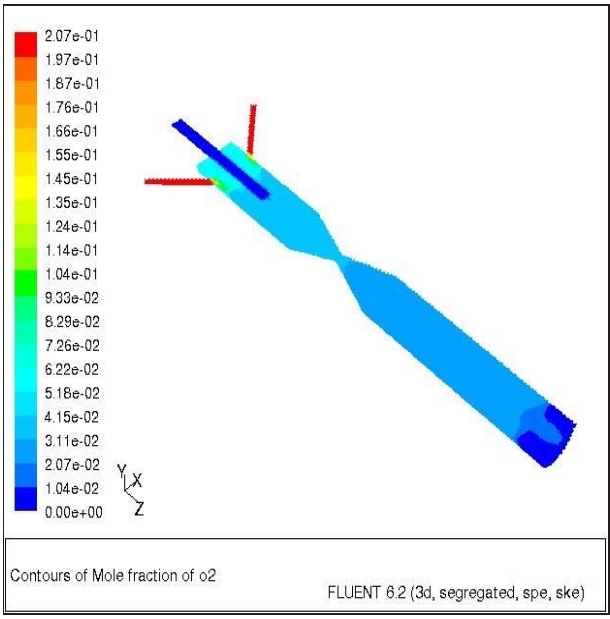

Figure 6.20 Visualization of molar fraction contours of O_2.

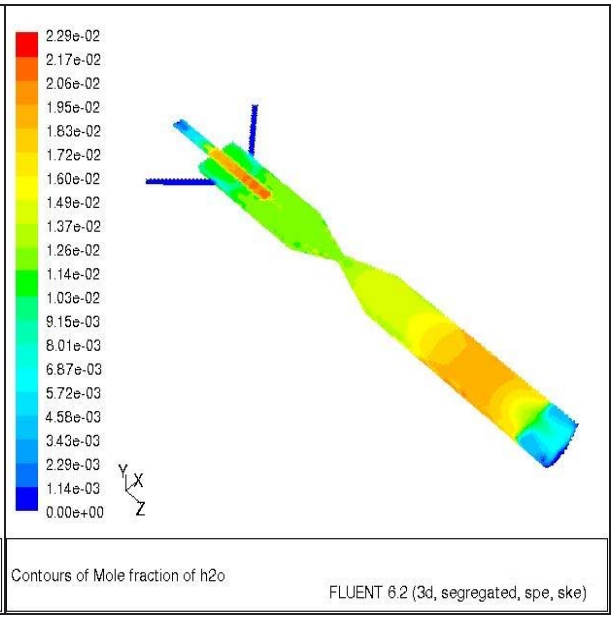

Figure 6.21 Visualization of molar fraction contours of H_2O

For nitrogen the evolution is not so clear, as it is not a reacting species. In Figure 6.22 N_2 presents a maximum in the air inlets, but them it remains in fractions relatively steadier than the reacting species.

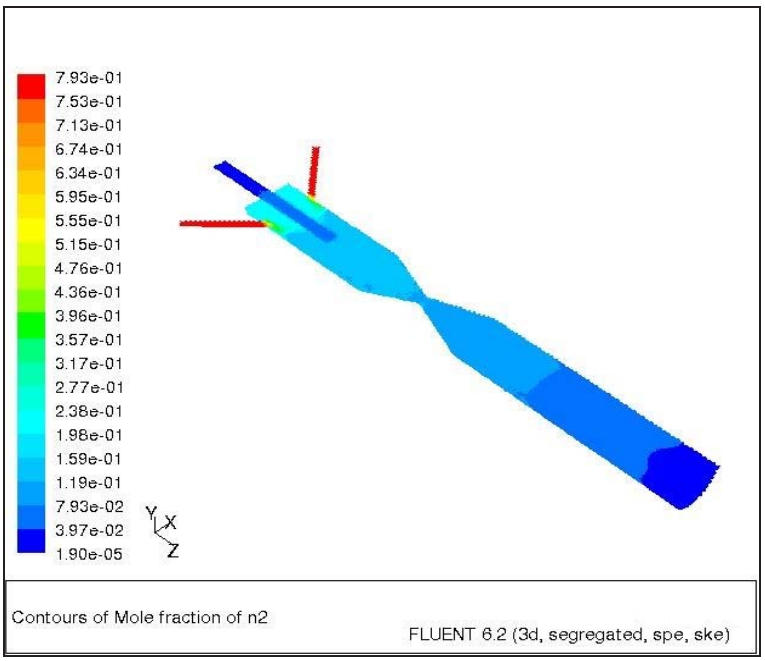

Figure 6.22 Visualization of molar fraction contours of N_2

In Figure 6.23 are presented the contours of density inside the equipment. These values reflect the composition from all the species, with a maximum in the injector inlet tube, while after the mixing with air and the reaction with O2 the density of the flow presents less variations.

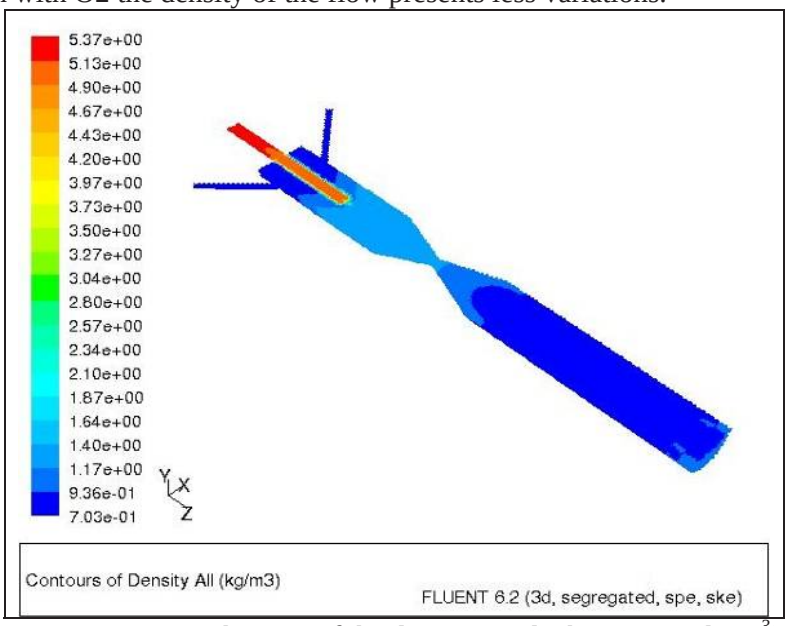

Figure 6.23 Visualization of the density inside the reactor (kg/m^3)

The effective diffusion coefficients are related with the efficacy of mixing between all the species and in the defined model they present a comparable evolution inside the reactor as can be seen in Figures 6.24 and 6.25 for the anthracene oil and for the pitch. For all the other species the evolution is practically equivalent.

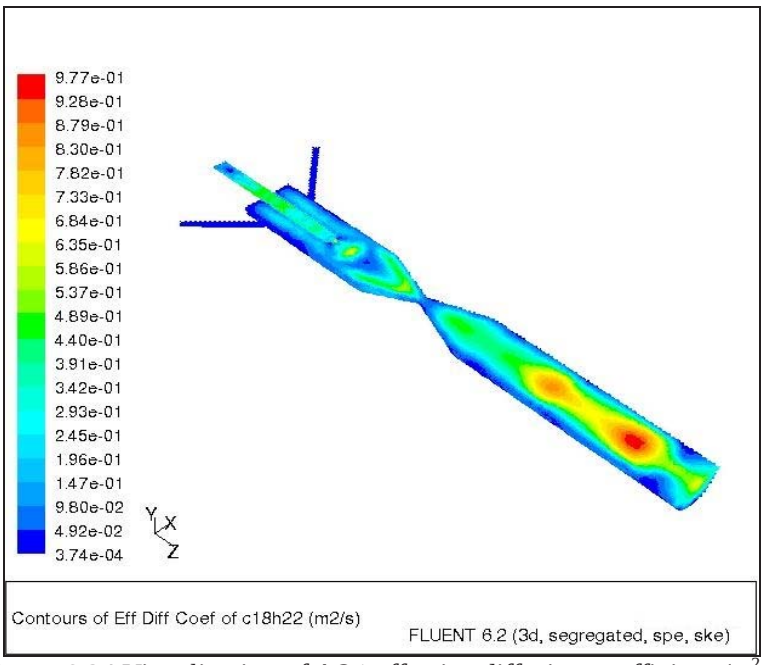

Figure 6.24 Visualization of AO1 effective diffusion coefficient (m^2/s)

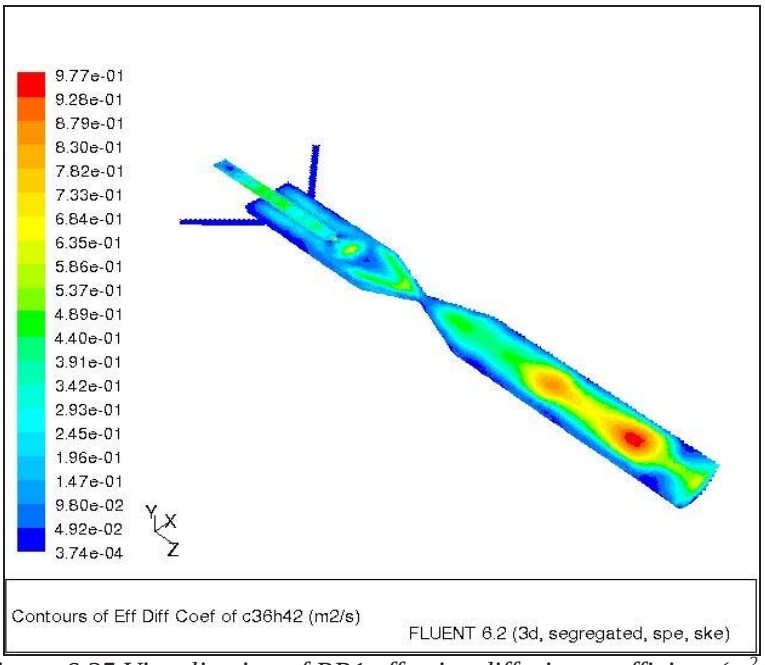

Figure 6.25 Visualization of RP1 effective diffusion coefficient (m^2/s)

In Figures 6.26 and 6.27 are presented the contours of turbulence kinetic energy and thermal conductivity inside the equipment. These values result from the underlying data of the used model. In Figure 6.26 are visible the zones inside the equipment where the turbulence is higher, mainly in the injection system. In Figure 6.27 the areas with higher thermal conductivity result from the composition inside the reactor.

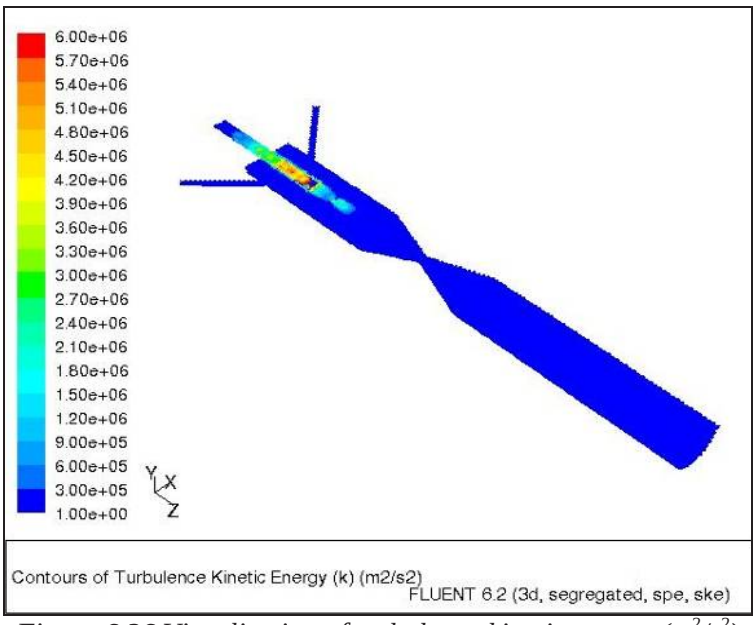

Figure 6.26 Visualization of turbulence kinetic energy (m^2/s^2)

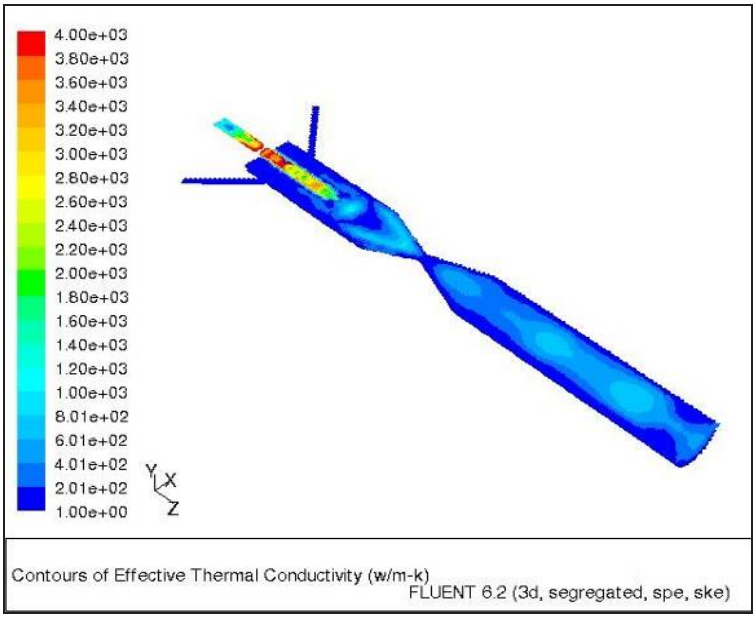

Figure 6.27 Visualization of thermal conductivity contours (W/m·K)

In Figure 6.28 are presented the contours of Enthalpy profile inside the equipment. The higher enthalpy zone, from the anthracene oil, is located in the injector area.

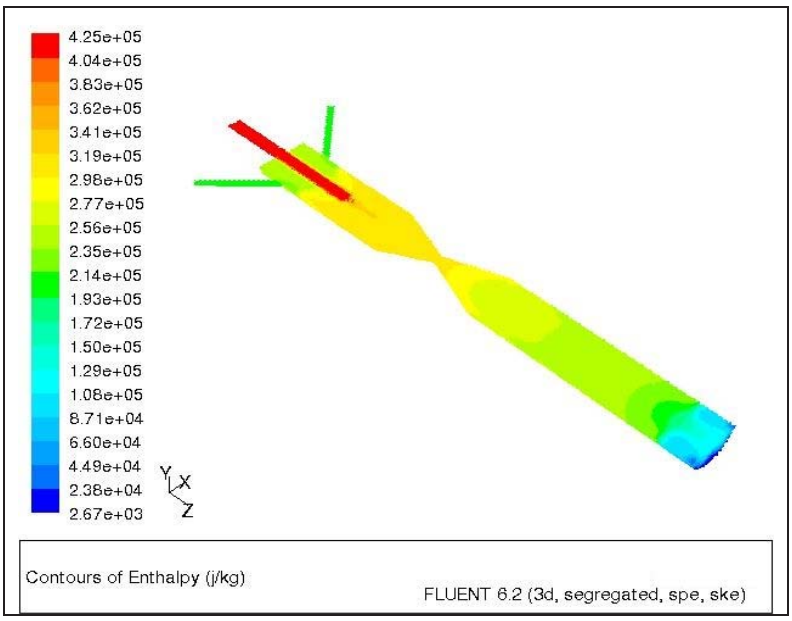

Figure 6.28 Visualization of the enthalpy contours (J/kg)

References

[1] A.L. Fernandez, M. Granda, J. Bermejo, R. Menendez (**2000**), Carbon 38, 1315-1322
[2] A.L. Fernandez, M. Granda, J. Bermejo, R. Menendez (**1999**), Carbon 37, 1247-1255
[3] J. Bermejo,A.L. Fernandez, M. Granda, I. Suelves, A.A. Herod, R. Kandiyoti, R. Menendez (**2001**) J. Chromatogr. A. 919, 255-266
[4] J. Bermejo,A.L. Fernandez, M. Granda, I. Suelves, A.A. Herod, R. Kandiyoti, R. Menendez (**2001**) J. Chromatogr. A. 919, 255-266
[5] Adela L. Ferna´ndez, Marcos Granda, Jenaro Bermejo, Rosa Menendez (**1998**), Energy & Fuels, vol. 12, No 5, 949-957
[6] Jenaro Bermejo, Rosa Menendez, Adela L. Fernandez, Marcos Granda, I. Suelves, A. A. Harold, R. Kandiyoti, (**2001**), Fuel, 2155-2162
[7] J. Bermejo, Adela L. Fernandez, Marcos Granda, F. Rubiera, I. Suelves, Rosa Menendez (**2001**) Fuel 80, 1229-1238.

Work Package Conclusions

The experimental work was executed in two different installations, both operating in batch mode, one operating at atmospheric pressure and another that was pressurized. The production of pitch from anthracene oil at atmospheric pressure was evaluated with a large range of temperatures, reaction times, and flow rates of air and nitrogen in the heating phase. The results obtained were compared with a supplied pitch sample, considering elemental composition, softening point and toluene insoluble fraction. The best fitting was obtained for the experiment done at a temperature of 275ºC, with a run time between 11 to 12 hour and an air flow rate of 0.30 g/min.

These results confirm the problems that were verified in the industrial installation. It was clear, from results presented in Table 6.9 that apparently small variations in reaction time or in air flow, gave very large variations on the chemical composition and on the physical characteristics of the obtained pitch. The results of a short reaction time are products with a very low softening point that will not solidify to a pitch with the desired behaviour. The effect of excessively long reaction times or excessive air flows is a pitch with a softening point that will be too elevated to its further practical use.

The set of pressurized experimental tests, to evaluate the possibility of pitch production at a temperature of 250ºC and a pressure between 1 to 10 bar was inconclusive, as no solid formation was observed.

These results and the experimental difficulties that where observed with the existing installation did not encourage the execution of an additional set of tests where the pressure and the reaction time would be both increased, to avoid further damage to the existing valves, flow meters and pressure regulators.

The modelling work made with “Fluent” included an accurate representation of both the physical process and the chemical reactions, inside the reactor. The simulation included all the available data, but A better validation could eventually have been achieved if internal values from a real system have been used, but the existing installation does not include the possibility of data acquisition to access internal properties inside the reactor, especially near the injector area, like temperature, pressure or gas composition.

It was possible to conclude from the developed model that the reaction occurs in a very short time, and that due to the exothermal nature of the process it would be difficult to try to affect externally the reactor conditions. The high velocity of the conversion reaction, is also related with the higher temperatures found, through the model, in the injector area. There is a zone of high turbulence, with a noticeable release of energy, which through the high flow velocities involved in the process lead to a very fast mixing of the chemical species. It is possible to conclude from the model that this zone near the injector can be considered a critical point of the whole reactor. Any changes due to accumulation of residues on the injector or near the reactor walls, which could produce a noticeable effect on the high turbulence zone, would have a very negative impact on the process, with significant changes on the pressure and temperature profiles and a disruption of the chemical species flows.

The more promising way to affect the pitch production reaction would be to eventually change the air/anthracene oil ratio, to achieve any changes on the produced pitch characteristics. The requirements for alterations on the control mechanism could be achieved including intermediate data acquisition points inside the reactor instead of relying only on the output conditions of the reactor. These measurement points should be mainly located near the injector area. This could be a method to enable an early detection of the eventual operating problems, allowing a faster process actuation and control, before the negative impact becomes too problematic for the reactor.

It is then possible to conclude from these experimental tests that it will be necessary a thorough control of the experimental conditions to better adjust the conditions inside the industrial reactor. In the industrial installation the problems that are verified after long operation must be due to a slow accumulation of solid pitches inside the reactor. It could be necessary to take some periodic samples at different distances from the injector to evaluate the evolution of the reactor performance over time. The data thus accumulated could allow an earlier identification of possible problems on the process, allowing for some preventive measures on the temperature profile or air flow rates that would ultimately avoid a total shut-down of the pitch production process.

Conclusions

Partial conclusions have been presented at the end of each Work package. In more general terms it can be concluded that:

- A process for producing pitches with specific properties from anthracene oil by oxidative treatment was developed.
- Anthracene oil pitches with different composition and molecular structure were obtained by introducing only small modifications in the operational conditions. Impregnation and binder pitches with properties similar to those of standard coal-tar pitches were prepared. Additionally, the benzo[a]pyrene content of anthracene oil pitches was found to be much lower than that of coal-tar pitches. The industrial tests of the anthracene oil pitches showed that the impregnating capacity of these pitches makes them highly suitable candidates for the densification of graphite cathode blocks. The use of anthracene oil pitches for binder purposes requires further investigation.
- The detailed characterization of all the samples generated during the anthracene oil processing made it possible to establish the criteria for understanding the mechanisms of anthracene oil polymerization under the different conditions used. Moreover, the low-medium molecular weight of the compounds generated in the initial stages of anthracene oil polymerization served as a powerful testing-tool for validating different advanced analytical methods based on laser desorption mass spectroscopy and nuclear magnetic resonance.
- The high aromaticity, the total absence of solid particles (mainly QI particles) and their capacity to generate carbons with different microstructures, make anthracene oil derivatives suitable precursors for different type of carbon materials. Carbon fibres, graphitic carbons activated carbons for application in energy storage, are some of the applications that were found for the samples prepared in this study.
- A modeling work with ‘Fluent’ for the anthracene oil polymerization by air-blowing was elaborated. This model, based on physical and chemical variables, established that the reaction is highly exothermic and occurs in a very short time. Preferential zones of reaction were also identified by this model. This information will be crucial for the further enhancement of the process.

Exploitation and impact of the research results

The execution of this project has been highly beneficial for all the partners involved. The development of low benzo[a]pyrene content pitches based on anthracene oil provides IQNSA with opportunities to open up new markets. The transformation of anthracene oil into pitch implies a significant increase in the global yield of the coal tar processing (feedstock from which anthracene oil is obtained). Although from an economical point of view the market situation does not necessarily favour the transformation of anthracene oil into pitch, IQNSA has proceeded with the design of an industrial plant with a capacity for processing 170,000 t of anthracene oil per year. Due to the current world economic situation, the construction of this plant has been postponed to a later date.

This project has also demonstrated the suitability and versatility of the anthracene oil derivatives for producing mesophase-based materials with very different characteristics. A consequence of this has been the presentation of a new RFCS project (acronym, EUROFIBRES) which is currently in the phase of contract negotiation. The main goal of this project is to prepare carbon fibre precursors from anthracene oil-based mesophase. This will entail the development of a new route for the upgrading of a low-cost raw material (anthracene oil) and the preparation of a highly strategic product for preparing advanced carbon materials (mesophase-based fibres).

Furthermore, the first stages of the anthracene oil production process provided samples with a less complex composition to those of the standard pitches. These samples may be used in the future for calibrating and validating other advanced analytical techniques.

In addition to the benefits mentioned above, this project has given rise to some publications (articles in ISI journals and extended abstracts/proceedings at congresses) in which financing by the RFCS Ecopitch project has been acknowledged. These publications are:

1. Sutil J., Alvarez P., Blanco, C., Santamaría R., Menéndez R., Granda M., Polygranular synthetic graphites from anthracene oil-based mesophase. The International Conference on Carbon, Aberdeen (United Kingdom), 2006, 1P10.
2. Alvarez P., Menéndez P., Granda M., Carbon-embedded iron oxide nanoparticles. The International Conference on Carbon, Aberdeen (United Kingdom), 2006, 1P32.
3. Sutil J., Alvarez P., Menéndez R., Granda M., Viña, J.A., Fernández J.J., The effect of the severity of anthracene oil treatment on the chemical composition of resultant pitches. The International Conference on Carbon, Aberdeen (United Kingdom), 2006, 2P66.
4. Sutil J., Alvarez P., Blanco, C., Santamaría R., Menéndez R., Granda M., Obtención de grafitos poligranulares autosinterizables a partir de aceite de antraceno. IX Congreso Nacional de Materiales, Vigo, 2006, Vol. I, 263-265.
5. Sutil J., Alvarez P., Blanco C., Santamaría R., Menéndez R., Granda M., Preparation of mesophase from anthracene oil. 2007 International Conference on Coal Science and Technology, Nottingham (United Kingdom), 2007, CD ROM 2P19.pdf.
6. Alvarez P., Blanco C., Granda M., Menéndez R., Santamaría R., Sutil J., Anthracene oil-based graphites containing iron nanoparticles. Internacional Conference on Carbon, Seatle (United States), 2007, CD ROMM P149.
7. Granda M., INCAR research on coal derivatives. ITA Internacional Tar Association: General Assembly & Annual Conference, 2007, Palma de Mallorca (Spain), 56-103.
8. Krol M., Kierzek K., Gryglewicz G., Machnikowski J., Variation of porosity development on KOH activation with carbonization progress of pitch-derived precursor, The 2nd International Conference, CESEP`07, Carbon for Energy Storage and Environment Protection, Abstracts Book p. 158, Krakow (Poland), 2007.
9. Machnikowski J., Kierzek K., **O**n the role of of precursor nature on the fine structure of the KOH activated carbon, The 2nd International Conference, CESEP`07, Carbon for Energy Storage and Environment Protection, Abstracts Book p. 48, Krakow (Poland), 2007.

10. Frackowiak E., Kierzek K., Lota G., Machnikowski J., Lithium insertion/deinsertion of boron doped graphitic carbons synthesized by different procedure, ISIC2007, 14th International Symposium on Intercalation Compounds, Seoul (Korea) 2007, CD ROM.
11. Alvarez P., Sutil J., Granda M., Menéndez R., Mejora de las propiedades de materiales de carbono mediante la aditivación con nanopartículas de óxido de hierro, VII Congreso Nacional de Materiales Compuestos, Valladolid (Spain) 2007, 311-316.
12. Alvarez P., Blanco C., Granda M., Menéndez R., Santamaría R., Sutil J., Anthracene oil-based graphites containing iron nanoparticles, Carbon 2007, Seatle (USA), P149.
13. Alvarez P., Blanco C., Granda M., Santamaría R., Sutil J., Menéndez R., Preparación de mesofase a partir de breas de aceite de antraceno. IX Reunión del Grupo Español del Carbón, Teruel (Spain) 2007, 45-46.
14. Alvarez P., Granda M., Sutil J., Menéndez R., Dopado de grafitos poligranulares autosinterizables con óxido de hierro nanoparticulado. IX Reunión del Grupo Español del Carbón, Teruel (Spain) 2007, 233-234.
15. Alvarez P., Granda M., Sutil J., Menéndez R., Preparación de coques de aguja a partir de derivados de aceite de antraceno. IX Reunión del Grupo Español del Carbón, Teruel (Spain) 2007, 235-236.
16. **Alvarez P., Granda M., Sutil J., Menéndez R., Fernández J.J., Viña J.A., Morgan T.J., Millán M., Herod A.A., Kandiyoti R., Characterization and pyrolysis behaviour of novel anthracene oil derivatives, Energy & Fuels 22 (6), 4077-4086, 2008.**
17. **Alvarez P., Sutil J., Santamaría R., Blanco C., Menéndez R., Granda M., Mesophase from anthracene oil-based pitches, Energy & Fuels 22 (6), 4146-4150, 2008.**
18. Sutil J., Alvarez P., Menéndez R., Granda M., Preparation of leedle coke from anthracene oil-based pitches, Internacional Conference on Carbon (Carbon'08), Nagano (Japan), 2008, P0277.
19. Sutil J., Alvarez P., Granda M., Menéndez R., Mejora de las propiedades de materiales de carbono mediante la aditivación con nanopartículas de óxido de hierro, X Congreso Nacional de Materiales, San Sebastián (Spain), 2008, Vol. II, 787-789.
20. **Frackowiak E., Kierzek K., Lota G., Machnikowski J. Lithium insertion/deinsertion of boron doped graphitic carbons synthesized by different procedure. J. Phys. Chem. Solids 2008, 69 (5-6), 1179-1181.**
21. Machnikowski J., Machnikowska H., Lota G., Frąckowiak E. On the contribution of heteroatoms to the capacitance properties of nitrogen enriched carbons. Carbon'2008, International Carbon Conference, CD-ROM, paper PO 534, Nagano 2008.
22. **Morgan T., George A., Alvarez P., Millan M., Herod A., Kandiyoti R., Characterization of molecular mass ranges of two coal tar distillate fractions (creosote and anthracene oils) and aromatic standards by LD-MS, GC-MS, probe-MS & size exclusion chromatography. Energy & Fuels, 2008, 22 (5), 3275-3292.**
23. Kierzek K., Krol M., Gryglewicz G., Machnikowski J., Optimizing porous texture of KOH activated karbon for electrochemical capacitors, submitted for CESEP'09, III International Conference on Carbons for Energy Storage and Environment Protection. Torremolinos-Málaga, Spain, 25-29 October 2009.
24. **Alvarez P., Sutil J., Menéndez R., Granda M., Matriz-iron interactions in carbon-embedded iron oxide nanoparticles, Journal of Nanoscience and Nanotechnology, in press.**
25. **Krol M., Gryglewicz G., Machnikowski J. Tailoring porosity development of pitch-derived KOH activated carbons, Carbon, under review.**

List of figures and tables

Figures

Figure 5.3. TG (left) and DTG (right) curves of the green and stabilized fibres obtained from Meso-2.

Figure 5.4. SEM micrograph of carbon fibres obtained from Meso-2 stabilized at (a) 225, (b) 250 and (c) 300 °C.

Figure 5.5 Flowsheet of boron-doped graphite preparation routes used in the study.

Figure 5.6. Changes in the volatile matter content (a) and H/C atomic ratio (b) on the heat-treatment of pitches P1 and P4.

Figure 5.7. N_2 adsorption isotherms for the series of activated carbons produced at 700^{o}C from P-1 carbonization products.

Figure 5.8. Relation between BET surface area of KOH activated carbon derived from P-1 (■,□) and P-4 (▲,△) and the volatile matter content (a) and the H/C atomic ratio (b) for series of precursors derived from pitch P-1 and P-4. Open points - activation at 800^{o}C, filled points - at 700^{o}C.

Figure 5.9. Variation of microporosity parameters: micropore volume V_{DR} (a) and V_{DR}/V_T ratio (b) with carbonization degree $(H/C)_{at}$ for pitch derived carbons AP-1 (■,□) and AP-4 (▲,△)activated with KOH at 700^{o}C and 800^{o}C.

Figure 5.10. Particle size distribution of KOH activated carbons (700^{o}C) from P-1 and P-4 derived precursors of different carbonization degree.

Figure 5.11. Pore size distribution of activated carbons produced at 700^{o}C using different KOH/P-4 semi-coke ratio.

Figure 5.12. N_2 adsorption isotherms of steam and CO_2 activated carbons from PAN and pitch/PAN blend.

Figure 5.13. The optical texture of chars from P-1/MF (a) and P-1/Mox (b) blends.

Figure 5.14. N1s spectra of AP1-520/700-N450 (a) and AP1-520/700-N700 (b).

Figure 5.15. Effect of particle size on nitrogen up-take during ammonization at 700^{o}C of coke powder (a) and KOH activated carbons of BET surface area of ~1500 m^2/g (b, c) and ~ 2500 m^2/g produced from P-1 pitch.

Figure 5.16. Optical microscopy of the cokes (a) C1, (b) C2, (c) C3, (d) C4, (e) C5 and (f) C6 obtained from the reaction product RP-1 under different experimental conditions (see Table 5.11).

Figure 5.17. Galvanostatic lithium insertion/deinsertion for undoped and boron doped P-1 derived graphites

Figure 5.18. Variation of electric capacitance with current load for a series of KOH activated carbons derived from P-4 pitch.

Figure 5.19. Voltammetry characteristics of a capacitor built from the selected KOH activated carbons at different scan rates of voltage. Electrolytic solution: 1M H_2SO_4.

Figure 5.20. Variation of electric capacitance with current load for steam and CO_2 activated carbons derived from the blends of pitch with N-polymers.

Figure 5.21. Relationship between electrochemical properties and nitrogen/oxygen content in parent and ammonized materials.

Tables

List of references

A list of references has been in each individual Work Package.

European Commission

EUR 24193 — Development of a new generation of coal-derived environmentally friendly pitches

R. Menéndez, M. Granda, R. Kandiyoti, M. Millán, I. Gulyurtlu, F. Pinto, J. J. Fernández, S. Lacroix, B. Allard, J. Machnikowski

Luxembourg: Publications Office of the European Union

2009 — 139 pp. — 21 × 29.7 cm

Research Fund for Coal and Steel series

ISBN 978-92-79-14238-3

doi 10.2777/82435

ISSN 1018-5593

Price (excluding VAT) in Luxembourg: EUR 7